DISRUPTION OF NEURORESPIRATORY CONTROL BY ACUTE INFLAMMATION, NEONATAL INFLAMMATION, AND PERINATAL OPIOIDS

by

AUSTIN DEAN HOCKER

A DISSERTATION

Presented to the Department of Human Physiology
and the Graduate School of the University of Oregon
in partial fulfillment of the requirements
for the degree of
Doctor of Philosophy

September 2019

DISSERTATION APPROVAL PAGE

Student: Austin Dean Hocker

Title: Disruption of Neurorespiratory Control by Acute Inflammation, Neonatal Inflammation, and Perinatal Opioids

This dissertation has been accepted and approved in partial fulfillment of the requirements for the Doctor of Philosophy degree in the Department of Human Physiology by:

Adrianne G. Huxtable, PhD	Advisor
Andrew T. Lovering, PhD	Core Member
Carrie E. McCurdy, PhD	Core Member
Cris M. Niell, PhD	Institutional Representative

and

Janet Woodruff-Borden	Vice Provost and Dean of the Graduate School

Original approval signatures are on file with the University of Oregon Graduate School.

Degree awarded September 2019

DISSERTATION ABSTRACT

Austin Dean Hocker

Doctor of Philosophy

Department of Human Physiology

September 2019

Title: Disruption of Neurorespiratory Control by Acute Inflammation, Neonatal Inflammation, and Perinatal Opioids

Adequate respiratory control is vital, but is disrupted by stressors such as inflammation or opioids. Additionally, early-life stressors may have long-lasting consequences for adult breathing, increasing the risk of disease. This dissertation focuses on how acute inflammation impairs adult respiratory control mechanisms and explores the consequences of two early life stressors, neonatal inflammation and perinatal opioids.

Respiratory plasticity is a key feature of respiratory control, commonly studied in the form of phrenic long-term facilitation (LTF), evoked by acute intermittent hypoxia. Two distinct molecular pathways evoke LTF: the Q-pathway which is impaired by low-level inflammation, and the S-pathway which is inflammation-resistant. Chapters II and III further our mechanistic understanding of how inflammation impacts respiratory plasticity.

Chapter II demonstrates spinal activation of the interleukin-1 (IL-1) receptor is necessary for impairing Q-pathway LTF after inflammation. However, IL-1β, the endogenous ligand of IL-1R, is not sufficient to impair LTF in healthy animals, suggesting other inflammatory signals are required.

While LPS or simulated sleep apnea induces inflammation and impairs Q-pathway-evoked LTF, chapter III demonstrates these impairments are generalizable to viral-mimetic induced inflammation which impairs Q-pathway, but not S-pathway-evoked pLTF.

Chapter IV demonstrates the long-lasting impairment of adult respiratory plasticity following a single bout of LPS-induced early-life inflammation. Early-life inflammation impaired both Q-pathway and S-pathway-evoked LTF in male and female rats. Despite a lack of adult pro-inflammatory gene expression, Q-pathway LTF was restored by adult anti-inflammatory treatment, demonstrating ongoing inflammatory signaling after neonatal inflammation. S-pathway-evoked LTF was revealed by adenosine receptor agonism, suggesting upstream impairment in adenosine release.

Chapter V investigates the impact of maternal opioid use, another common perinatal stressor. Maternal methadone increases neonatal apneas and mitigates acute methadone-induced respiratory depression, demonstrating perinatal opioids destabilize neonatal respiratory control in rats.

These studies demonstrate neurorespiratory control is disrupted by acute inflammation, neonatal inflammation, and perinatal opioids. The research contributes to our fundamental understanding of how inflammation impairs adult respiratory plasticity, both acutely and after a single early-life exposure. Further, it lays the foundation for future studies investigating how perinatal opioids alter the developing respiratory control system. This dissertation includes previously published, coauthored material.

CURRICULUM VITAE

NAME OF AUTHOR: Austin Dean Hocker

GRADUATE AND UNDERGRADUATE SCHOOLS ATTENDED:

University of Oregon, Eugene, Oregon
Linfield College, McMinnville, Oregon

DEGREES AWARDED:

Doctor of Philosophy, Human Physiology, 2019, University of Oregon
Master of Science, Human Physiology, 2014, University of Oregon
Bachelor of Science, Exercise Science, 2011, Linfield College

AREAS OF SPECIAL INTEREST:

Neural control of breathing
Respiratory plasticity

PROFESSIONAL EXPERIENCE:

Teaching and Administrative Consultant, 2018-present

Graduate Education Mentor, Science Literacy Program, 2017-2018

Instructor and Laboratory Coordinator, University of Oregon, 2014-2015

GRANTS, AWARDS, AND HONORS:

Jan Broekhoff Graduate Scholarship	2019
Shapiro Family Scholarship	2019
APS Respiration Section Usha Award	2019
Dissertation Research Fellowship University of Oregon Graduate School	2018
Jan Broekhoff Graduate Scholarship	2018
Shapiro Family Scholarship	2018
Therapeutic Intermittent Hypoxia Retreat, Travel Award University of Florida	2018
APS Respiration Section Usha Award	2018

Marthe E. Smith Memorial Science Scholarship	2017
Jan Broekhoff Graduate Scholarship	2017
Shapiro Family Scholarship	2017
Department of Human Physiology, Graduate Teaching Award	2016
National Skeletal Muscle Research Center - Muscle Physiology Workshop, UCSD	2013
U. Oregon CAMCOR Training Scholarship	2012
Linfield College: Outstanding Exercise Science Student of the Year	2011

PUBLICATIONS:

1. **Hocker AD**, Huxtable AG. 2019. Viral mimetic-induced inflammation abolishes Q-pathway, but not S-pathway, respiratory motor plasticity in adult rats. Front Physiol **2019** 10:1039.

2. **Hocker AD**, Beyeler SA, Gardner AN, Johnson SM, Watters JJ, Huxtable AG. One bout of neonatal inflammation impairs adult respiratory motor plasticity in male and female rats. eLife **2019**;8:e45399 PMID: 30900989.

3. Johnson SM, Randhawa KS, Epstein JJ, Gustafson E, **Hocker AD**, Huxtable AG, Baker TL, Watters JJ. Gestational intermittent hypoxia increases susceptibility to neuroinflammation and alters respiratory motor control in neonatal rats. Respir Physiol Neurobiol. **2018** Oct;256:128-142. PMID: 29174411.

4. **Hocker AD**, Huxtable AG. IL-1 receptor activation undermines respiratory motor plasticity after systemic inflammation. J Appl Physiol (1985). **2018** Aug 1;125(2):504-512. PMID: 29565772.

5. Chicco AJ, Le CH, Gnaiger E, Dreyer HC, Muyskens JB, D'Alessandro A, Nemkov T, **Hocker AD,** Prenni JE, Wolfe LM, Sindt NM, Lovering AT, Subudhi AW, Roach RC. Adaptive remodeling of skeletal muscle energy metabolism in high-altitude hypoxia: Lessons from AltitudeOmics. J Biol Chem. **2018** May 4;293(18):6659-6671. PMID: 29540485.

6. **Hocker AD**, Stokes JA, Powell FL, Huxtable AG. The impact of inflammation on respiratory plasticity. Exp Neurol. **2017** Jan;287(Pt 2):243-253. Review. PMID: 27476100.

7. Clayton ZS, Wilds GP, Mangum JE, **Hocker AD,** Dawson SM. Do targeted written comments and the rubric method of delivery affect performance on future human physiology laboratory reports? Adv Physiol Educ. **2016** Sep;40(3):359-64. PMID: 27445286.

8. Romero SA, **Hocker AD,** Mangum JE, Luttrell MJ, Turnbull DW, Struck AJ, Ely MR, Sieck DC, Dreyer HC, Halliwill JR. Evidence of a broad histamine footprint on the human exercise transcriptome. J Physiol. **2016** Sep 1;594(17):5009-23. PMID: 27061420.

9. Muyskens JB, **Hocker AD,** Turnbull DW, Shah SN, Lantz BA, Jewett BA, Dreyer HC. Transcriptional profiling and muscle cross-section analysis reveal signs of ischemia reperfusion injury following total knee arthroplasty with tourniquet. Physiol Rep. **2016** Jan;4(1). pii: e12671. PMID: 26733251.

10. Dreyer HC, Strycker LA, Senesac HA, **Hocker AD**, Smolkowski K, Shah SN, Jewett BA. Essential amino acid supplementation in patients following total knee arthroplasty. J Clin Invest. 2013 Nov;123(11):4654-66. PMID: 24135139.

11. **Hocker AD**, Boileau RM, Lantz BA, Jewett BA, Gilbert JS, Dreyer HC. Endoplasmic Reticulum Stress Activation during Total Knee Arthroplasty. Physiol Rep. **2013** Aug 1;1(3):e00052. PMID: 24159375.

12. Bailey AN, **Hocker AD**, Vermillion BR, Smolkowski K, Shah SN, Jewett BA, Dreyer HC. MAFbx, MuRF1, and the stress-activated protein kinases are upregulated in muscle cells during total knee arthroplasty. Am J Physiol Regul Integr Comp Physiol. **2012** Aug 15;303(4):R376-86. PMID: 22761181.

13. Ratchford SM, Bailey AN, Senesac HA, **Hocker AD**, Smolkowski K, Lantz BA, Jewett BA, Gilbert JS, Dreyer HC. Proteins regulating cap-dependent translation are downregulated during total knee arthroplasty. Am J Physiol Regul Integr Comp Physiol. **2012** Mar 15;302(6):R702-11. PMID: 22204954

ACKNOWLEDGMENTS

As a graduate student, I have had so many opportunities for my personal and professional development. First, Thank you to my advisor Adrianne Huxtable for training, your availability and research guidance. Thank you for the autonomy to design experiments, build equipment, and try new things. Most importantly, thank you for letting me serve on committees and explore other career options over the last few years. Thank you to the rest of my committee: Andy Lovering gave the first research talk I ever saw and blew my mind with bubbles. Thank you for always willing to drop everything to talk about science and help troubleshoot problems. Without Andy I would never have made it to Bolivia for my first research expedition and wouldn't have ended up studying respiratory physiology. Carrie McCurdy played a critical role in these projects, allowing me to use lab space and equipment. Portions of these projects would not be possible without her time and assistance. Cris Neill inspires me with his excitement for science and willingness to pursue new research directions. From what I see, genuine curiosity and collaboration drives his work – just the way I think science should be done. Thank you to Sierra Dawson, the best mentor and ally I have had in my time at University of Oregon. I have learned so much from Sierra professionally and as a person and am looking forward to continuing our work together. Thank you to Elly Vandegrift and the Science Literacy Program for countless professional development opportunities. Thank you to the graduate school for the graduate research fellowship which funded my last year and opened up possibilities for me to explore and find the perfect job. Thank you to funding from the University of Oregon and the National Institute of Health which made all of these

experiments possible. Finally, thank you to everyone on the animal care team – your care for our animals makes all of our work possible.

TABLE OF CONTENTS

Chapter Page

LIST OF FIGURES

Figure Page

Figure Page

LIST OF TABLES

Table Page

CHAPTER I

INTRODUCTION AND BACKGROUND

This chapter includes previously published co-authored material (Hocker et al., 2017). F. Powell, J. Stokes, and A.G. Huxtable contributed to writing and provided editorial input.

Appropriate ventilatory control is critical for preserving life and must adapt to ensure adequate breathing after diseases, disorders, and injuries. The respiratory control system modulates breathing to maintain homeostasis under changing physiological and environmental conditions, but also utilizes adaptive control mechanisms (e.g. respiratory plasticity) to maintain adequate breathing in the face of disease or injury. Furthermore, respiratory plasticity can be used therapeutically to enhance breathing when respiratory function is compromised. However, theses therapeutic benefits are thought to be limited by inflammation. This dissertation examines how two stressors, inflammation and opioids, alter the neural control of breathing and undermine the system's capacity to adapt. I will examine 1) how acute inflammation, which is common in injury and diseases, undermines adult respiratory plasticity 2) how early-life inflammation can have lasting consequences for adult respiratory control and 3) the effects of perinatal opioids, which inhibit respiratory control centers in the brain, and how they influence the development of the respiratory control system.

The first chapter of this thesis reviews the neural control of breathing and how it is influenced by inflammation and opioids. This includes a discussion of the functions of

the respiratory control networks and their capacity for plasticity, as well as how acute inflammation and opioids alter these functions.

Neurorespiratory Control System

The respiratory system is a vital homeostatic system for maintaining blood gasses and appropriate pH. The respiratory system must be robust, yet highly adaptable to changes in the environment, metabolic demand, and injury or disease. This adaptability is created through both modulation and, a less well appreciated form of adaptation in the respiratory control system, neuroplasticity.

The neural network controlling breathing is comprised of regions in the pons, medulla, and spinal cord that integrate sensory feedback and shape inspiratory and expiratory muscle activation patterns to control ventilation. These respiratory-related regions contain a heterogenous population of excitatory and inhibitory neurons, named according to how the firing patterns correspond with inspiration and expiration. However, most regions have a generally agreed upon function supported by lesion, pharmacological, and optogenetic experiments.

Neural Circuitry Controlling Breathing

The primary site of respiratory control is the ventral respiratory column (VRC) in the medulla (Feldman, 1986), a long column of regions responsible for respiratory rhythm generation and pattern formation (Fig. 1.1).

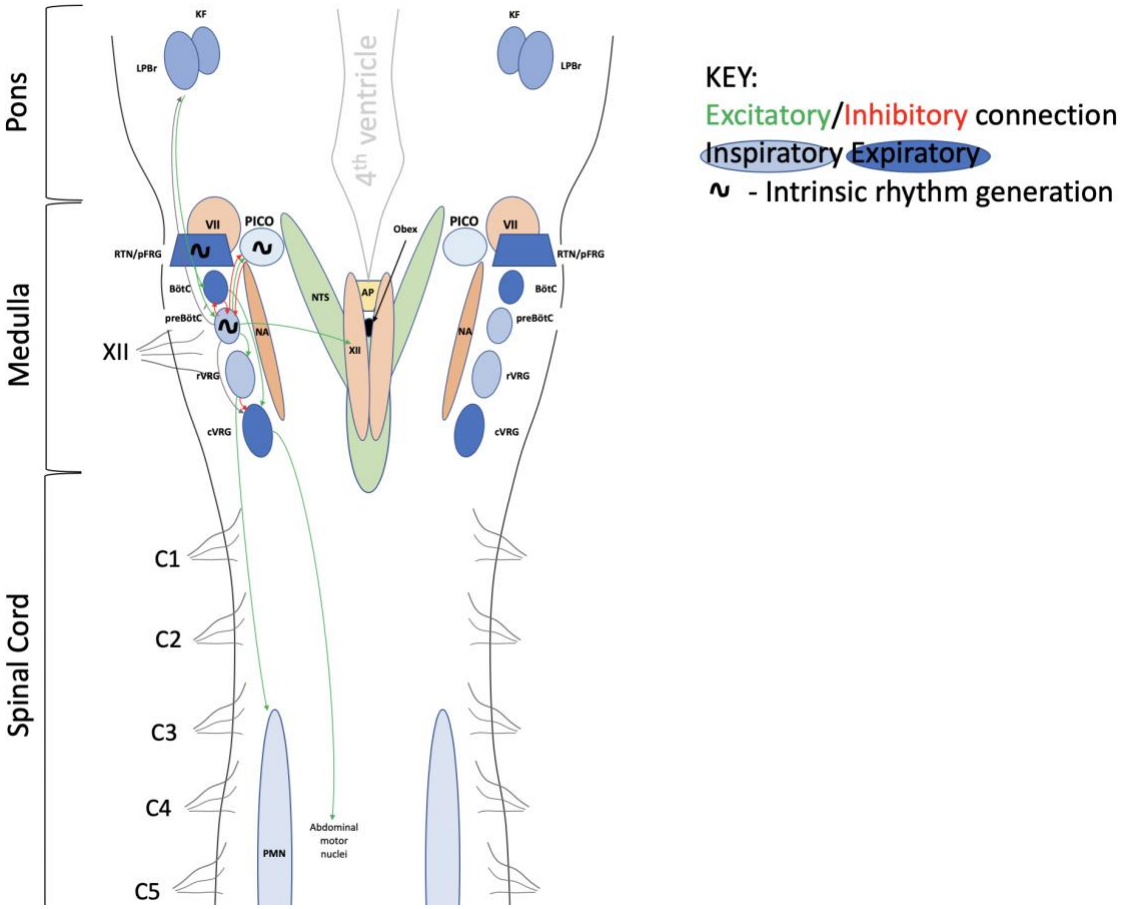

Figure 1.1. Brainstem and spinal cord circuitry controlling breathing. Respiratory networks in the pons, medulla, and spinal cord control breathing. Rhythmogenic regions send excitatory outputs to bulbospinal neurons innervating phrenic motor neurons, which innervate the diaphragm, the primary inspiratory muscle. Ventral Respiratory Column (VRC), Bötzinger complex (BötC), preBötzinger complex (preBötC), ventral respiratory group (VRG), rostral VRG (rVRG), caudal VRG (cVRG), facial nucleus (VII), hypoglossal motor nucleus (XII), retrotrapezoid nucelus (RTN), parafacial respiratory group (pFRG/RTN), nucleus of the solitary tract (NTS), nucleus ambiguous (NA), area postrema (AP), post-inspiratory complex (PICO), phrenic motor nucleus (PMN), lateral parabrachial region (LPBr), Kölliker Fuse nucleus (KF). (Adapted from Smith, Abdala, Borgmann, Rybak, & Paton, 2013; Smith, Abdala, Rybak, & Paton, 2009; Tan, Pagliardini, Yang, Janczewski, & Feldman, 2010)

The most rostral component of the VRC is the parafacial respiratory group/retrotrapezoid nucleus (pFRG/RTN) containing Phox2b-positive neurons (Thoby-Brisson et al., 2009) with intrinsic rhythmic activity in perinatal rodents (Onimaru and Homma, 2003). This

early rhythmic activity shifts in adults to tonic activity (Mulkey et al., 2004), regulated by CO2/pH and inputs from peripheral chemoreceptors (Gourine et al., 2010; Takakura et al., 2006), and may be responsible for expiratory abdominal muscle activation during active expiration (Huckstepp et al., 2018). The Bötzinger complex (BötC) is caudal to the RTN and is primarily made up of inhibitory interneurons which fire primarily during expiration and project to the preBötC (Smith et al., 2009) (Fig. 1.1). Caudal to the BötC is the preBötzinger complex (preBötC), which has been widely studied because of its critical role in inspiratory rhythm generation (Smith et al., 1991). It is composed of inhibitory and excitatory propriobulbar neurons projecting to the BötC, rostral ventral respiratory group (rVRG), and suprapontine regions (Yang and Feldman, 2018). These connections coordinate rhythmic activity between regions and may mediate the emotional and other complex behaviors that can be altered by breathing (Tan et al., 2010b; Yang and Feldman, 2018). Importantly, this region can autonomously produce rhythmic bursting output via multiple potentially overlapping mechanisms, discussed in more detail below. The ventral respiratory group makes up the caudal aspect of the VRC and can be subdivided into rostral and caudal portions. Both the rVRG and caudal VRG (cVRG) contain premotor bulbospinal neurons which transmit respiratory activity from the medulla to cranial and spinal respiratory motor neurons driving respiratory muscles (Smith et al., 2013). Neurons in the rVRG are primarily inspiratory, while neurons in the cVRG are primarily expiratory (Smith et al., 2013) (Fig. 1.1).

Other brainstem areas contain important respiratory modulating regions, but are not required for rhythmic respiratory motor output. The pontine respiratory groups project to the VRC to modulate breathing and contribute to respiratory phase transitions

(Smith et al., 2009) (Fig. 1.1). The dorsal respiratory group (DRG) is located in the nucleus of the solitary tract (NTS) and relays afferent input from peripheral and central chemoreceptors, as well as stretch receptors in the lung (Hamnid et al., 2005). Lesions to the DRG greatly diminishes the hypoxic ventilatory response in rats (Cheng et al., 2002). The NTS is also involved in cardiovascular reflexes and contributes to cardiorespiratory coupling. A diagrammatic view of the major pontine, medullary, and spinal regions controlling breathing is shown in Figure 1.1.

Rhythm Generation

Respiratory rhythm is generated from bilateral preBötC interneurons in the VRC of the medulla (Gray et al 2001, Gray et al., 1999, Smith et al 1991). Single cell, laser ablation studies demonstrate approximately 80% of the 700 preBötC neurons are necessary for rhythm generation (Hayes et al., 2012). These cells are networked with nearby respiratory-related medullary regions and work together to produce coordinated, rhythmic output to premotor neurons, which relay signals to respiratory motor neurons and the muscles responsible for breathing. Despite significant advances in the last 30 years, the precise cellular mechanisms underlying rhythm generation remain unclear. Proposed mechanisms include the pacemaker hypothesis (Rekling and Feldman, 1998), group pacemaker hypothesis (Feldman and Del Negro, 2006), and burstlet hypothesis (Feldman and Kam, 2015).

The pacemaker hypothesis posits that a group of synaptically connected pacemaker neurons independently generate rhythm and is modulated by other neural inputs from the network (Rekling and Feldman, 1998). In support of this theory, there are

two types of endogenously bursting pacemaker neurons identified in the preBötC. However, these intrinsic pacemaker cells are not required for respiratory rhythm generation in all conditions (Del Negro et al., 2002; Feldman et al., 2013; Pace et al., 2007; Paton et al., 2006; Peña et al., 2004). It is likely that in different *in vitro* experimental preparations, including either more or less respiratory circuitry, each region contributes to distinct breathing patterns such as sighs, gasps, and eupenic breathing (Peña et al., 2004)

The group pacemaker hypothesis suggests that rhythm is generated through emergent network properties (Feldman and Del Negro, 2006), in contrast to rhythm being driven by groups of intrinsically rhythmic neurons. While the network contains cells capable of endogenous bursting, they are not necessary for rhythmic respiratory motor activity. The network contains synaptically coupled excitatory neurons which provide positive feedback to excite each other. Excitatory inward currents amplify this feedback and drive high frequency bursting activity (Feldman and Del Negro, 2006). The ability for emergent bursting from synaptically coupled excitatory neurons can be easily modeled as two synaptically coupled leaky, integrate-and-fire neurons (Rubin et al., 2009). These emergent bursting properties, because they are driven by positive feedback between excitatory cells, require activity dependent, inhibitory outward currents to depress their activity (Rubin et al., 2009). Additionally, synaptic depression between preBötC interneurons occurs during physiologically relevant firing patterns and could also contribute to deactivation of group pacemaker activity (Kottick and Del Negro, 2015). *In vivo*, this likely occurs through synaptic inhibition, though inhibition is not necessary for rhythm generation (Feldman and Del Negro, 2006).

More recent models focus on the properties of microcircuits within the preBötC to understand how groups of neurons contribute to the entire circuit output (Feldman and Kam, 2015). The burstlet hypothesis suggests a small population (a microcircuit) of preBötC cells can generate small burstlets, which recruit larger populations of neurons to create a full population burst (Feldman and Kam, 2015). Burstlets occur rhythmically at the shortest inter-burst interval and are thought to set the rhythm of respiratory networks. Specifically, when the excitability of the network is decreased experimentally, inspiratory bursts are sometimes absent, but burstlets persist at the same rhythm (Kam et al., 2013a). This slowing of full population bursts is described as "quantal" slowing because the periods between full population bursts are integer (or quantal) multiples of the basal burstlet rhythm (Kam et al., 2013a). A recent study, using light-activated release of glutamate, showed activation of only nine randomly selected preBötC neurons reproducibly triggered a burst triggering a XII nerve burst (Kam et al., 2013b). As preBötC neurons are a heterogenous group of excitatory and inhibitory neurons with pre-inspiratory, inspiratory, and post-inspiratory firing patters, the random selection of cells in this study suggests a smaller microcircuit is sufficient to induce burstlets driving breathing rhythm. Thus, it is possible a small subset of preBötC neurons create burstlets and are the source of respiratory rhythm generation.

Taken together, it is likely there are overlapping mechanisms within the respiratory network producing rhythmic breathing-related activity. Redundancy of these mechanisms is beneficial because it makes respiratory output robust in the face of potential insults. It also has made the search for the smallest necessary unit of rhythm generation difficult. Different preparations at different ages and in different states may

rely on different rhythm generating mechanisms. For example, as mentioned above, some endogenous rhythmic bursting mechanisms are necessary for gasping *in situ*, but not eupneic respiratory output (Paton et al., 2006). Therefore, the mechanisms responsible for respiratory rhythm generation may change under different conditions making them difficult to fully elucidate.

Though the preBötC is the accepted kernel of respiratory rhythm generation, there are at least two other distinct rhythmogenic regions in the medulla involved in rhythm generation. The parafacial respiratory group/retrotrapezoid nucleus (pFRG/RTN) is the most rostral component of the VRC, contains endogenous pacemaker neurons, and can fire before and drive preBötC rhythm early in development (Onimaru and Homma, 2003). The pFRG is important early in life for driving inspiratory rhythm as it is hypothesized to maintain breathing shortly after birth when the preBötC is inhibited by an endogenous opioid surge (Jacquin et al., 1996). Additionally, these two synchronous pacemakers in the developing respiratory network create the conditions required for quantal slowing of breathing. This occurs when the preBötC is inhibited by opioids and the pFRG rhythm maintains the rhythm of breathing, but transmission failure through the preBötC leads to reductions in inter-burst intervals in predictable integers of the basal frequency (Mellen et al., 2003). Importantly, this phenomenon demonstrates the interactions between these two oscillators (Wittenmeir et al., 2008). However, the pFRG/RTN is only involved in inspiratory rhythm generation early in life (Janczewski and Feldman, 2006). Later in adolescence, the pFRG/RTN shifts to predominantly driving expiratory motor output during exercise or hypercapnia (Huckstepp et al., 2016a, 2018; Leirão et al., 2017).

A separate, rhythmic post-inspiratory oscillator has been described dorsal and caudal to preBötC called post-inspiratory complex (PICO) (Anderson et al., 2016). PICO is an excitatory network thought to regulate the post-inspiratory phase of breathing and is autonomously rhythm generating in phase with respiratory motor output (Anderson et al., 2016). This discovery suggests the possibility that three distinct oscillatory regions control separate phases of the respiratory cycle: preBötC for inspiratory rhythm, PICO for post-inspiratory rhythm, and pFRG for expiratory rhythm. However, it remains unclear if the role of PICO changes during early post-natal development similar to the pFRG.

Feedback Control Mechanisms

The rhythmic respiratory control centers also must be capable of considerable adaptability to compensate for changes in activity and environment, and thus respond to inputs to maintain homeostasis. Afferent inputs from central and peripheral chemoreceptors mediate the hypoxic and hypercapnic ventilatory responses to maintain appropriate blood gasses, and vagal inputs from the lung relay information about lung stretch and irritation (Feldman, 1986).

The hypoxic ventilatory response (HVR) is a triphasic response to reflexively ensure adequate oxygen delivery. Peripheral chemoreceptors located in the carotid body rapidly detect changes in arterial oxygen (PaO_2) and are responsible for the initial rapid phase of hypoxic ventilatory response. The initial phase consists of a rapid increase in breathing frequency and increasing tidal volume within the first two minutes of hypoxic exposure (Powell et al., 1998). If hypoxia occurs for more and a few minutes, the

secondary phase of the HVR is evident as a decrease and eventual plateau of ventilation termed hypoxic ventilatory depression (HVD) (Powell et al., 1998). This secondary depression is primarily mediated by changes in frequency (Powell et al., 1998) and may be attributed to central mechanisms (Gourine and Funk, 2017). Lasting hypoxic exposure for days leads to ventilatory acclimatization, the third phase of the HVR (Powell et al., 1998).

The HVR develops significantly during the early post-natal period. Very young neonatal animals have significant HVD which depresses breathing below baseline levels within a few minutes of exposure to hypoxia (Liu et al., 2006; Moss et al., 1987; Rajani et al., 2018; Thoby-brisson and Greer, 2010; Wong-Riley and Liu, 2008). During the first two weeks of life, HVD becomes less severe, such that hypoxic responses remain above baseline ventilation levels and animals can more adequately maintain oxygen saturation. The precise mechanisms underlying this change in the HVD remains unclear, but it likely reflects central shifts in neurochemical signaling. Shifting adenosine receptor expression and alterations in the expression of glutamate receptors contribute to HVD (Funk, 2013). Additionally, changes in hypoxia induced hypometabolism may contribute to the development of the HVR (Liu et al., 2006). The significant HVD in young animals makes them more vulnerable to hypoxia. Thus, appropriate development of the HVR after birth is critical.

Central chemoreceptors sense CO_2 indirectly through changes in local pH (Guyenet and Bayliss, 2015). CO_2 is able to cross the blood-brain barrier and is converted to changes in pH by reaction with carbonic acid. pH sensitive neurons in the ventrolateral medulla, RTN, VRG, Locus coeruleus, medullary raphe, and NTS all contribute to

central chemoreception (Guyenet et al., 2008; Nattie, 1999). However, the RTN is more sensitive to physiological ranges of pH and contributes to the majority of the hypercapnic ventilatory response making it a strong candidate for physiological control of $PaCO_2$ (reviewed in Guyenet and Bayliss, 2015). Further, some medullary regions may increase the gain of pH sensitivity in other regions and together multiple regions may have cumulative effects on breathing under physiological conditions (Nattie and Li, 2009). It is likely that overlapping pH sensitive mechanisms in the medulla work together to mediate physiological responses to changes in $PaCO_2$, and that the overlapping mechanisms add malleability and create a more robust network response.

The carotid bodies, which primarily sense PaO_2, also contribute to the HCVR. Thus, not all of the HCVR is due to central mechanisms. Remarkable studies in dogs demonstrate locally perfused carotid bodies determine the pH sensitivity of central responses to increasing $PaCO_2$ (Blain et al., 2010; Smith et al., 2015). A hypercapnic carotid body can double or triple the central response to $PaCO_2$ (Blain et al., 2010; Smith et al., 2015). Thus, cumulative effects of simultaneous activation of distinct CO_2 sensing regions, both peripheral and central, are important for the ventilatory response to changing CO_2/pH.

Respiratory Motor Plasticity

Respiratory plasticity is a fundamental feature of the respiratory control circuitry. Plasticity, defined as a change in future behavior based on prior experience (Mitchell and Johnson, 2003), can occur at any point within the respiratory circuitry, including the carotid bodies, integration and rhythm generating sites within the medulla, and motor

pools innervating respiratory muscles. Respiratory plasticity is thought to be critical for maintaining adequate breathing in the face of lung and neural control disorders by affording adaptability of the respiratory system to changing internal and external environments (Fuller and Mitchell, 2017; Mitchell and Johnson, 2003).

The most well-studied model of respiratory plasticity is phrenic long-term facilitation (pLTF), a long-term increase in phrenic burst amplitude induced by acute intermittent hypoxia (AIH, Fig. 1.2). pLTF occurs in or around phrenic motor neurons in the cervical spinal cord (Baker-Herman et al., 2004; Dale et al., 2017; Devinney et al., 2015a) and is induced by at least two distinct cellular signaling pathways: the Q-pathway and the S-pathway (Dale-Nagle et al., 2010) (Fig. 1.3). The Q-pathway is serotonin-dependent and induced by moderate AIH (mAIH, 3x5 minute hypoxic episodes, PaO_2 35-45 mmHg) (Baker-Herman and Mitchell, 2002), while the S-pathway involves activation of adenosine receptors and is induced by severe AIH (sAIH, PaO_2 25-35 mmHg) (Nichols et al., 2012) (Fig. 1.3). The cellular mechanisms of Q- and S-pathway plasticity are distinct (Turner et al., 2018), but evoke a similar lasting facilitation of phrenic motor output. The mechanisms leading to prolonged phrenic motor output after AIH (Fig. 1.1) are hypothesized to involve phosphorylation of phrenic motor neuron glutamate receptors (Turner et al., 2018). In support of this hypothesis, multiple reports have demonstrated that a NMDA receptor antagonist prevents development of pLTF after mAIH (McGuire et al., 2005, 2008). Furthermore, after S-pathway activation with intermittent adenosine receptor agonism, NMDA receptor antagonism inhibits the development of pLTF (Golder, 2009), suggesting Q-pathway and S-pathway-evoked plasticity converge by regulating NMDA receptors to elicit plasticity.

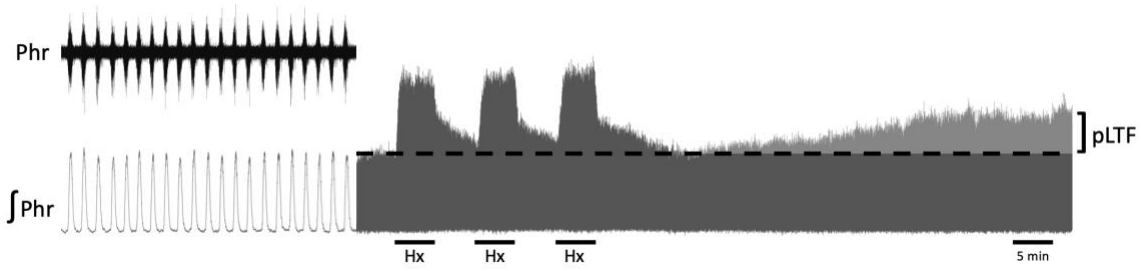

Figure 1.2. Acute intermittent hypoxia elicits long-term facilitation of phrenic burst amplitude. Integrated phrenic (∫ Phr) nerve recording from an anesthetized, ventilated, paralyzed, and vagotomized adult rat. Phrenic long-term facilitation (pLTF) is evident as the progressive increase in phrenic burst amplitude 60 minutes after acute intermittent hypoxia (AIH, 3, 5-minute bouts of hypoxia). pLTF is quantified as the percent change of phrenic burst amplitude from baseline (dashed line) 60 minutes after AIH.

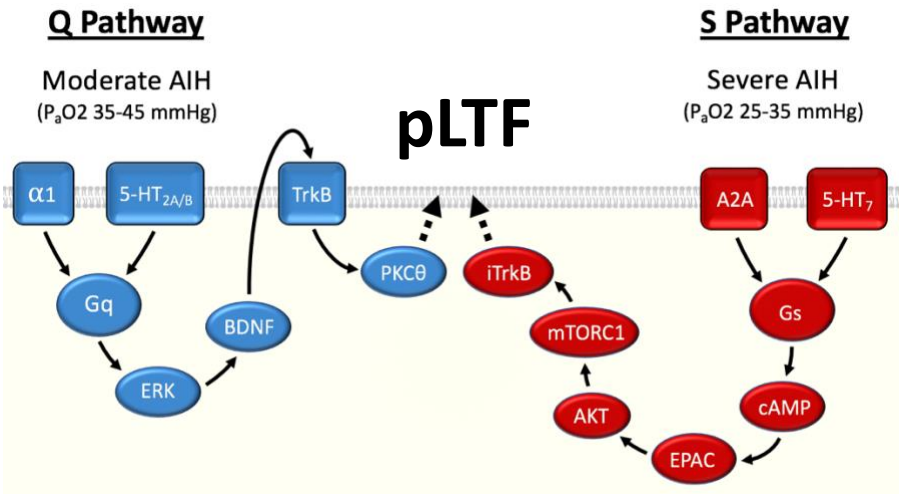

Figure 1.3. Distinct cellular pathways induce pLTF after either moderate or severe AIH. The working mechanistic model of pLTF in phrenic motor neurons. Moderate AIH activates G_q-coupled receptors leading to Q-pathway-evoked pLTF, while severe AIH activates a G_s-coupled S-pathway-evoked pLTF. (Adapted from Turner et al., 2018).

In disease and injuries compromising ventilation, plasticity within the respiratory system is thought to compensate and stabilize breathing (Fuller and Mitchell, 2017). However, AIH-induced motor plasticity is not limited to respiratory-related motor output. AIH facilitates motor output from all studied spinal motor pools (Baker-Herman and

Mitchell, 2002; Christiansen et al., 2018; Hayes et al., 2014; Mitchell and Johnson, 2003; Trumbower et al., 2017), suggesting it has significant therapeutic value for patients with motor limitations. In fact, multiple clinical trials have now demonstrated AIH-induced improvements in upper and lower limb motor function in patients with incomplete spinal cord injuries (Hayes et al., 2014; Trumbower et al., 2012, 2017). Therefore, understanding the mechanisms underlying AIH-induced motor plasticity may have broader clinical relevance beyond the neural control of breathing.

Inflammation

Undermining the respiratory control system poses a significant threat to maintaining homeostasis. Multiple studies have examined how pharmacological agents (like opioids) or diseases (like sleep apnea) cause dysfunction in the respiratory system, but more recent studies have begun to investigate the interplay between the immune system and the respiratory system. A common attribute of almost all diseases and disorders, respiratory or other, is inflammation. Increasing evidence supports a dynamic role for inflammation in promoting or inhibiting different forms of neuroplasticity (Di Filippo et al., 2008; Liu et al., 2011; Stemkowski and Smith, 2012; Watkins and Maier, 2002; Woolf and Salter, 2000). Since the therapeutic benefits of AIH-induced motor plasticity may be impaired by underlying inflammation, many investigations into the role of inflammation in the respiratory system have focused on plasticity. Understanding how inflammation alters the respiratory system is vital for development of better therapeutic interventions to promote breathing and to utilize plasticity as a clinical treatment.

Models of Systemic Inflammation

Since LPS activates endogenous inflammatory pathways and much is known about its signaling cascade, it serves as a relevant ligand to induce systemic inflammation experimentally. LPS is a component of gram-negative bacterial cell walls and activates the innate immune response via Toll-like Receptor 4 (TLR4). TLR4 activation induces pro-inflammatory gene expression through activation of MAPKs JNK, ERK, p38 MAPK, and the transcription factor NF-κB (Kuzmich et al., 2017). Many endogenous ligands also activate TLR4 including proteins released from dead or dying cells, heat shock proteins, and modified low-density lipoproteins (Erridge, 2010; Lehnardt et al., 2008; Ohashi et al., 2000). As both bacterial and endogenous activation of TLR4 are possible sources of inflammation throughout our lives, LPS serves as a relevant model to understand the impact of inflammation.

Viral infections are also common models of inflammation and induce similar inflammatory signaling pathways to LPS-induced inflammation. RNA viruses induce inflammation through activation of TLR3, TLR7, and TLR8 (Carrithers, 2014). The most common model of viral infections is the viral mimetic, polyinosinic:polycytidylic acid (polyIC), a synthetic dual-stranded RNA (dsRNA) molecule activating TLR3. TLR3 activation elicits overlapping inflammatory profiles to other TLRs, including activation of NF-kB and MAPKs, and increased pro-inflammatory gene expression (Konat et al., 2009; Krasowska-Zoladek et al., 2007; Yamato et al., 2014). However, the inflammatory cascade and gene expression profile from viral inflammation is distinct from bacterial inflammation (Hu et al., 2013). Furthermore, polyIC can compromise the blood-brain barrier (Wang et al., 2004), though other mechanisms of peripheral to central

inflammatory transmission are similar between polyIC and LPS. Importantly, polyIC-induced inflammation induces temporally slower onset of inflammatory genes in the CNS compared to LPS (Konat et al., 2009; Krasowska-Zoladek et al., 2007; Yamato et al., 2014), and therefore, it has the potential to have different effects on pLTF. Overall, both bacterial and viral-induced inflammation are common (Obasi et al., 2014) and elicit overlapping, but distinct, inflammatory profiles.

CNS Inflammation

The mechanisms of peripheral to CNS transmission of inflammation are still an active area of investigation, but at least four possible routes of inflammatory transmission have been demonstrated. Peripheral immune cells and pro-inflammatory molecules can cross the BBB under certain conditions or induce inflammatory signaling within the CNS via cross-talk between endothelial cells, neurons, and glia (Lampron et al., 2013). Circumventricular organs also play a role in CNS responses to inflammation by allowing either LPS or cytokines to interact directly with neurons and glia. The area postrema contains cells activated by LPS, TNFα, and IL-1β (Wuchert et al., 2008; Wuchert et al., 2009). However, the capacity for LPS penetration across the BBB is low (Banks and Robinson, 2010), yet even low-dose LPS (intraperitoneal or intratracheal) is sufficient to induce inflammatory gene and protein expression in the CNS without LPS crossing the BBB (Balan et al., 2011; Banks and Robinson, 2010; Laye et al., 1995). Vagal afferents moderate communication of low-level systemic inflammation to the CNS, since vagotomy eliminates the febrile response associated with sickness and inflammation after very low doses of LPS (1 μg/kg), but not higher doses. At higher doses, there are likely

alternative routes for transmission and induction of CNS inflammation (Romanovsky et al., 1997), as evident by subdiaphragmatic vagotomy inhibiting CNS gene expression of IL-1β after i.p. LPS (Laye et al., 1995), and cervical vagotomy inhibiting medullary IL-1β after intratracheal LPS (Balan et al., 2011).

Therefore, there is considerable communication between the peripheral and central immune responses. In the experiments below, I use bacterial and viral inflammatory stimuli to induce systemic inflammatory responses, which are then transmitted to the CNS to mediate neurophysiological effects. These paradigms represent physiologically relevant stimuli for inducing central inflammatory responses compared to direct immune stimulation in the CNS, which is rare. Additionally, the doses of inflammation used in the following experiments are relatively low in most cases and do not evoke sepsis. Therefore, the models of inflammation used here are relevant for understanding low-level inflammation, such as would be expected in diseases and injuries.

Inflammation and Respiratory Motor Plasticity

Q-pathway-evoked respiratory motor plasticity is exquisitely sensitive to even low-levels of inflammation. In adults, Q-pathway-evoked plasticity is undermined by low levels of acute, systemic inflammation induced by a TLR4 agonist (lipopolysaccharide, LPS) (Huxtable et al., 2011; Vinit et al., 2011) or 8 hours of intermittent hypoxia (Huxtable et al., 2015, 2017) and restored by the non-steroidal anti-inflammatory, ketoprofen (Huxtable et al., 2013, 2015). On the contrary, S-pathway-evoked adult respiratory motor plasticity is inflammation resistant (Agosto-Marlin et al., 2017), and

therefore it has the potential to serve as a "backup" pathway to preserve plasticity after inflammation.

Since AIH-induced plasticity is being translated to clinical populations (e.g. after spinal cord injury) (Hayes et al., 2014; Trumbower et al., 2012, 2017) with low-levels of systemic/neuroinflammation, interest in the impact of inflammation on motor plasticity is growing. Previous studies on inflammation-induced impairments in pLTF have focused on lipopolysaccharide (LPS, bacterial induced-inflammation) (Huxtable et al., 2013; Vinit et al., 2011) or simulated sleep apnea induced by nocturnal intermittent hypoxia (Huxtable et al., 2015, 2017). LPS induces systemic inflammation, increases brain inflammatory cytokines, and undermines pLTF within 3 hours (Huxtable et al., 2013), while nocturnal intermittent hypoxia is a relevant physiological perturbation (Huxtable et al., 2015). However, the signaling mechanisms by which inflammation undermines respiratory motor plasticity are not yet fully understood. The anti-inflammatory, ketoprofen, restores Q-pathway-evoked pLTF after LPS or nocturnal intermittent hypoxia (Huxtable et al., 2013, 2015). Ketoprofen inhibits both COX and NF-κB (Cashman, 1996; Yin et al., 1998). However, as COX inhibition alone does not restore Q-pathway-evoked pLTF after inflammation, the restoration of pLTF from ketoprofen is likely due to NF-κB inhibition (Huxtable et al., 2017). Additionally, after nocturnal intermittent hypoxia, spinal p38-MAPK inhibition restores pLTF (Huxtable et al., 2015). Thus, inflammation is responsible for impairing pLTF and activates inflammatory signaling via p38 MAPK within phrenic motor neurons. However, the inflammatory signaling molecules responsible for inducing inflammation in the phrenic motor pool remain to be elucidated and will be the topic of my first aim.

Though studies to date have focused on LPS or intermittent-hypoxia induced impairments in pLTF, viral infections are also common (Obasi et al., 2014) and induce an overlapping, but unique, inflammatory profile. As inflammation comes from diverse stimuli during our lives, understanding the effects of viral-induced inflammation on respiratory motor plasticity broaden our understanding of the impact of inflammation on respiratory control. Additionally, while the inflammatory impairment of Q-pathway-evoked plasticity has been confirmed in multiple models, S-pathway-evoked plasticity has only been studied after LPS-induced inflammation (Agosto-Marlin et al., 2017, 2018). Therefore, my second aim will investigate the effects of viral-induced inflammation on Q- and S-pathway-evoked pLTF. Because S-pathway plasticity may serve important roles as a backup pathway during inflammation, this study will significantly contribute to our understanding of how respiratory motor plasticity manifests during inflammation and potential strategies for therapeutic use.

Lasting Consequences of Neonatal Inflammation

We are beginning to understand the potential for long-term physiological consequences after early life inflammation, including impairments of adult immune function (Bilbo et al., 2010; Mouihate et al., 2010; Spencer et al., 2011), adult stress reactivity (Grace et al., 2014; Shanks et al., 2000; Wang et al., 2013), adult learning and hippocampal plasticity (Bilbo, 2005; Bilbo et al., 2006), age-related cognitive decline (Bilbo, 2010), and increased risk of neuropsychiatric disorders (Hornig et al., 1999; Rantakallio et al., 1997). However, despite the prevalence of early life inflammation (Stoll

et al., 2002, 2004), little is known about the long-lasting consequences of neonatal inflammation on adult neurorespiratory control.

At birth, neonates transition from a sterile maternal environment into an environment filled with pathogens and inflammatory stimuli and must simultaneously begin robust, rhythmic breathing. Respiratory problems represent a significant clinical problem for neonatologists (Martin et al., 2012), especially in preterm infants where breathing is unstable (Poets et al., 1994; Poets and Southall, 1994) and infections are common (Stoll et al., 2002, 2004). Further, inflammation appears to augment respiratory dysfunction in neonates, whereby inflammation depresses hypoxic responses (Olsson et al., 2003; Rourke et al., 2016) and induces recurrent apneas (Hofstetter et al., 2007). Despite the prevalence of early life inflammation, little is known about the long-lasting consequences of neonatal inflammation on adult neurorespiratory control. Furthermore, few studies have investigated sex-differences in pLTF (Behan et al., 2002; Dougherty et al., 2017) and we know even less about sex-differences in respiratory control in response to inflammation. However, there are sex differences in inflammatory responses whereby females are typically protected from some negative consequences of inflammation due to more rapid resolution of inflammation (Rathod et al., 2017) and the protective effects of female sex hormones (Bouman et al., 2005; Rathod et al., 2017). Furthermore, females are less susceptible to long-term effects of neonatal inflammation on adult behaviors (Kentner et al., 2010). Given the profound effects of neonatal inflammation on other physiological systems, the third aim of this dissertation will examine the hypothesis that neonatal inflammation induces lasting impairments in respiratory motor plasticity in adult male and female rats.

Opioids

Opioids are among the most potent analgesics, yet their use is limited by significant side-effects such as sedation, dizziness, nausea, constipation, itching, allodynia, physical dependence, tolerance, and respiratory depression (Benyamin et al., 2008). The misuse of opioids has become a national and public health crisis with more than 118 US residents dying from opioid overdoses daily in 2016, representing a 27% increase from the previous year and accounting for two thirds of drug-overdose deaths in the USA (CDC WONDER, 2018). Not only is this a major public health concern, but it carries a significant economic burden, estimated to be >$78.5 billion in 2013 (Florence et al., 2016).

Repeated opioid use induces tolerance leading to the use of higher opioid doses which cause profound respiratory depression, thought to be the most life-threatening side-effect of opioids (reviewed in Hutchinson et al., 2011). Since the respiratory control system does not develop opioid-induced tolerance (Emery et al., 2016; Levitt and Williams, 2018), respiratory depression is a potentially lethal risk of opioid misuse.

Opioids and Respiratory Rhythm Generation

The physiological effects of opioids are complicated by opioid receptor (OR) subtypes, interactions with other non-opioid receptors, divergent signal transduction cascades, and interactions between opioids and inflammatory signaling (Hutchinson et al., 2009). Three main types of ORs (μ, δ, and κ) are largely responsible for mediating the effects of opioids, and a less well understood fourth type (nociceptin) (Hutchinson et

al., 2011). ORs are primarily inhibitory G_i-protein-coupled receptors hyperpolarizing neurons through activating protein kinase A (PKA), inhibiting voltage-dependent Ca^{2+} channels, reducing Na^+ conductance, and activating inward-rectifying K^+ channels (Montandon et al., 2011, 2016). Within the respiratory control circuitry, MOR are expressed in the ventral respiratory column with the highest density of receptor expression near the preBötC and very little receptor expression in the more rostral pFRG/RTN (Kennedy, 2014). *In vitro* and *in vivo* data from rodents demonstrate the major effect of opioids is to depress breathing through the preBötC (Montandon et al., 2011), while the pFRG/RTN is relatively opioid insensitive (Mellen et al., 2003; Takeda et al., 2001). The organization of these two coupled oscillators and their differential sensitivity to opioids creates the conditions for opioid-induced quantal slowing of respiratory rhythm. Quantal slowing indicates a reduction in frequency at integer multiples of the control period. The proposed mechanism for this effect is the opioid-insensitive pFRG/RTN continues to oscillate at the control period, but there is transmission failure through the inhibited preBötC, causing some breaths to be skipped (Mellen et al., 2003). The appearance of quantal slowing demonstrates preBötC and pFRG activities are coordinated and suggests the pFRG could act as a backup in the presence of opioids to promote breathing.

Perinatal Opioids and Respiratory Control

Recently, there has been a disproportionate rise in opioid use during pregnancy (Epstein et al., 2013; Krans et al., 2015; Stover and Davis, 2015). Maternal opioid use leads to diverse negative outcomes for the developing infant, including; irritability,

nystagmus, sleep disturbances, respiratory deficits, and even death (McQueen and Murphy-Oikonen, 2016). Clinically these infants (55-94%, Finnegan *et al.*, 1975; Hudak *et al.*, 2012) are diagnosed with neonatal abstinence syndrome (NAS), described as dysfunction in the central and autonomic nervous systems, and gastrointestinal system, though the pathophysiology and treatments for these infants remains unclear. The increase maternal use of opioids and risk of NAS leads to a significant need to develop better treatments for neonates born from mothers using opioids (Kraft et al., 2016). However, discrepancies are abundant regarding how neonates with NAS should be treated clinically (McQueen and Murphy-Oikonen, 2016). Current treatments for NAS include methadone, morphine, or buprenorphrine (Kocherlakota, 2014); however, ideal dosing guidelines are not clear (McQueen and Murphy-Oikonen, 2016). Overall, as maternal opioid use increases, understanding the impacts of gestational opioids and how to best treat infants represents a critical clinical need (McQueen and Murphy-Oikonen, 2016).

As maternal opioids cross the placenta (Hauser and Knapp, 2018; Kopecky et al., 1999) and suppress respiratory rhythm generation in the preBötC, they may inhibit appropriate development of the respiratory control system. The respiratory system must be fully functional at birth and capable of robust, rhythmic breathing. Rhythmic neural activity, initiating at the preBötzinger complex (preBötC, the kernel for respiratory rhythmogenesis) is required for adequate development of neural circuitry, respiratory muscles, and the lungs (Greer, 2012; Pagliardini et al., 2003). In rats, development of respiratory neural networks begins around embryonic day 17 (E17) and continues until birth (Pagliardini *et al.*, 2003). As soon as preBötC cells migrate to their final location in

the medulla, they begin rhythmic activity which activates respiratory motor neurons and drive fetal breathing movements (Greer, 2012; Pagliardini et al., 2003). Importantly, the preBötC is exceptionally sensitive to opioids and is responsible for many of the respiratory depressant effects of neonatal opioids (Montandon et al., 2011, 2016; Stucke et al., 2015). Therefore, in the presence of prenatal opioids, the respiratory control networks need to compensate to maintain adequate development and appropriate respiratory function at birth (Gourévitch *et al.*, 2017). However, controlled studies on neonatal breathing after maternal opioids are extremely limited. One study demonstrated medullary respiratory network reorganization after maternal opioid exposure in neonatal rats (Gourévitch *et al.*, 2017) and another study in guinea pigs demonstrates hypercapnic ventilatory responses are enhanced in pups exposed to prenatal opioids (Nettleton et al., 2008), suggesting changes in chemosensitivity after maternal opioids. To our knowledge, the study presented in Chapter V will be the first investigating changes in neonatal breathing after maternal opioid use in rats. Additionally, since NAS infants are typically treated with exogenous opioids to alleviate withdrawal symptoms (Pryor et al., 2017), the final aim of this dissertation will also assess neonatal ventilatory responses after maternal opioid use and repeated, acute, neonatal methadone exposure.

As maternal opioid use increases, understanding the acute and long-term effects will be critical to effectively treating neonates exposed to perinatal opioids. Additionally, understanding how maternal opioid use alters the respiratory effects of acute opioid exposure in neonates will contribute to our understanding of how to best treat neonates to alleviate symptoms of NAS without severe respiratory disturbance.

Specific Aims

This dissertation focuses on furthering our understanding of how inflammation or opioids undermine the neurorespiratory control system. These studies provide novel findings on the mechanisms of inflammatory impairment of respiratory plasticity and how maternal opioids impact neonatal breathing. The first aim will focus on the effects of acute inflammation and the mechanisms by which they impair adult respiratory plasticity. These mechanistic insights may help in developing clinical strategies to promote plasticity after inflammation. Next, I compare the generalizability of inflammation-induced impairments in respiratory plasticity between bacterial and viral sources of inflammation. These studies suggest distinct inflammatory stimuli can impair respiratory plasticity and suggest inflammation, regardless of the source, could limit respiratory control mechanisms. The remainder of the dissertation focuses on perinatal challenges when the respiratory system is vulnerable and relatively unstable. Chapter IV will describe the lasting effects of a single bout of early life inflammation on adult respiratory motor plasticity and broadens our understanding of motor plasticity to both males and female rats. Chapter V of this dissertation investigates the respiratory consequences of perinatal opioids to better understand how maternal opioid use alters the neurorespiratory control system and how neonatal opioids affect breathing after *in utero* exposure. These studies lay a solid foundation for future work understanding and treating neonates exposed to *in utero* methadone.

CHAPTER II

INTERLEUKIN-1 SIGNALING AFTER ACUTE, SYSTEMIC INFLAMMATION UNDERMINES ADULT RESPIRATORY MOTOR PLASTICITY

This chapter includes co-authored material previously published in the *Journal of Applied Physiology* (Hocker and Huxtable 2018). I designed and implemented the experiments, collected and analyzed data, and wrote the manuscript. Dr. Adrianne Huxtable designed, contributed to writing, provided guidance and editorial assistance.

Introduction

Our understanding of how systemic inflammation alters CNS function has accelerated with the identification of peripheral cytokines inducing CNS inflammation by crossing the blood brain barrier, entering the CNS at circumventricular organs, activating vagal afferents (Hosoi et al., 2000; Laye et al., 1995), or activating blood brain barrier endothelial cells and glia (Ching et al., 2007; Iwase et al., 2000; Quan et al., 2003). In turn, this peripheral to central inflammatory signaling alters CNS function by modulating glia (Liddelow et al., 2017) and significantly affecting neuroplasticity (Di Filippo et al., 2008). The inflammatory deficits in plasticity can limit neural control mechanisms and impair physiological regulatory processes.

A complicated relationship exists between inflammatory signaling and neuroplasticity. Inflammatory signaling in the CNS promotes and inhibits distinct forms of neuroplasticity in different CNS regions through the actions of the interleukin-1 (IL-1) signaling cascade. CNS IL-1β and its corresponding IL-1 receptor (IL-1R) are upregulated after systemic inflammation induced experimentally by lipopolysaccharide

(LPS) (Di Filippo et al., 2008; Huxtable et al., 2013; Turrin et al., 2001). IL-1β is sufficient to inhibit hippocampal-dependent memory formation and long-term potentiation, a form of plasticity important for learning and memory formation (Katsuki et al., 1990). However, a genetic knockout of the IL-1R undermines hippocampal-dependent memory formation and abolishes plasticity in the form of long-term potentiation (Avital et al., 2003; Di Filippo et al., 2013; Schneider et al., 1998), demonstrating IL-1 signaling both contributes to and undermines hippocampal plasticity. Conversely, spinal pain hypersensitivity, a form of neuroplasticity in the spinal dorsal horn, is induced by inflammatory stimuli involving IL-1R activation (Cunha et al., 2008; Maier et al., 1993; Zhang et al., 2008). Thus, IL-1β and IL-1Rs have complicated effects on neuroplasticity, whereby IL-1R signaling can either promote or inhibit plasticity depending where in the CNS region plasticity is occurring.

The respiratory control system, like other CNS regions, undergoes plasticity to confer stability and adaptability to respiratory output (Devinney et al., 2015b; Mitchell and Johnson, 2003). Phrenic long-term facilitation (pLTF) is a frequently studied model of neuroplasticity in the respiratory control system (Mitchell and Johnson, 2003). pLTF is induced by acute intermittent hypoxia (AIH: three 5-min hypoxic episodes, separated by 5 min normoxic periods) and manifests as a progressive increase in phrenic nerve burst amplitude following AIH. Previously, we have shown pLTF is abolished by systemic inflammation and IL-1β gene expression increases after systemic inflammation in the cervical spinal cord (Huxtable et al., 2013, 2015). However, the inflammatory signaling cascades involved in undermining plasticity in the respiratory system are not fully understood.

Given the central role for IL-1R signaling in other forms of plasticity and increased IL-1β gene expression in the cervical spinal cord (where purportedly pLTF occurs (Baker-Herman et al., 2004; Dale et al., 2017)) after systemic inflammation, we investigated the necessity and sufficiency of IL-1 signaling to undermine pLTF after systemic inflammation. We demonstrate that IL-1R activation, both systemically and centrally, undermines pLTF after LPS-induced systemic inflammation. Yet, in healthy rats, acute, exogenous IL-1β spinally was not sufficient to undermine pLTF. Overall, our findings further our mechanistic understanding of how plasticity in the neural control of breathing is abolished by systemic inflammation.

Methods

All experiments were approved by the Institutional Animal Care and Use Committee at the University of Oregon and conformed to the policies of the National Institute of Health *Guide for the Care and Use of Laboratory Animals*. Male Sprague Dawley Rats (300-400g; 3-4 months; Envigo Colony 217 and 206) were housed under standard conditions with a 12:12h light/dark cycle with food and water *ad libitum*.

Drugs and Materials

Lipopolysaccharide (LPS; 0111:B4, Sigma Chemical) was dissolved and sonicated in sterile saline to a working concentration of 100 μg/mL given via intraperitoneal (i.p.) injections. The IL-1R antagonist, AF-12198 (Toronto Research Chemicals) was dissolved in 10% ethanol and sterile saline for peripheral injections (0.5 mg/mL) or in fresh artificial cerebrospinal fluid (aCSF; 120mM NaCl, 3mM KCl, 2mM $CaCl_2$, 2mM $MgCl_2$, 23mM $NaHCO_3$, and 10mM glucose) for intrathecal (i.t.) injections

(1 mM). Recombinant rat IL-1β (rIL-1β, BioVision 4130) was dissolved in aCSF for i.t. injections (0.25-10 ng/μL).

Experimental Groups

To investigate the necessity of peripheral IL-1R activation in undermining pLTF, we used the following experimental groups: 1) LPS (100 μg/kg i.p., 24 hours before AIH) + AF-12198 (0.5 mg/kg i.p., 24 hours before AIH) (n = 5); 2) LPS + Vehicle (10% ethanol in sterile saline) (n = 5); 3) Saline (i.p.; LPS Vehicle) + AF-12198 (n = 6); 4) Saline + Vehicle (n = 5); 5) Time control (TC), which consists of rats from each of the previous treatment groups (LPS + AF-12198 (i.p.), n=4; Saline + AF-12198 (i.p.), n=5; LPS + Vehicle (i.p.), n=4; Saline + Vehicle (i.p.) n=4).

To investigate the necessity of spinal IL-1R activation in undermining pLTF after systemic inflammation, we used the following experimental groups: 1) LPS (100 μg/kg i.p., 24 hours before AIH) + AF-12198 (1 mM, 15 μL, i.t., 20 min before AIH) (n = 4); 2) LPS + Vehicle (10% ethanol in sterile saline, i.t.) (n = 5); 3) Saline (i.p.) + AF-12198 (i.t.) (n = 4); 4) Saline + Vehicle (i.t.) (n = 4); 5) TCs, which consist of rats from each of the previous treatment groups (LPS + AF-12198 (i.t.), n=4; Saline + AF-12198 (i.t.), n=3; LPS + Vehicle (i.t.), n=4; Saline + Vehicle (i.t.), n=4).

To investigate the sufficiency of acute, exogenous, spinal rIL-1β to undermine pLTF, we performed a dose-response with exogenous rIL-1β (i.t.) at 1 ng (n = 3), 10 ng (n = 3), 100 ng (n = 4), and 300 ng (n = 4). AIH was performed 20 minutes after spinal rIL-1β injections.

To investigate the effects of acute, exogenous, spinal rIL-1β on phrenic burst facilitation in the absence of AIH, rIL-1β (i.t., 1 ng (n = 3), 10 ng (n = 4), 100 ng(n = 3),

300 ng (n = 3)) was applied over the cervical spinal cord and phrenic neural output monitored over the next 105 minutes.

Electrophysiological studies

Electrophysiological studies have been described in detail previously (Huxtable et al., 2015). Rats were anesthetized with isoflurane, tracheotomized, ventilated (Rat Ventilator, VetEquip®) and bilaterally vagotomized. A venous catheter was placed for drug delivery and fluid replacement, and a femoral arterial catheter was used for arterial blood analysis and monitoring blood pressure. Arterial blood samples were analyzed (PaO_2, $PaCO_2$, pH, base excess; Siemens RAPIDLAB® 248) before AIH, during the first hypoxic response, and 15, 30 and 60 minutes post-AIH. Temperature was measured with a rectal temperature probe (Kent Scientific Corporation) and maintained between 37 and 38°C with a heated table. Using a dorsal approach, hypoglossal and phrenic nerves were dissected, cut distally, and desheathed. Rats were converted to urethane anesthesia (1.8 g/kg i.v.; Sigma-Aldrich), allowed to stabilize over the next hour, and paralyzed with pancuronium dibromide (1 mg/rat; Selleck Chemicals).

In rats receiving i.t. injections, a laminectomy was performed at cervical vertebrae 2 (C2) and a primed, silicone catheter was inserted two millimeters through a small incision in the dura. The catheter tip extended toward the rostral margin of C4 (Baker-Herman and Mitchell, 2002). AF-12198 (1 mM) or vehicle (aCSF) was injected (15 µL) 20 minutes before AIH. rIL-1β was applied i.t. 20 minutes before the start of AIH at doses of 1ng (4 µL of 0.2 ng/µL), 10ng (10 µL of 1 ng/µL), 100ng (10 µL of 10 ng/µL), and 300ng (30 µL of 10 ng/µL in 10 µL boluses over 3 minutes). In rats receiving rIL-1β (i.t.) but not AIH, all time points were matched with rIL-1β + AIH experiments.

Nerves were bathed in mineral oil and placed on bipolar silver wire electrodes. Raw nerve recordings were amplified (10k), filtered (0.1-5 kHz), integrated (50 ms time constant), and recorded (10 kHz sampling rate) for offline analysis (PowerLab and LabChart 8.0, AD Instruments). Apneic and recruitment CO_2 thresholds were determined by changing inspired CO_2 with continuous end-tidal CO_2 monitoring (Kent Scientific Corporation). End tidal CO_2 was set 2 mmHg above the recruitment threshold and arterial blood samples were used to establish baseline $PaCO_2$, which was maintained within 1.5 mmHg of the baseline value throughout. Blood volume and base excess were maintained (±3 MEq/L) by continuous infusion (1-3 mL/h i.v.) of hetastarch (0.3%) and sodium bicarbonate (0.99%) in lactated ringers. Experiments were excluded if mean arterial pressure deviated more than 20 mmHg from baseline versus 60 minutes after AIH.

All rats (except for TC rats) received three, 5 minute bouts of hypoxia (~10.5% O_2, PaO_2 35-45 mmHg) separated by 5 minutes of normoxia. The average amplitude and frequency of 30 consecutive integrated phrenic bursts were analyzed at baseline, during the first acute hypoxic response, and 15, 30, and 60 minutes after AIH and made relative to baseline amplitude. Physiological variables and phrenic nerve activity data for each experimental group were compared using two-way, repeated measures ANOVA with Fisher LSD post hoc tests. Time control data were grouped for each experimental design since no significant differences between experimental groups were found (ANOVA RM, Fisher LSD post-hoc). Mean arterial pressure is reported from baseline, the end of the final hypoxic exposure, and 60 minutes after AIH. Acute hypoxic responses were compared using an ANOVA with Fisher LSD post hoc test. Values are means ± SD.

Results

Peripheral IL-1R activation is necessary for undermining pLTF after peripheral LPS.

Saline + AF-12198 Vehicle (i.p.) and saline + AF-12198 (i.p.) rats exhibited pLTF 60 minutes after AIH (57 ± 25%, $p < 0.0001$, n=6; 44 ± 14%, $p < 0.0001$, n=5, respectively, Fig. 2.1A and B). As expected (Huxtable et al., 2013), pLTF was eliminated in LPS + Vehicle (i.p.) rats (12 ± 18%, $p < 0.05$, n=6, Fig. 2.1A and B). pLTF was restored by peripheral antagonism of IL-1Rs (LPS ± AF-12198 i.p.; 63 ± 13%, $p < 0.0001$, n=5, Fig. 2.1) and was not evident in any TC groups (-1 ± 9 % $p = 0.24$, n=17). No significant differences in the magnitude of pLTF was evident between LPS + AF-12198 (i.p.) and saline + AF-12198 (i.p.) groups.

The acute hypoxic phrenic response was unaffected by LPS or IL-1R antagonism (Saline + Vehicle (i.p.); 133 ± 39%, LPS + Vehicle (i.p.); 129 ± 49%, Saline + AF-12198 (i.p.); 104 ± 46%, LPS + AF-12198 (i.p.); 129 ± 30%, Fig. 2.1C); no significant differences were present between groups.

LPS caused a small, but significant, increase in baseline phrenic burst frequency compared to saline controls (LPS + Vehicle (i.p.), 51 ± 6 bursts/min; Saline + Vehicle (i.p.), 43 ± 8 bursts/min; $p = 0.021$). However, AF-12198 had no effect on baseline burst frequency between groups (LPS ± AF-12198 (i.p), 49 ± 5 bursts/min; Saline + AF-12198 (i.p.), 45 ± 5 bursts/min). Frequency LTF was not evident 60 minutes post-AIH in any experimental group.

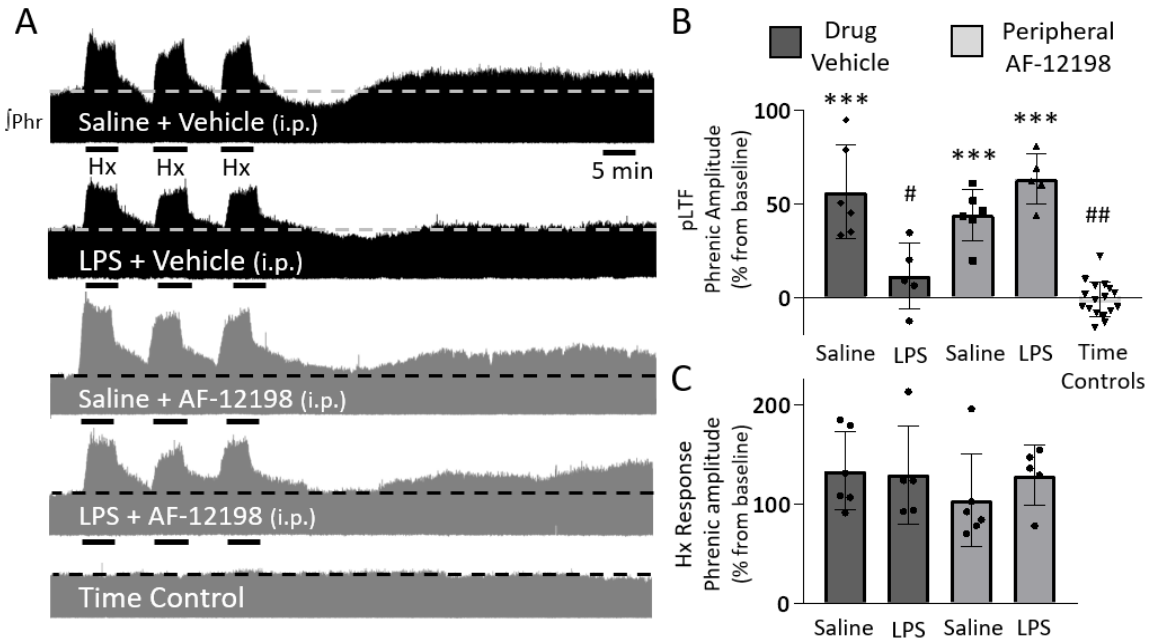

Figure 2.1. Peripheral IL-1R antagonism restores pLTF after systemic inflammation. Representative integrated phrenic neurograms **(A)** for acute intermittent hypoxia (AIH)-treated rats receiving Saline + Vehicle (i.p.), LPS (100 μg/kg; i.p.) + Vehicle (i.p), Saline + AF-12198 (i.p.), LPS + AF-12198 (i.p.), and a time control (no AIH). pLTF is evident as the progressive increase in phrenic nerve amplitude from baseline (dashed line) over 60 minutes following AIH. Group data **(B)** demonstrate pLTF is abolished by LPS (Vehicle treated, dark bars) and restored by peripheral IL-1R antagonism (AF-12198 treated, grey bars). Acute hypoxic responses **(C)** were not significantly altered by any treatment (ANOVA). *** $p < 0.0001$ significant difference in phrenic amplitude from baseline; # different from Saline + Vehicle ($p < 0.001$), Saline + AF-12198 ($p < 0.05$), and LPS + AF-12198 ($p < 0.001$); ## $p < 0.001$ different from Saline + Vehicle, Saline + AF-12198, and LPS + AF-12198 (ANOVA RM, Fisher LSD).

Small variations were evident in physiological parameters (Table 1), but remained within experimental limits. As expected, all experimental groups displayed significantly decreased MAP and PaO_2 during hypoxia (Huxtable et al., 2015). Temperature 60 minutes after AIH was significantly different in Saline + Vehicle and LPS + AF-12198 (i.p.) groups relative to baseline, but remained within experimental limits noted above. Similarly, 60 minutes after AIH, small differences were evident between groups in PaO_2 and pH, but remained within acceptable limits (Table 1).

Table 1.1. Physiological parameters during electrophysiology experiments with systemic AF-12198 (0.5 mg/kg, i.p.) treatment.

Experimental Group		Temperature	PaO_2	$PaCO_2$	pH	MAP
Baseline	AF12198 + LPS	37.4 ± 0.3	315.4 ± 17.3	44.6 ± 3.3	7.34 ± 0.04 [c]	145 ± 5
	AF12198 + Saline	37.6 ± 0.3	281.9 ± 29.1[d]	43.3 ± 3.5	7.34 ± 0.02 [c]	115 ± 13 [d,e]
	Vehicle + LPS	37.5 ± 0.2 [c]	295.8 ± 19.7	43.5 ± 3.3	7.36 ± 0.01	146 ± 7
	Vehicle + Saline	37.7 ± 0.1	295.8 ± 22.9	41.7 ± 2.7	7.38 ± 0.03	126 ± 12
	Grouped TC	37.6 ± 0.3	295.0 ± 24.8	42.4 ± 3.1	7.36 ± 0.03	131 ± 23
Hypoxia	AF12198 + LPS	37.5 ± 0.2	39.9 ± 3.0 [a,b]	44.9 ± 3.2	7.33 ± 0.05 [a,b]	101 ± 24 [a,b]
	AF12198 + Saline	37.4 ± 0.2	40.9 ± 3.7 [a,b]	43.0 ± 3.4	7.34 ± 0.02 [a]	63 ± 12 [a,b,d]
	Vehicle + LPS	37.6 ± 0.2	41.1 ± 1.5 [a,b]	43.4 ± 3.7	7.36 ± 0.03 [a]	106 ± 15 [a,b,c]
	Vehicle + Saline	37.5 ± 0.2	39.1 ± 2.4 [a,b]	42.0 ± 2.8	7.37 ± 0.03	73 ± 26 [a,b,d]
	Grouped TC	37.5 ± 0.2	298.2 ± 25.0	42.1 ± 3.3	7.36 ± 0.03	127 ± 27
60 min	AF12198 + LPS	37.7 ± 0.1 [a]	297.3 ± 13.5 [a]	44.8 ± 2.7	7.37 ± 0.04	132 ± 12 [a]
	AF12198 + Saline	37.4 ± 0.2	277.0 ± 27.8	44.0 ± 2.7	7.37 ± 0.03	115 ± 9 [e]
	Vehicle + LPS	37.6 ± 0.3	299.9 ± 20.8 [c]	44.1 ± 3.5	7.39 ± 0.01	140 ± 9
	Vehicle + Saline	37.5 ± 0.2 [a]	273.7 ± 26.1 [a,b]	42.5 ± 2.4 [a]	7.38 ± 0.02	119 ± 20
	Grouped TC	37.5 ± 0.2	297.1 ± 22.4	42.6 ± 3.4	7.38 ± 0.03 [a]	128 ± 21

MAP, mean arterial pressure, [a] $p < 0.05$ different from baseline within group, [b] $p < 0.05$ different from grouped TC within time point, [c] $p < 0.05$ different from Vehicle + Saline within time point, [d] $p < 0.05$ different from AF-12198 + LPS within time point AF12198 + LPS; n=5, AF12198 + Saline; n=6, Vehicle + LPS; n=5, Vehicle + Saline; n=6, Grouped TC; n=17

Spinal IL-1R activation is necessary for undermining pLTF after peripheral LPS.

We next tested the hypothesis that acute, spinal IL-1R activation is necessary to undermine pLTF 24 hours after peripheral LPS (Fig 2A and B). Saline + Vehicle (i.t.) rats exhibited pLTF 60 minutes after AIH (60 ± 18%, $p < 0.0001$, n=4). AF-12198 (i.t.) did not significantly increase the magnitude of pLTF in saline treated rats (Saline + AF-12198 (i.t.); (72 ± 26%, $p < 0.0001$, n=4). As expected, LPS (100 µg/kg; i.p.) eliminated pLTF (LPS + Vehicle (i.t.), 11 ± 10%, $p = 0.165$ from baseline, n=5). pLTF was restored after spinal IL-1R antagonism (LPS + AF-12198 (i.t.), 53 ± 15%, $p < 0.0001$ from baseline, n=4). pLTF was not apparent in the TC group (6 ± 17%, $p = 0.241$, n=15).

The acute hypoxic phrenic response was not significantly affected by LPS or spinal IL-1R antagonism (Saline + Vehicle (i.t.); 117 ± 23%, LPS + Vehicle (i.t.); 169 ± 45%, Saline + AF-12198 (i.t.); 150 ± 61%, LPS ± AF-12198 (i.t.); 104 ± 36%).

Baseline phrenic burst frequency was not significantly different between any group (Saline + Vehicle (i.t.); 45 ± 6 bursts/min, Saline + AF-12198 (i.t.); 45 ± 3 bursts/min, LPS + Vehicle (i.t.); 44 ± 4 bursts/min, LPS ± AF-12198 (i.t); 47 ± 10 bursts/min, p = 0.9528). Frequency LTF was evident in Saline + AF-12198 (i.t.) rats 60 minutes after AIH (4 ± 2 bursts/min, p = 0.0138), but not in any other group.

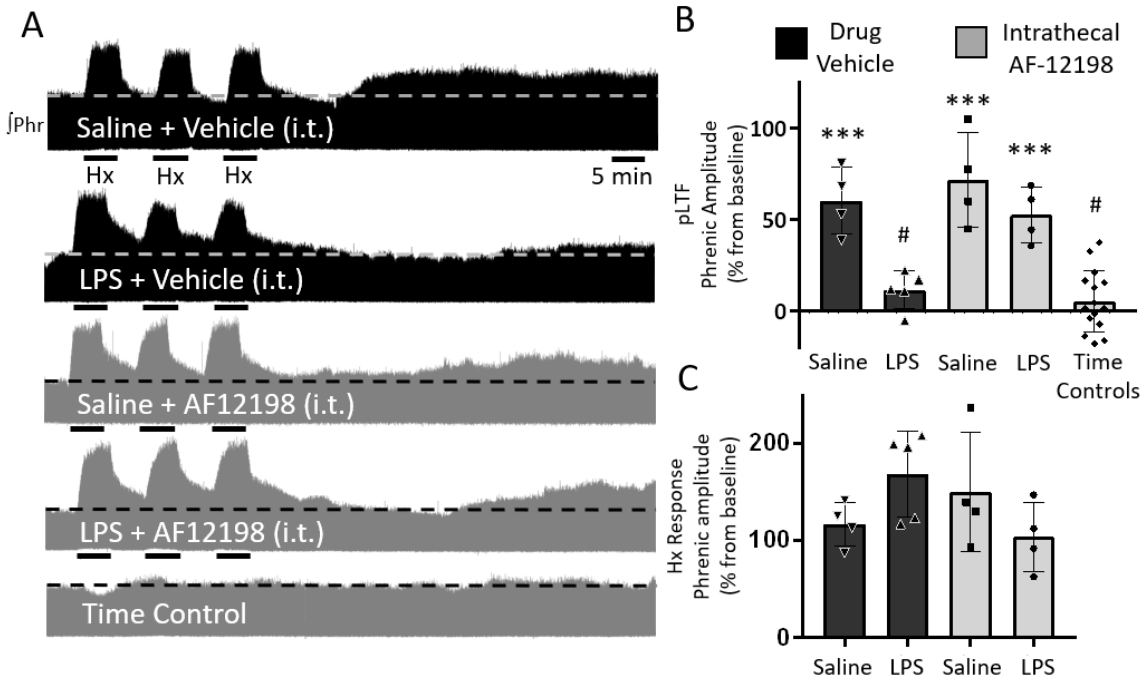

Figure 2.2. Spinal IL-1R antagonism restores pLTF after systemic inflammation. Representative integrated phrenic neurograms **(A)** for AIH-treated rats receiving Saline + Vehicle (i.t.), LPS (100 μg/kg; i.p.) + Vehicle (i.t.), Saline + AF-12198 (1 mM, 15 μL; i.t.), LPS (i.p.) + AF-12198 (i.t.), and a time control (no AIH). pLTF is evident as the progressive increase in phrenic nerve amplitude from baseline (dashed line) over 60 minutes following acute intermittent hypoxia (AIH). Group data **(B)** demonstrate pLTF is abolished by LPS + Vehicle (dark bars) and restored by intrathecal IL-1R antagonism (AF-12198 treated, grey bars). Acute hypoxic responses **(C)** were not significantly affected by any treatment. *** $p < 0.0001$ significant difference in phrenic amplitude from baseline; # $p < 0.001$ different from Saline + Vehicle, Saline + AF-12198, and LPS + AF-12198 (ANOVA RM, Fisher LSD).

Small variations were evident in physiological parameters (Table 2), but they remained within experimental limits. As expected, all experimental groups displayed

significantly decreased MAP and PaO_2 during hypoxia. There were no significant differences in temperature, $PaCO_2$, or pH at baseline between groups. The significant decrease in PaO_2 at 60 min in the saline + Vehicle (i.t.) group was within normal limits. At baseline, LPS treatment increased MAP relative to saline-treated groups with AF-12198 or vehicle (Table 2).

Table 2.2. Physiological parameters during electrophysiology experiments after spinal AF-12198 (1 mM, 15uL).

Experimental Group		Temperature	PaO_2	$PaCO_2$	pH	MAP
Baseline	AF12198 + LPS	37.5 ± 0.3	294.2 ± 31.0	47.5 ± 2.5	7.35 ± 0.03	145 ± 19
	AF12198 + Saline	37.4 ± 0.3	276.9 ± 22.1	45.1 ± 2.2	7.37 ± 0.03	127 ± 20 [b]
	Vehicle + LPS	37.5 ± 0.3	284.6 ± 29.0	44.0 ± 2.7	7.37 ± 0.01	144 ± 11 [c]
	Vehicle + Saline	37.7 ± 0.3	288.9 ± 33.5	43.5 ± 3.2	7.38 ± 0.02	102 ± 11 [b]
	Grouped TC	37.5 ± 0.2	278.7 ± 16.1	44.8 ± 3.2	7.35 ± 0.04	125 ± 25
Hypoxia	AF12198 + LPS	37.5 ± 0.2	37.6 ± 2.1 [a,b]	47.6 ± 3.4	7.33 ± 0.02	106 ± 37 [a,c]
	AF12198 + Saline	37.6 ± 0.1	39.1 ± 2.0 [a,b]	44.1 ± 2.3	7.37 ± 0.02	66 ± 14 [a]
	Vehicle + LPS	37.4 ± 0.1	37.5 ± 2.1 [a,b]	44.5 ± 3.8	7.37 ± 0.02	95 ± 10 [a]
	Vehicle + Saline	37.7 ± 0.2	38.6 ± 8.0 [a,b]	43.4 ± 3.8	7.36 ± 0.03	56 ± 12 [a]
	Grouped TC	37.6 ± 0.2	283.7 ± 33.8	44.9 ± 3.2	7.36 ± 0.03	122 ± 25
60 min	AF12198 + LPS	37.4 ± 0.3	289.5 ± 18.8	47.2 ± 2.3	7.37 ± 0.02	137 ± 15
	AF12198 + Saline	37.6 ± 0.2	272.5 ± 19.0	45.4 ± 3.3	7.37 ± 0.03	115 ± 18
	Vehicle + LPS	37.5 ± 0.3	283.7 ± 20.3	43.9 ± 2.3	7.39 ± 0.02	132 ± 13
	Vehicle + Saline	37.5 ± 0.1	260.5 ± 20.9 [a]	43.6 ± 2.8	7.40 ± 0.03	99 ± 23
	Grouped TC	37.4 ± 0.2	270.1 ± 24.7	45.1 ± 3.2	7.38 ± 0.02	120 ± 22

MAP, mean arterial pressure, [a] $p < 0.05$ different from baseline within group, [b] $p < 0.05$ different from grouped TC within time point, [c] $p < 0.05$ different from Vehicle + Saline within time point, AF12198 + LPS; n=4, AF12198 + Saline; n=4, Vehicle + LPS; n=5, Vehicle + Saline; n=4, Grouped TC; n=15

Spinal exogenous rIL-1β does not abolish AIH-induced pLTF in healthy rats.

pLTF remains after spinal, exogenous rIL-1β (1ng ± AIH; 66 ± 26%, n=3, p = 0.012, 10ng ± AIH; 102 ± 49%, n=4, p < 0.0001, 100ng + AIH; 93 ± 51%, n=3, p < 0.0001, 300ng ± AIH; 37 ± 40%, n=3, p = 0.028). However, after 300ng rIL-1β, AIH elicited pLTF with lower magnitude than 10ng (p = 0.008) and 100ng doses (p = .014, Fig. 2.3A and B). Thus, rIL-1β is not sufficient to abolish pLTF in healthy rats.

Furthermore, rIL-1β had no effect on the acute hypoxic phrenic responses at any dose (1ng; 154 ± 63%, 10ng; 220 ± 131%, 100ng; 143 ± 55%, 300ng; 96 ± 52%).

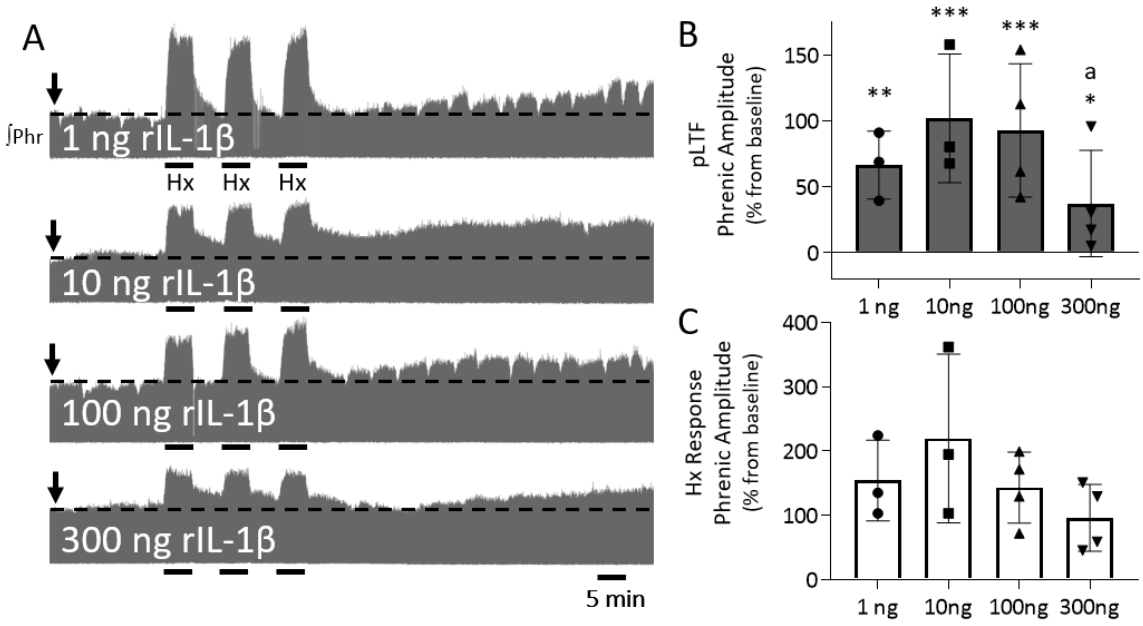

Figure 2.3. Exogenous, spinal rIL-1β does not abolish pLTF in healthy animals. Representative integrated phrenic neurograms (**A**) after intrathecal rIL-1β (1ng, 10ng, 100ng, 300ng; indicated by ↓) 20 minutes before acute intermittent hypoxia (Hx). pLTF is evident as the progressive increase in phrenic nerve amplitude from baseline (dashed line) over 60 minutes following acute intermittent hypoxia. Intrathecal rIL-1β does not abolish pLTF at any dose. Group data (**B**) demonstrate pLTF at all doses of intrathecal rIL-1β, but the magnitude of pLTF at high doses (300 ng) is reduced compared to lower doses (10 and 100 ng). Acute hypoxic phrenic responses (**C**) were not significantly affected by any treatment. * $p < 0.05$; ** $p < 0.01$; *** $p < 0.001$ significantly different from baseline; a, $p < 0.05$ significantly different from 10ng + AIH and 100ng + AIH (ANOVA RM, Fisher LSD).

Minor changes in physiological variables occurred in animals receiving intrathecal rIL-1β and AIH (Table 3). Temperature was decreased at 60 minutes in the 1ng + AIH group, but remained within acceptable ranges. There were no significant differences in $PaCO_2$ and small, but significant, changes in pH during hypoxia in 1ng +

AIH and 300ng + AIH groups. PaO_2 and MAP were significantly decreased during hypoxia (Table 3).

Spinal exogenous rIL-1β facilitates phrenic amplitude in healthy rats.

Since exogenous IL-1β is sufficient to induce plasticity in the spinal dorsal horn in the form of pain hypersensitivity (Cunha et al., 2008), we next tested the hypothesis that spinal rIL-1β was sufficient to facilitate phrenic nerve amplitude. Low doses of rIL-1β (1 ng and 10 ng) did not significantly alter phrenic amplitude (1 ng; -3 ± 5%, n=3, p = 0.738, 10 ng; 8 ± 22%, n=3, p = 0.380); however, higher doses of rIL-1β induced progressive phrenic amplitude facilitation (100 ng; 31 ± 12%, p = 0.005 relative to baseline, n=4, 300 ng; 51 ± 17%, p <0 .0001 relative to baseline, n=4). Therefore, high doses of rIL-1β are sufficient to facilitate phrenic amplitude.

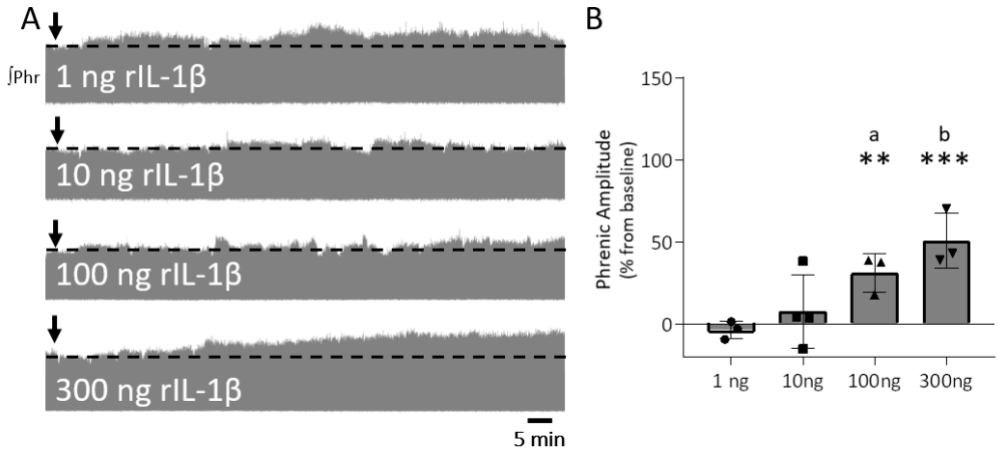

Figure 2.4. Exogenous, spinal rIL-1β induces dose-dependent facilitation of phrenic amplitude. Representative integrated phrenic neurograms (**A**) for rats receiving intrathecal rIL-1β (1ng, 10ng, 100ng, 300ng; indicated by ↓). Phrenic amplitude facilitation is evident as the progressive increase in phrenic nerve amplitude from baseline (dashed line) following intrathecal rIL-1β. Group data (**B**) demonstrate a dose-dependent increase in phrenic nerve amplitude 60 minutes after intrathecal rIL-1β. ** p < 0.01; *** p < 0.001 significantly different from baseline; a, p < 0.05 significantly different from 1ng + TC; b, p < 0.01 significantly different from 1ng + TC and 10ng + TC; (ANOVA RM, Fisher LSD).

Physiological variables were stable throughout electrophysiology experiments without any significant changes (Table 3).

Table 2.3. Physiological parameters during electrophysiology experiments after spinal rIL-1β.

Experimental Group		Temperature	PaO_2	$PaCO_2$	pH	MAP
Baseline	1 ng + AIH	37.7 ± 0.3	272.9 ± 34.8	42.8 ± 2.0	7.38 ± 0.01	117 ± 12
	10 ng + AIH	37.5 ± 0.2	267.9 ± 11.1	40.0 ± 4.8	7.40 ± 0.05	111 ± 21
	100 ng + AIH	37.6 ± 0.1	258.7 ± 11.1	43.9 ± 2.8	7.37 ± 0.01	115 ± 18
	300 ng + AIH	37.6 ± 0.4	289.0 ± 6.2	41.5 ± 2.9	7.40 ± 0.03	103 ± 10
Hypoxia	1 ng + AIH	37.4 ± 0.3	38.0 ± 3.5 [a]	42.9 ± 3.7	7.36 ± 0.04 [a]	69 ± 17 [a]
	10 ng + AIH	37.4 ± 0.3	38.2 ± 4.0 [a]	38.8 ± 5.8	7.40 ± 0.05	72 ± 21 [a]
	100 ng + AIH	37.4 ± 0.2 [f]	42.6 ± 1.4 [a]	43.4 ± 2.8	7.36 ± 0.02	60 ± 25 [a]
	300 ng + AIH	37.6 ± 0.3	37.6 ± 4.3 [a]	42.2 ± 3.7	7.40 ± 0.01 [a]	62 ± 15 [a]
60 min	1 ng + AIH	37.3 ± 0.1 [a]	247.7 ± 45.2 [a]	42.9 ± 1.3	7.37 ± 0.02	120 ± 5
	10 ng + AIH	37.3 ± 0.2	281.3 ± 18.4	40.5 ± 4.9	7.39 ± 0.05	123 ± 17
	100 ng + AIH	37.4 ± 0.2	249.5 ± 16.3	44.2 ± 2.3	7.37 ± 0.02	107 ± 20 [a]
	300 ng + AIH	37.5 ± 0.4	262.4 ± 15.0 [a]	42.1 ± 3.2	7.37 ± 0.01	115 ± 14
Experimental Group		**Temperature**	**PaO_2**	**$PaCO_2$**	**pH**	**MAP**
Baseline	1 ng	37.6 ± 0.4	282.1 ± 26.1	42.5 ± 1.2	7.38 ± 0.02	127 ± 27
	10 ng	37.5 ± 0.2	255.3 ± 19.0	42.4 ± 2.2	7.37 ± 0.01	117 ± 12
	100 ng	37.6 ± 0.3	264.4 ± 23.6	45.4 ± 2.4	7.37 ± 0.01	135 ± 9
	300 ng	37.7 ± 0.3	258.8 ± 24.3	40.5 ± 6.5	7.40 ± 0.04	123 ± 11
60 min	1 ng	37.6 ± 0.3	279.6 ± 15.0	43.0 ± 0.7	7.39 ± 0.03	132 ± 17
	10 ng	37.7 ± 0.3	254.6 ± 7.2	42.8 ± 1.8	7.38 ± 0.02	120 ± 17
	100 ng	37.4 ± 0.2	263.0 ± 25.2	45.7 ± 2.5	7.36 ± 0.01	131 ± 7
	300 ng	37.6 ± 0.2	234.2 ± 22.6	40.2 ± 7.2	7.38 ± 0.01	134 ± 18

MAP, mean arterial pressure, [a] $p < 0.05$ different from baseline within group, [b] $p < 0.05$ different from all AIH experimental groups within time point,1 ng + AIH; n=3, 10 ng + AIH; n=4, 100 ng + AIH; n=3, 300 ng + AIH; n=3, 1 ng + TC; n=3, 10 ng + TC; n=3, 100 ng + TC; n=4, 300 ng + TC; n=4,

Discussion

Here, we demonstrate a role for IL-1R activation, both peripherally and centrally, in systemic inflammation-induced impairment of respiratory motor plasticity. In healthy rats, however, activation of IL-1Rs with exogenous rIL-1β is insufficient to abolish AIH-induced pLTF, yet it induces phrenic amplitude facilitation in the absence of AIH. Thus, IL-1R activation is necessary to abolish pLTF after systemic inflammation, but not

sufficient to abolish pLTF in healthy rats. These data demonstrate IL-1R activation is an important signaling step in abolishing respiratory plasticity after systemic inflammation.

CNS responses to IL-1β have been widely studied because IL-1β plays a role in modulating many physiological systems, including thermoregulation and behavioral responses (Matsuwaki et al., 2017; Zhu et al., 2010), and IL-1β is rapidly upregulated in the CNS after LPS-induced systemic inflammation (Rothwell and Luheshi, 2000). More recently, IL-1 signaling in the CNS has been shown to modulate different forms of neuroplasticity, including hippocampal dependent learning and pain sensitivity in the dorsal spinal cord (Cunha et al., 2008; Maier et al., 1993; Zhang et al., 2008). We now demonstrate a role for IL-1R activation in undermining respiratory plasticity in the cervical spinal cord.

The restoration of pLTF by peripheral IL-1R antagonism suggests IL-1R activation is necessary for transmitting relevant inflammatory information to the CNS after LPS-induced inflammation. Additionally, since IL-1R signaling likely contributes significantly to time-dependent changes in serum cytokine levels (Terrando et al., 2010), peripheral IL-1R antagonism may indirectly mitigate CNS inflammation by inducing changes in other cytokines and restore plasticity. While we did not assess CNS inflammation directly in these experiments, others have shown peripheral IL-1R activation is required for brain inflammatory responses after i.p LPS (Giles et al., 2015; Maier et al., 1993) and peripheral and spinal IL-1β gene expression is upregulated after peripheral LPS (Huxtable et al., 2013). Thus, we suggest the primary action of peripheral IL-1R antagonism is to inhibit peripheral inflammatory responses induced by LPS. It remains possible, however, that AF-12198 crosses the blood-brain barrier and also

directly reduces CNS inflammatory responses. Since AF-12198 is a small peptide, we believe it is unlikely to cross the blood-brain barrier at sufficient concentrations to directly reduce CNS inflammation. Thus, the actions of peripheral IL-1R antagonism are most likely by inhibiting peripheral inflammatory responses. Together, we propose peripheral IL-1R antagonism indirectly reduces relevant spinal inflammation, and thus, restores pLTF.

Our data demonstrating restoration of pLTF by spinal IL-1R antagonism is consistent with the hypothesis that persistent IL-1 signaling around the phrenic motor pool is necessary for undermining pLTF. IL-1R signaling in phrenic motoneurons could directly alter their properties to eliminate pLTF or could promote the release of other inflammatory cytokines from nearby cells (such as microglia) which undermine pLTF. IL-1R signaling can activate diverse intracellular pro-inflammatory pathways, including NF-kB and stress activated protein kinases (Dinarello, 2009), which may inhibit pLTF. Additionally, in a separate model of systemic inflammation, spinal p38-MAPK activation, a kinase downstream of IL-1R (Molina-Holgado et al., 2000), is necessary to undermine pLTF after systemic inflammation (Huxtable et al., 2015). Future investigations should assess the link between spinal IL-1 signaling and activation of p38-MAPK in undermining pLTF.

Though we demonstrate the necessity of IL-1R activation in undermining plasticity, the effects of direct application of rIL-1β are more complicated. Here, no rIL-1β dose abolished plasticity after AIH in healthy rats. The 300ng rIL-1β dose did reduce the magnitude of pLTF compared to other doses. Thus, it is possible higher doses of rIL-1β may be sufficient to undermine pLTF; however, 300ng is the highest dose possible

due to solubility and volume limitations for intrathecal injections. Exogenous rIL-1β may be insufficient to undermine pLTF if complementary inflammatory molecules are necessary to completely undermine pLTF or if systemic inflammation primes the CNS to augment the response to IL-1β. IL-1R expression is upregulated after peripheral LPS (Turrin et al., 2001), such that healthy animals not exposed to LPS have a blunted response to exogenous rIL-1β. Alternatively, the cellular mechanisms undermining pLTF may take longer to develop than 20 minutes after spinal, exogenous rIL-1β. However, in hippocampal slices, rIL-1β inhibits long-term potentiation within 10 minutes of exposure (Bellinger et al., 1993), demonstrating rIL-1β can have rapid effects. In the absence of AIH, high doses of rIL-1β facilitated phrenic burst amplitude, demonstrating rIL-1β evoked a lasting increase in phrenic amplitude after rIL-1β is likely degraded (Reimers et al., 1991). While the mechanisms mediating this plasticity are unknown, other reports show dose-dependent IL-1β changes in synaptic strength or cell excitability in response to IL-1R activation, such as increased calcium-dependent glutamate release from hippocampal neurons, upregulated NMDA receptor activity (Galic et al., 2012), and increased dorsal root ganglion neuron excitability after IL-1β (Binshtok et al., 2008; Takeda et al., 2007). Taken together, rIL-1β exerts dose-dependent alterations of phrenic motor output, capable of both inducing facilitation and reducing the magnitude of, but not abolishing, pLTF.

Though our study demonstrates an important role of IL-1 signaling in spinal motor respiratory plasticity, IL-1 signaling is likely not the only inflammatory molecule involved in modulating respiratory neural activity. For example, inactivity-induced phrenic motor facilitation, another model of spinal respiratory motor plasticity, requires

the activation of TNF receptor 1, an inflammatory cytokine receptor (Broytman et al., 2013). Additional inflammatory molecules, such as prostaglandins, have also been shown to modulate central respiratory networks. While prostaglandins mediate profound respiratory modulation (Forsberg et al., 2016; Koch et al., 2015; Olsson et al.; Siljehav et al., 2012), they are unlikely to play a significant role in undermining respiratory motor plasticity after systemic inflammation since inhibition of cyclooxygenase, the rate-limiting enzyme in the production of prostaglandins, does not restore pLTF (Huxtable et al., 2017). However, the relationship between the various types of inflammatory cytokines and their downstream effects in respiratory control remains mostly unknown. Improving our understanding of the actions of individual and combined inflammatory signaling molecules, as well as their cellular sources, in neural respiratory control will be the topic of future investigations.

Our study builds on these and other recent studies investigating the effects of IL-1 signaling in respiratory control networks (Aleksandrova and Danilova, 2010; Ribeiro et al., 2017). Similar to previous reports (Aleksandrova and Danilova, 2010; Gresham et al., 2011), we found a tendency for systemic inflammation to increase baseline phrenic burst frequency. While the mechanisms mediating the increased frequency after systemic inflammation are unclear, direct intracerebroventricular rIL-1β increases minute ventilation, suggesting a direct effect of IL-1β on respiratory frequency (Aleksandrova and Danilova, 2010). Additionally, acute hypoxic ventilatory responses are attenuated after intratracheal LPS due to spinal IL-1R activation (Ribeiro et al., 2017); however, no significant changes were seen in the acute hypoxic phrenic amplitude response after systemic inflammation. Furthermore, frequency LTF was only evident in one

experimental group, which supports previous work suggesting frequency LTF is small and inconsistent (Baker-Herman and Mitchell, 2008). Less is known about the mechanisms underlying frequency LTF, which may be distinctly different from the amplitude change known as pLTF. Thus, we have focused our analyses on amplitude changes since much more is known about the mechanisms of pLTF using this experimental preparation and the AIH paradigm, where the consistent and significant changes are reflected in amplitude. In summary, IL-1 signaling seems to have widespread roles in the neural control of breathing.

In conclusion, we demonstrate IL-1R activation peripherally and centrally is necessary for undermining respiratory plasticity after systemic inflammation. Our study is the first to investigate the effects of IL-1 signaling on spinal respiratory plasticity, and builds on other recent studies investigating the effects of IL-1 signaling in medullary respiratory networks (Aleksandrova and Danilova, 2010; Ribeiro et al., 2017). Taken together, inflammatory signaling through IL-1R attenuates chemosensitivity (Aleksandrova and Danilova, 2010) and respiratory plasticity. Furthermore, such results suggest uncovering how inflammation impacts the neural control of breathing is fundamental to understand changes in respiratory function during pathological conditions. Furthermore, for respiratory motor plasticity to be used clinically (Hayes et al., 2014; Trumbower et al., 2012, 2017), we must also understand the interaction between plasticity and inflammation, which is common in many pathologies.

CHAPTER III

VIRAL MIMETIC-INDUCED INFLAMMATION ABOLISHES Q-PATHWAY-EVOKED BUT NOT S-PATHWAY-EVOKED ADULT RESPIRATORY MOTOR PLASTICITY IN RATS

This chapter includes material previously published in the *Frontiers in Physiology: Respiratory Physiology* (Hocker et al., 2019) which was co-authored by Adrianne G. Huxtable. I designed and led these studies, collected and analyzed all data, and wrote the paper. Adrianne Huxtable designed, contributed to writing the manuscript, provided guidance, oversight, and editorial assistance.

Introduction

Neuroplasticity of the respiratory control system is an important feature of the control of breathing thought to confer stability and adaptation when the respiratory system is challenged (Fuller and Mitchell, 2017). One frequently studied model of adult respiratory neuroplasticity is phrenic long-term facilitation (pLTF), induced by acute intermittent hypoxia (AIH). At least two pathways to pLTF exist: the Q-pathway and the S-pathway (Reviewed in Turner et al., 2018). The Q-pathway is serotonin-dependent and induced by moderate AIH (mAIH, 3x5 minute hypoxic episodes, PaO_2 35-45 mmHg) (Baker-Herman and Mitchell, 2002), while the S-pathway is induced by severe AIH (sAIH, PaO_2 25-35 mmHg) and involves activation of adenosine receptors (Nichols et al., 2012). The cellular mechanisms of Q- and S-pathway plasticity are distinct (Turner et al., 2018) and the two pathways are differentially affected by adult, systemic inflammation (Agosto-Marlin et al.,

2017). Adult Q-pathway plasticity is abolished by low levels of acute, systemic inflammation induced by a TLR4 agonist (lipopolysaccharide, LPS) (Huxtable et al., 2011; Vinit et al., 2011) or 8 hours of intermittent hypoxia (Huxtable et al., 2015, 2017) and restored by the non-steroidal anti-inflammatory, ketoprofen (Huxtable et al., 2013, 2015). On the contrary, S-pathway-evoked adult respiratory motor plasticity is inflammation resistant (Agosto-Marlin et al., 2017), and therefore it has the potential to serve as a "backup" pathway to preserve plasticity after inflammation.

Since AIH-induced plasticity is being translated to clinical populations (e.g. after spinal cord injury) (Hayes et al., 2014; Trumbower et al., 2012, 2017) with low-levels of systemic/neuroinflammation, interest in the impact of inflammation on motor plasticity is growing. Studies on inflammation-induced impairments in pLTF have focused on lipopolysaccharide (LPS, bacterial induced-inflammation) (Huxtable et al., 2013; Vinit et al., 2011) or simulated sleep apnea induced by nocturnal intermittent hypoxia (Huxtable et al., 2015, 2017). LPS is the most common model of acute, systemic inflammation, induces a rapid upregulation of brain inflammatory cytokines, and abolishes pLTF within 3 hours and for at least 24 hours (Huxtable et al., 2013), while nocturnal intermittent hypoxia is a clinically relevant physiological perturbation also abolishing pLTF (Huxtable et al., 2015). However, viral infections are very common (Obasi et al., 2014) and induce unique, but overlapping, inflammatory profiles through TLR3 activation (Reimer et al., 2008). Polyinosinic:polycitidylic acid (polyIC) is an agonist for TLR3 and is used experimentally to investigate the effects of systemic viral inflammation (Nicodemus and Berek, 2010). PolyIC-induced inflammation induces a temporally slower onset of inflammatory genes in the brain compared to LPS (Konat et al., 2009; Krasowska-Zoladek et al., 2007; Yamato

et al., 2014), and therefore, it has the potential to have differential effects on pLTF. Since inflammation arises from diverse stimuli throughout our lives, understanding the effects of polyIC on respiratory motor plasticity broadens our understanding of the impact of inflammation on respiratory control. Additionally, while the inflammation sensitivity of Q-pathway-evoked plasticity has been confirmed in two models of systemic inflammation (reviewed in Hocker et al., 2017), the sensitivity of S-pathway-evoked plasticity has only been investigated after LPS-induced inflammation (Agosto-Marlin et al., 2017). Here, we hypothesize polyIC will induce CNS inflammation and abolish Q-pathway, but not S-pathway, evoked pLTF. Further, since we hypothesize slower neuroinflammation onset after peripheral polyIC, where Q-pathway-evoked LTF will be abolished at 24 hours, but not 3 hours.

Methods

All experiments were approved by the University of Oregon Institutional Animal Care and Use Committee and conformed to the policies of the National Institute of Health *Guide for the Care and Use of Laboratory Animals*. Male Sprague Dawley Rats (300-400g; 3-4 months; Envigo, Colony 206) were housed under standard conditions (12:12h light/dark cycle) with food and water *ad libitum*.

Drugs and Materials

PolyIC (P9582, Sigma Chemical) was dissolved in sterile saline, heated to 50°C, cooled for re-annealing, and injected (intraperitoneal, i.p.) at doses ranging from 250 µg/kg to 2 mg/kg. S-(+) Ketoprofen (Keto, Sigma Chemical) was dissolved in ethanol (50% V/V, 0.39 g/kg) and sterile saline for acute, adult injections (12.5 mg/ml/kg, i.p., 3 hr).

Experimental Groups

To investigate the temporal actions of polyIC and the sufficiency of polyIC to abolish Q-pathway-evoked pLTF, we used the following groups: 3 hr polyIC (750 µg/kg, n = 5), 24 hr polyIC (750 µg/kg, n = 4), 24 hr polyIC (500 µg/kg, n = 4), 24 hr polyIC (250 µg/kg, n = 4). A time control group consisted of rats from each of the groups: 3 hr polyIC (750 µg/kg, n = 3), 24 hr polyIC (750 µg/kg, n = 2), 24 hr polyIC (500 µg/kg, n = 1), 24 hr polyIC (250 µg/kg, n = 1).

To investigate if acute, anti-inflammatory treatment restores Q-pathway-evoked pLTF after polyIC, rats were treated ketoprofen (12.5 mg/kg, i.p.) three hours before electrophysiology experiments. We used the following experimental groups: 24 hr vehicle (saline) + Keto (n = 4), 24 hr polyIC (750 µg/kg) + Keto (n = 4), and time controls made up of two animals from each treatment group (n = 4).

To investigate the impact of polyIC-induced inflammation on S-pathway-evoked respiratory pLTF, we used the following experimental groups: 24 hr vehicle (n = 4), 24 hr polyIC (750 µg/kg) (n = 5), and time controls made up of two animals from each treatment group (n = 4).

Electrophysiological Studies

Electrophysiological studies have been described in detail previously (Bach and Mitchell, 1996; Baker-Herman and Mitchell, 2002). Briefly, rats were anesthetized with isoflurane, tracheotomized, ventilated (Rat Ventilator, VetEquip®), and bilaterally vagotomized. A venous catheter was placed for drug delivery and fluid replacement, and a femoral arterial catheter was used to monitor blood pressure and for arterial blood

sampling. Arterial blood samples were assessed (PaO_2, $PaCO_2$, pH, base excess; Siemens RAPIDLAB® 248) during baseline, the first hypoxic response, and 15, 30 and 60 minutes post-AIH. Rectal temperature was measured (Kent Scientific Corporation) and maintained between 37°C and 38°C with a custom heated surgical table. Using a dorsal approach, phrenic nerves were isolated, cut distally, and de-sheathed. Rats were converted to urethane anesthesia (1.8 g/kg i.v.; Sigma-Aldrich), allowed to stabilize for one hour, and paralyzed with pancuronium dibromide (1 mg; Selleck Chemicals). Nerves were bathed in mineral oil and placed on bipolar silver electrodes. Raw nerve recordings were amplified (10k), filtered (0.1-5 kHz), integrated (50 ms time constant), and recorded (10 kHz sampling rate) for offline analysis (PowerLab and LabChart 8.0, AD Instruments). Apneic and recruitment CO_2 thresholds were determined by continuous end-tidal CO_2 monitoring (Kent Scientific Corporation) while changing inspired CO_2. End-tidal CO_2 was set 2 mmHg above the recruitment threshold, where baseline $PaCO_2$ was established and then maintained within 1.5 mmHg for the duration of the experiment. Blood volume and base excess were maintained (±3 MEq/L) by continuous infusion (0-3 mL/h, i.v.) of hetastarch (0.3%) and sodium bicarbonate (0.99%) in lactated ringers. Experiments were excluded if mean arterial pressure deviated more than 20 mmHg from baseline.

Rats (excluding time control rats) received three, 5-minute bouts of either mAIH (~10.5% O_2, PaO_2 35-45 mmHg) or sAIH (~7% O_2, PaO_2 25-35 mmHg). The average frequency and amplitude of 30 consecutive integrated phrenic bursts were assessed during baseline, the first acute hypoxic response, and 15, 30, and 60 minutes after AIH. Data are presented as the percent relative to baseline and compared using two-way, repeated measures ANOVA with Fisher LSD post hoc tests (GraphPad Prism v8). Physiological

variables were compared using two-way, repeated measures ANOVA with Tukey's post hoc test. Mean arterial pressure is reported for baseline, the end of the third hypoxic episode, and 60 minutes after AIH. Acute hypoxic phrenic responses were compared using an ANOVA with Fisher LSD post hoc test. Values are presented as mean ± SD.

RNA isolation and Quantitative PCR Experiments

Male rats were injected with either vehicle (saline) or polyIC (750 µg/kg, i.p.) 3 or 24 hours (n = 6 per group) before tissue collection. Rats were anesthetized with isoflurane and perfused with transcardiac PBS (pH 7.4). Ventral cervical spinal cords (C3-C7), medullas, and spleens were dissected and flash frozen until homogenization in TRIzol Reagent (Invitrogen, Carlsbad, CA, USA). RNA was isolated with PureLink columns (Invitrogen, Carlsbad, CA, USA) according to the manufacturer's protocol. cDNA was reverse transcribed from 1 µg of total RNA using qScript cDNA Synthesis Kit (QuantaBio) reverse transcriptase and analyzed using qPCR with PerfeCTa SYBR Green FastMix (QuantaBio) on a CFX-384 system (BioRad). Inflammatory gene expression was analyzed in ventral cervical spinal cord, medullary, and spleen homogenates using the following primers:

IL-6: 5'-GTG GCT AAG GAC CAA GAC CA and 5'-GGT TTG CCG AGT AGA CCT CA;

IL-1β: 5'-CTG CAG ATG CAA TGG AAA GA and 5'-TTG CTT CCA AGG CAG ACT TT;

COX-2: 5'-TGT TCC AAC CCA TGT CAA AA and 5'-CGT AGA ATC CAG TCC GGG TA;

TNF-α: 5’-TCC ATG GCC CAG ACC CTC ACA C and 5’-TCC GCT TGG TGG TTT GCT ACG;

iNOS: 5’-AGG GAG TGT TGT TCC AGG TG and 5’-TCT GCA GGA TGT CTT GAA CG;

18s: 5’-CGG GTG CTC TTA GCT GAG TGT CCC G and 5’-CTC GGG CCT GCT TTG AAC AC.

Wherever possible, primers (purchased from ThermoFisher) were designed to span introns (Primer 3 software). Primer efficiency was assessed by use of standard curves, as previously reported (Crain and Watters, 2015). Expression of inflammatory genes was made relative to 18s ribosomal RNA calculated using the $2^{-\Delta\Delta CT}$ method (Livak and Schmittgen, 2001).

Results

PolyIC induces transient inflammatory gene expression in the ventral cervical spinal cord

Ventral cervical spinal inflammatory gene expression 3 and 24 hours after polyIC (750 μg/kg, i.p., Fig. 3.1A) was assessed since previous studies have demonstrated peripheral LPS abolishes Q-pathway-evoked pLTF within 3 hours and for at least 24 hours (Huxtable et al., 2013), and involves activation of spinal IL-1 receptors (Hocker and Huxtable, 2018). In ventral cervical spinal homogenates, IL-1β, IL-6, TNFα and iNOS gene expression were not significantly different from saline controls at 3 or 24 hours (Fig. 3.1A). However, COX-2 gene expression transiently increased at 3 hours ($n = 6$, $p < 0.001$, Fig. 3.1A), but returned to baseline by 24 hours after polyIC. At 24 hours, expression of

TNFα and iNOS genes was significantly increased relative to 3-hour polyIC ($p = 0.01$ and $p = 0.003$ respectively), but they were not different from 24-hour saline controls ($p > 0.05$). Thus, inflammatory gene expression increases in regions of the central nervous system important for pLTF 3 hours after polyIC, with some regions remaining insignificantly elevated at 24 hours. Medullary gene expression (Fig. 3.1B) was also assessed to investigate regional differences in CNS inflammatory responses and splenic gene expression (Fig. 3.1C) as a marker of systemic inflammation. In medullary and splenic homogenates, no significant changes in inflammatory genes (IL-6, IL-1β, COX-2, TNF-α, iNOS) were evident at 3 or 24 hours (Fig. 3.1B and C), suggesting polyIC induces minimal systemic or medullary inflammation.

Q-pathway-evoked pLTF is abolished 24 hours after polyIC

Q-pathway-evoked pLTF is evident as the increase in integrated phrenic nerve activity 60 minutes after mAIH (PaO_2 35-45 mmHg) in anesthetized rats (Bach and Mitchell, 1996) (Fig. 3.2A). PolyIC (750 μg/kg) was sufficient to induce transient cervical spinal inflammatory gene expression, but was insufficient to abolish Q-pathway-evoked pLTF at 3 hours (67 ± 21% change from baseline, $n = 5$, $p < 0.001$, Fig. 3.2B). At 24 hours, a dose response to polyIC revealed 750 μg/kg was sufficient to abolish Q-pathway-evoked pLTF (17 ± 15% change from baseline, $n = 5$, $p = 0.058$, Fig. 3.2B). Lower doses of polyIC were insufficient to significantly abolish pLTF (500 μg/kg = 24 ± 33% change from baseline, $n = 4$, $p = 0.019$; 250 μg/kg = 63 ± 19% change from baseline, $n = 4$, $p < 0.001$, Fig. 3.2B). Variability in pLTF magnitude 24 hours after 500 μg/kg polyIC suggests this dose is near the threshold to abolish plasticity. Phrenic amplitude in time controls (not

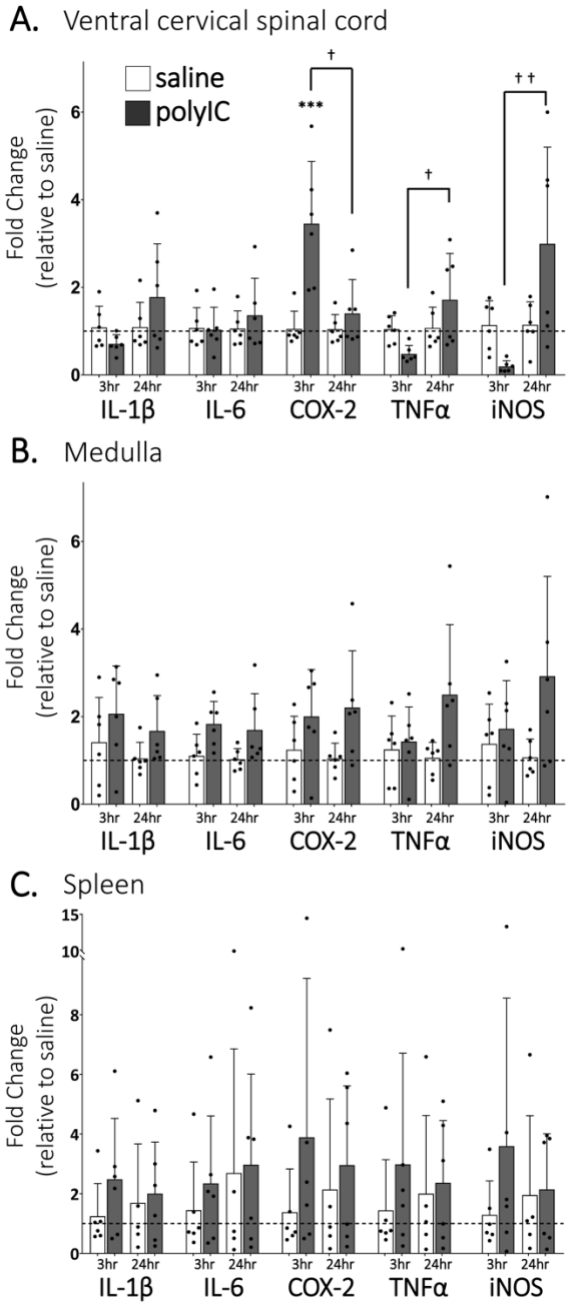

Figure 3.1. PolyIC (750 μg/kg, i.p.) transiently increases inflammatory gene expression in ventral cervical spinal cord homogenates, but not in the medulla or spleen. Ventral spinal cord homogenate COX-2 mRNA significantly increased 3 hours after polyIC and returned to baseline by 24 hours **(A)**. TNFα and iNOS mRNA significantly increased in the ventral spinal cord at 24 hours compared to 3 hours after polyIC (n = 6 per group), but mRNA was not different from saline controls **(A)**. Other inflammatory genes were not significantly altered by polyIC in ventral cervical spinal cords **(A)**, medullas **(B)** or spleens **(C)**. Horizontal dashed line indicates 1-fold change from 3hr saline control. (*** $p<0.001$ significant difference from saline control, † $p<0.01$ between groups, †† $p<0.001$ between groups. ANOVA, Tukey)

receiving mAIH) did not differ from baseline (6 ± 18% change from baseline, n = 6, p = 0.466, Fig. 3.2B), demonstrating no effect of polyIC on experiment stability. Between groups, phrenic amplitude 60 minutes after mAIH was significantly reduced ($p < 0.01$) after 24 hour polyIC (500 µg/kg) and 24 hour polyIC (250 µg/kg, and time controls) compared to 3hr polyIC (750 µg/kg) and 24 hr polyIC (250 µg/kg) groups. Thus, polyIC-induced impairment of pLTF occurs slower than LPS-induced impairment and after inflammatory gene expression has returned to baseline. Phrenic nerve responses to moderate hypoxia were not different among groups (Fig. 3.2C).

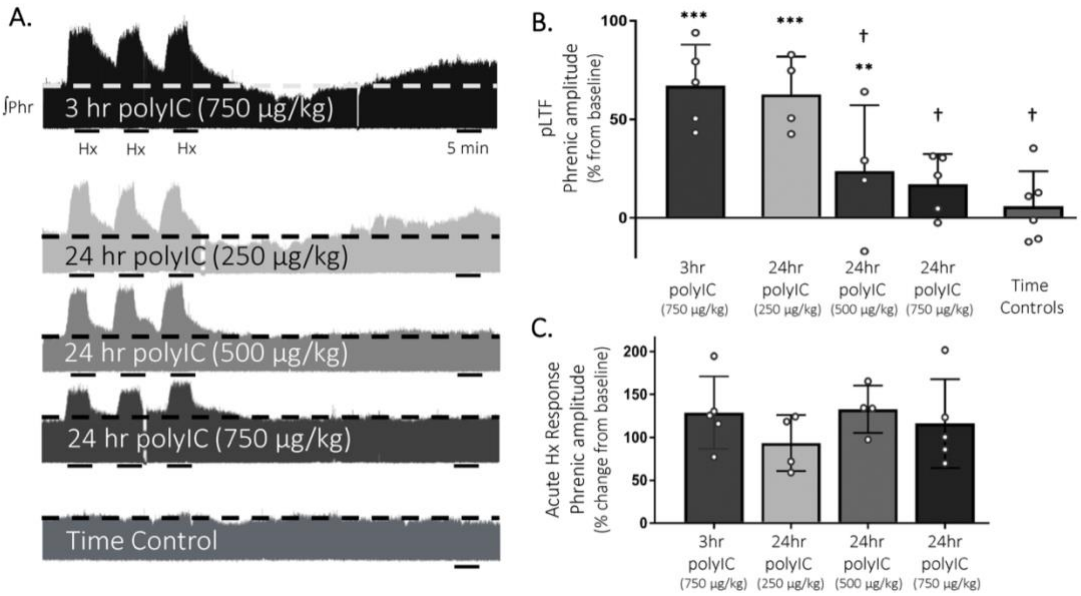

Figure 3.2. The viral mimetic, polyIC, abolishes Q-pathway-evoked pLTF at 24 hours, but not at 3 hours. Representative integrated phrenic neurograms after polyIC (250-750 µg/kg, 3 or 24 hours, i.p.) **(A)**. Q-pathway-evoked pLTF is evident as the progressive increase in phrenic nerve amplitude from baseline (dashed line) over 60 minutes following moderate acute intermittent hypoxia (mAIH, 3 x 5 minute episodes, PaO_2 35-45 mmHg). Group data **(B)** demonstrate 750 µg/kg polyIC was insufficient to abolish Q-pathway-evoked pLTF at 3 hours (n = 5). However, Q-pathway-evoked pLTF is abolished 24 hours after 750 µg/kg polyIC (n = 4), but not at lower doses of polyIC (500 µg/kg, n = 4; 250 µg/kg, n = 4). Time controls (no AIH, n = 7) are not different from baseline, but were significantly reduced from 3hr polyIC (750 µg/kg) and 24 hr polyIC (250 µg/kg) groups. Acute hypoxic phrenic nerve responses (**C**) were not altered by polyIC at any dose. *** $p < 0.0001$ significant difference in phrenic amplitude from baseline; ** $p < 0.001$ from baseline, † $p < 0.01$ different from 3hr polyIC 750 µg/kg and 24hr polyIC 250 µg/kg (ANOVA RM, Fisher LSD).

Ketoprofen restores Q-pathway-evoked pLTF after polyIC induced inflammation

To test the hypothesis that inflammatory signaling after polyIC (750 µg/kg, 24 hours) was undermining Q-pathway-evoked pLTF, the anti-inflammatory ketoprofen (12.5 mg/kg, i.p., 3 hours) was used to acutely diminish inflammatory signaling (Fig. 3.3A). As expected, Q-pathway-evoked pLTF was evident in vehicle + ketoprofen treated rats 60 minutes after mAIH (64 ± 24% change from baseline, $n = 4$, $p < 0.001$, Fig. 3.3B). Ketoprofen restored Q-pathway-evoked pLTF after polyIC (55 ± 13% change from baseline, $n = 5$, $p < 0.001$, Fig. 3.3B), suggesting polyIC-induced inflammation abolishes Q-pathway-evoked pLTF. pLTF was not apparent in time control rats (8 ± 10% change from baseline, $n = 4$, $p = 0.431$, Fig. 3.3B). Phrenic amplitude 60 minutes after mAIH was significantly greater ($p < 0.001$) in vehicle + Keto and polyIC + Keto groups relative to time controls. Phrenic nerve responses to hypoxia were not different among groups (Fig. 3.3C).

S-pathway-evoked pLTF is resistant to polyIC induced inflammation

S-pathway-evoked pLTF was evident as the significant increase in integrated phrenic amplitude 60 minutes after sAIH (PaO_2 25-35 mmHg, Fig. 3.4A) in adult rats treated with vehicle (65 ± 33% change from baseline, $n = 4$, $p < 0.001$, Fig. 3.4B). PolyIC at the same dose undermining Q-pathway-evoked pLTF (750 µg/kg, i.p., 24 hours) was insufficient to abolish S-pathway-evoked pLTF (72 ± 25% change from baseline, $n = 5$, $p < 0.001$, Fig. 3.4B), suggesting S-pathway-evoked pLTF is resistant to polyIC-induced

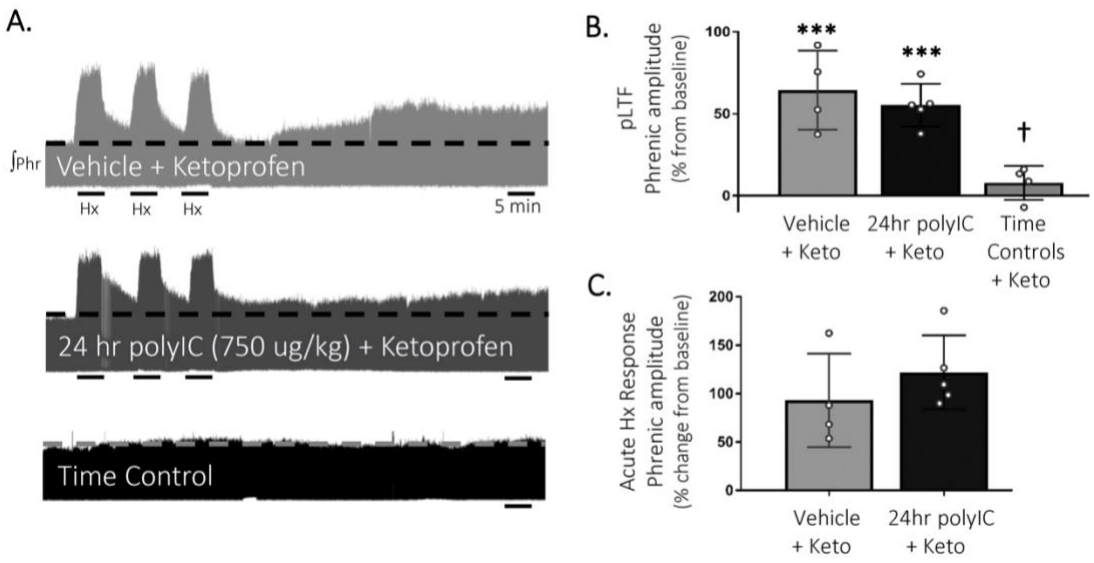

Figure 3.3. Acute, anti-inflammatory ketoprofen restores Q-pathway-evoked pLTF after polyIC-induced inflammation at 24 hours. Representative integrated phrenic neurograms after polyIC (750 μg/kg, i.p., 24h) and acute, adult ketoprofen (12.5 mg/kg, i.p., 3 hrs) (**A**). Q-pathway-evoked pLTF is evident as the progressive increase in phrenic nerve amplitude from baseline (dashed line) over 60 minutes following moderate acute intermittent hypoxia (mAIH, 3 x 5 minute episodes, PaO_2 35-45 mmHg). Group data (**B**) demonstrate Q-pathway-evoked pLTF is restored 24 hours after 750 μg/kg polyIC by the anti-inflammatory ketoprofen (n = 4). Time controls (no mAIH, n = 4) are not different from baseline and were significantly reduced from vehicle (n = 4) and 24h polyIC groups (n = 4). Acute hypoxic phrenic nerve responses (**C**) were not altered by polyIC or ketoprofen. *** $p < 0.0001$ significant difference in phrenic amplitude from baseline; † $p < 0.001$ different from all other groups (ANOVA RM, Fisher LSD).

inflammation. Phrenic amplitude did not change from baseline in time control rats (4 ± 9% change, n = 4, p = 0.670, Fig. 3.4B). Both vehicle and polyIC groups had significantly greater phrenic amplitude 60 minutes after sAIH (p = 0.027 and p = 0.002 respectively) compared to time controls. Phrenic nerve responses to severe hypoxia were not different among groups (Fig. 3.4C).

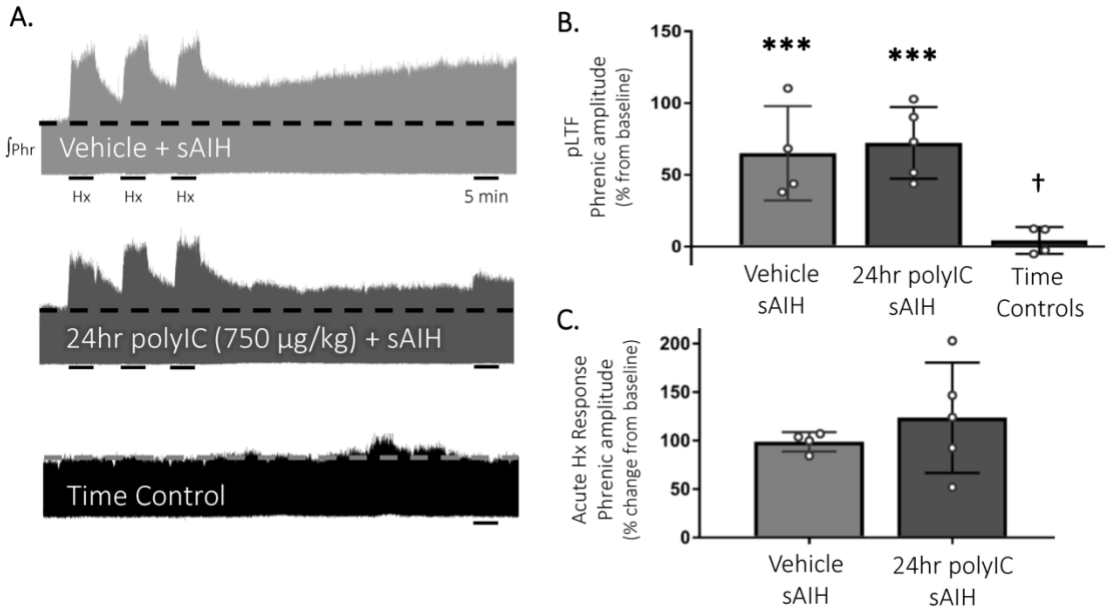

Figure 3.4. S-pathway-evoked pLTF persists 24 hours after the viral mimetic, polyIC. Representative integrated phrenic neurograms after polyIC (750 µg/kg, i.p., 24 hrs) (**A**). S-pathway-evoked pLTF is evident as the progressive increase in phrenic nerve amplitude from baseline (dashed line) over 60 minutes following severe acute intermittent hypoxia (sAIH, 3 x 5 minute episodes, PaO_2 25-35 mmHg). Group data (**B**) demonstrate S-pathway-evoked pLTF remains 24 hours after 750 µg/kg polyIC (n = 5). Time controls (no sAIH, n = 4) are not different from baseline and were significantly reduced from vehicle (n = 4) and 24hr polyIC groups. Acute hypoxic phrenic nerve responses to severe hypoxia (**C**) were not altered by polyIC. *** $p < 0.0001$ significant difference in phrenic amplitude from baseline; † $p < 0.001$ different from all other groups (ANOVA RM, Fisher LSD).

Physiological variables for all experimental groups were stable throughout electrophysiology experiments without any unexpected changes (Table 3.1).

Table 3.1. Physiological parameters during electrophysiology experiments.

Baseline	**Temperature (°C)**	**P_aO_2 (mmHg)**	**P_aCO_2 (mmHg)**	**pH**	**MAP (mmHg)**
750 µg/kg polyIC (3hr)	37.3 ± 0.2	282 ± 26	44.4 ± 1.1	7.36 ± 0.03	121 ± 14
750 µg/kg polyIC (24hr)	37.5 ± 0.4	268 ± 7	46.7 ± 2.4	7.35 ± 0.03	136 ± 24
500 µg/kg polyIC (24hr)	37.5 ± 0.3	287 ± 25	42.5 ± 3.4	7.38 ± 0.04	125 ± 17
250 µg/kg polyIC (24hr)	37.4 ± 0.3	279 ± 37	45.5 ± 3.9	7.34 ± 0.02	120 ± 26
Time Controls	37.5 ± 0.3	252 ± 29	45.6 ± 1.7	7.37 ± 0.02	123 ± 11
Vehicle + keto	37.5 ± 0.3	261 ± 28	43.8 ± 1.8	7.38 ± 0.02	123 ± 11
polyIC + keto	37.6 ± 0.1	267 ± 43	44.9 ± 2.3	7.35 ± 0.03	120 ± 22
Time Controls + keto	37.4 ± 0.4	246 ± 36	43.2 ± 2.0	7.37 ± 0.01	124 ± 28
Vehicle + sAIH	37.4 ± 0.3	262 ± 18	44.6 ± 2.4	7.39 ± 0.02	117 ± 5
polyIC + sAIH	37.3 ± 0.2	255 ± 29	44.9 ± 2.4	7.39 ± 0.03	118 ± 18
Time Controls	37.8 ± 0.1	260 ± 11	41.8 ± 1.1	7.4.0 ± 0.03	94 ± 19
Hypoxia					
750 µg/kg polyIC (3hr)	37.5 ± 0.2	42 ± 3 [ab]	43.6 ± 1.3	7.35 ± 0.02	98 ± 23 [a]
750 µg/kg polyIC (24hr)	37.4 ± 0.4	41 ± 4 [ab]	46.3 ± 1.8	7.34 ± 0.03	98 ± 35 [ab]
500 µg/kg polyIC (24hr)	37.3 ± 0.2	39 ± 2 [ab]	41.4 ± 4.3	7.38 ± 0.03	90 ± 30 [a]
250 µg/kg polyIC (24hr)	37.5 ± 0.4	41 ± 4 [ab]	45.5 ± 4.1	7.33 ± 0.02	102 ± 27
Time Controls	37.5 ± 0.3	260 ± 31 [c]	44.5 ± 1.9	7.37 ± 0.02	78 ± 29
Vehicle + keto	37.4 ± 0.4	35 ± 6 [ab]	42.4 ± 1.6	7.36 ± 0.01	78 ± 29 [ab]
polyIC + keto	37.7 ± 0.2	41 ± 4 [ab]	44.1 ± 1.8	7.33 ± 0.02	80 ± 30 [b]
Time Controls + keto	37.4 ± 0.4	260 ± 14 [c]	43.5 ± 2.0	7.38 ± 0.01	124 ± 28
Vehicle + sAIH	37.4 ± 0.3	29 ± 2 [ab]	43.7 ± 3.0	7.37 ± 0.04	70 ± 14 [ab]
polyIC + sAIH	37.4 ± 0.2	31 ± 4 [ab]	43.8 ± 1.2	7.37 ± 0.04	85 ± 15 [b]
Time Controls	37.8 ± 0.2	252 ± 8 [c]	41.0 ± 1.3	7.41 ± 0.01	94 ± 20
60 minutes					
750 µg/kg polyIC (3hr)	37.4 ± 0.4	272 ± 10	44.3 ± 1.6	7.37 ± 0.01	130 ± 12
750 µg/kg polyIC (24hr)	37.6 ± 0.2	238 ± 43	47.2 ± 2.8	7.34 ± 0.03	136 ± 32
500 µg/kg polyIC (24hr)	37.8 ± 0.3	250 ± 35	42.7 ± 3.5	7.38 ± 0.03	126 ± 20
250 µg/kg polyIC (24hr)	37.6 ± 0.3	247 ± 37	45.6 ± 3.9	7.33 ± 0.04	122 ± 21
Time Controls	37.6 ± 0.2	266 ± 66	45.2 ± 2.3	7.39 ± 0.02	114 ± 7
Vehicle + keto	37.5 ± 0.5	242 ± 40	44.9 ± 1.8	7.38 ± 0.02	114 ± 7
polyIC + keto	37.4 ± 0.3	268 ± 18	45.2 ± 2.3	7.34 ± 0.02	109 ± 21
Time Controls + keto	37.8 ± 0.0	236 ± 29	42.8 ± 1.8	7.39 ± 0.02	116 ± 28
Vehicle + sAIH	37.7 ± 0.4	250 ± 17	44.3 ± 2.0	7.38 ± 0.02	112 ± 13
polyIC + sAIH	37.6 ± 0.3	240 ± 19	44.9 ± 1.7	7.38 ± 0.03	115 ± 21
Time Controls	37.5 ± 0.3	252 ± 19	42.0 ± 1.0	7.40 ± 0.02	93 ± 20

MAP, mean arterial pressure; P_aO_2, arterial oxygen pressure; P_aCO_2, arterial carbon dioxide pressure. Statistical comparisons: ANOVA-RM, Tukey's post hoc: [a] different from 60 minutes timepoint within group, [b] different from baseline within group, [c] different from all other groups within timepoint

Discussion

To further our understanding of inflammation-induced impairment in adult respiratory motor plasticity, we investigated the impact of viral-mimetic-induced inflammation on Q- and S-pathway-evoked pLTF. Here, we demonstrate inflammatory impairment in respiratory motor plasticity is generalizable to viral-mimetic-induced inflammation. The viral-mimetic, polyIC, induced a transient increase in cervical spinal inflammatory gene expression and impaired Q-pathway-evoked pLTF. However, the time course of inflammatory impairment of pLTF is slower after polyIC compared to bacterial-induced inflammation (Huxtable et al., 2013). Additionally, S-pathway-evoked pLTF is resistant to polyIC-induced systemic inflammation, suggesting preferentially targeting S-pathway-evoked motor plasticity is an effective strategy to elicit a therapeutic benefit in conditions with coincident inflammation.

PolyIC is a commonly used viral-mimetic binding to TLR3 (Nicodemus and Berek, 2010) and is used here to induce systemic inflammation. In this study, 750 μg/kg polyIC (i.p.) was sufficient to induce ventral cervical spinal homogenate inflammatory gene expression within 3 hours, resolving by 24 hours. However, splenic inflammatory gene expression (a marker of systemic inflammation) showed no significant increase in inflammatory genes 3 or 24 hours after polyIC, suggesting this dose of polyIC induces relatively low-grade inflammation and has region-specific effects. These regional differences could be a result of differing mechanisms of peripheral to central inflammatory transmission, such as vagal transmission (Balan et al., 2011; Laye et al., 1995) or transmission through the blood brain barrier (Siljehav et al., 2012). Additionally, the blood-spinal cord barrier is more permeable to peripheral cytokines than the blood brain barrier

(Pan et al., 1997), suggesting increased spinal inflammation could be a result of faster peripheral inflammatory signal transmission from the periphery to the spinal cord relative to the medulla. However, our understanding of the detailed mechanisms underlying peripheral polyIC-induced central inflammation remain unclear (Dantzer, 2009; Konat et al., 2009) and warrant further investigation.

The time course of inflammatory gene expression after peripheral polyIC presented here is similar to increased cervical spinal inflammatory gene expression observed after peripheral LPS, which is elevated at 3 hours and similarly resolved by 24 hours (Huxtable et al., 2013). However, the magnitude of gene upregulation in spinal homogenates was substantially less following polyIC compared to LPS (Huxtable et al., 2013), suggesting 750 μg/kg polyIC is likely inducing a lower level of CNS inflammation. Yet, an inherent difficulty in comparing distinct inflammatory stimuli is identifying comparable doses. PolyIC dose-response experiments in rats demonstrate 750 μg/kg (i.p.) is sufficient to upregulate circulating cytokines and induce fever through an IL-1 dependent mechanism (Fortier et al., 2004). Therefore, 750 μg/kg polyIC is comparable to 100 μg/kg LPS since both induce similar febrile responses in rats (Boisse et al., 2005), and induce spinal inflammatory gene expression within 3 hours, but only LPS is sufficient to impair pLTF at 3 hours.

While LPS and polyIC both induce MAPKs, NF-κB, and increase pro-inflammatory gene expression, peripheral polyIC induces a slower onset and longer lasting upregulation of inflammatory gene expression in the CNS compared to LPS (Konat et al., 2009; Krasowska-Zoladek et al., 2007; Yamato et al., 2014). These differences may arise from differential downstream signaling mechanisms of polyIC compared to LPS, including

different TLR adaptor signaling (Matsumoto and Seya, 2008; Zhu et al., 2016) and TLR3-independent targets of polyIC (Hu et al., 2013; Matsumoto and Seya, 2008; McCartney et al., 2009; Starkhammar et al., 2012; Zhu et al., 2016). Alternatively, a temporal delay in polyIC-induced inflammatory protein expression may result in delayed or insufficient inflammation to impair plasticity 3 hours after polyIC. Additionally, we cannot rule out inflammatory changes in isolated cell types being diluted in homogenate samples, such as the changes seen in isolated microglia after LPS (Huxtable et al., 2013), nor the possibility of unmeasured inflammatory molecules playing an important role(s) in undermining plasticity. Any or all of these differences likely contribute to different time scales of pLTF impairment after polyIC (24 hour) compared to LPS (3 and 24 hour).

Q-pathway-evoked pLTF was not impaired 3 hours after polyIC, yet COX-2 gene expression transiently increased at 3 hours. Despite inducing neuroinflammation in regions of the CNS relevant to respiratory plasticity, it was not sufficient to impair plasticity. These findings support previous work demonstrating the inflammatory impairment of Q-pathway-evoked pLTF is COX-independent (Huxtable et al., 2017). However, 750 μg/kg polyIC was sufficient to abolish Q-pathway-evoked pLTF at 24 hours, when all measured inflammatory genes returned to baseline. Such findings match the results of Fortier et al., (2004), demonstrating 750 μg/kg polyIC was just above the threshold required to induce brain-mediated febrile responses. Thus, 750 μg/kg polyIC is above the threshold dose inducing CNS inflammatory responses and abolishing Q-pathway respiratory motor plasticity. Overall, these findings are similar to those observed 24 hours after LPS-induced inflammation (Huxtable et al., 2013), demonstrating the inflammatory impairment in Q-pathway-evoked plasticity is generalizable between inflammatory stimuli.

Acute ketoprofen after polyIC-induced inflammation restored Q-pathway-evoked pLTF, confirming the impairment of pLTF is inflammation-dependent. Ketoprofen inhibits both COX and NF-κB (Cashman, 1996; Yin et al., 1998). However, as COX inhibition does not restore Q-pathway-evoked pLTF after inflammation (Huxtable et al., 2017), the restoration of pLTF from ketoprofen is likely due to NF-κB inhibition, though we cannot rule out other off-target effects of ketoprofen. Regardless, our results indicate the viral mimetic polyIC induces cervical spinal inflammation and impairs Q-pathway-evoked pLTF in an inflammation-dependent manner. Previous work demonstrated the acute impairment of pLTF is downstream of serotonin receptors, upstream of BDNF signaling (Agosto-Marlin et al., 2018), and involves IL-1 receptors (Hocker and Huxtable, 2018) and p-38 MAPK activation (Huxtable et al., 2015). Future studies should further investigate more detailed cellular mechanisms by which inflammatory signaling impairs Q-pathway-evoked respiratory motor plasticity after both LPS- and polyIC-induced inflammation (summarized in Fig. 3.5).

S-pathway-evoked pLTF is a distinct molecular signaling pathway inducing facilitation of phrenic motor output and elicited by severe AIH through adenosine 2A receptor activation (Nichols et al., 2012). While Q-pathway-evoked pLTF is abolished by low-levels of inflammation from diverse stimuli (Huxtable et al., 2013, 2015), S-pathway-evoked pLTF is resistant to LPS-induced inflammation (Agosto-Marlin et al., 2017). Here, we demonstrate the inflammation resistance of S-pathway-evoked pLTF after polyIC-induced inflammation (Fig. 3.5). These findings contribute to the possibility S-pathway-evoked pLTF can serve as a "backup" mechanism to motor plasticity during low-level inflammation, even after Q-pathway-evoked pLTF is impaired.

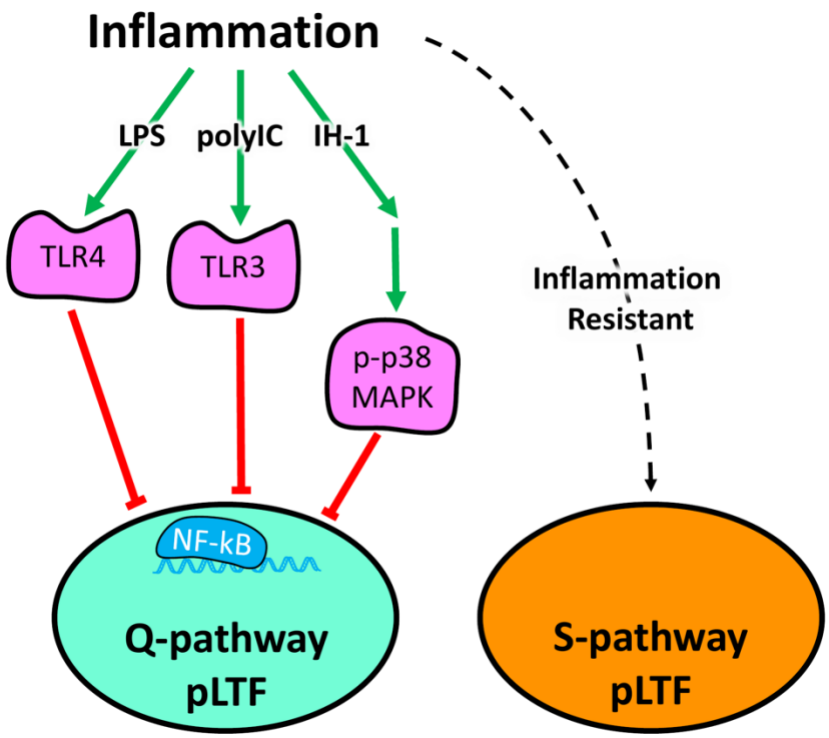

Figure 3.5. Schematic summarizing diverse inflammatory stimuli impair Q-pathway, but not S-pathway, adult respiratory motor plasticity. Lipopolysaccharide (LPS), polyinosinic:polycitidylic acid (polyIC), and one night of intermittent hypoxia (IH-1) activate peripheral inflammatory pathways and abolish Q-pathway-evoked pLTF. LPS and polyIC activate TLR4 and TLR3, respectively, to induce NF-kB activation and impair Q-pathway-evoked pLTF. IH-1-induced inflammation activates p38 MAPK and NF-kB to impair Q-pathway-evoked respiratory motor plasticity. Thus, multiple, diverse low-level inflammatory stimuli impair Q-pathway-evoked pLTF. S-pathway-evoked pLTF, however, is resistant to both LPS and polyIC-induced inflammation, suggesting it may act as a "backup" pathway after inflammation.

In summary, polyIC impairs Q-pathway, but not S-pathway-evoked, respiratory motor plasticity. Further, the inflammatory impairment of Q-pathway plasticity after polyIC relative to LPS is temporally delayed, though we do not have a detailed regional, time course of the inflammatory response following either polyIC or LPS. Such time course studies would facilitate a mechanistic understanding of the inflammatory impairment of Q-pathway plasticity. While the present studies were all performed in urethane-anesthetized rats, cellular mechanisms evoking respiratory plasticity appear similar between pLTF and

ventilatory LTF in freely behaving animals (McGuire et al., 2004, 2005, 2008), suggesting findings may be generalizable to ventilatory LTF. The present study focused on the impact of polyIC in adult male rats, highlighting the need for additional studies in females. However, the lack of sex differences observed in adults after neonatal inflammation (Hocker et al., 2019), suggest females would respond similarly to polyIC-induced inflammation. It is important to note pLTF in females is altered by cycling estrogen levels (Dougherty et al., 2017), which may also influence CNS inflammatory responses (Arakawa et al., 2014). Thus, future studies should address potential sex differences in the acute inflammatory impairment of pLTF and the inflammatory resistance of S-pathway-evoked plasticity in females.

In conclusion, this is the first study to evaluate the impact of viral-mimetic-induced inflammation on adult respiratory motor plasticity and demonstrates respiratory plasticity is profoundly sensitive to diverse inflammatory stimuli. Our results suggest the sensitivity of Q-pathway-evoked pLTF to inflammation is not stimulus specific and is impaired by viral, bacterial, and physiological inflammatory stimuli (Fig. 3.5). Further, S-pathway-evoked pLTF is resistant to viral mimetic-induced inflammation, supporting the notion S-pathway-evoked plasticity could compensate for Q-pathway impaired plasticity after inflammation (Fig. 3.5). Therefore, inflammation, which is common during disease and injury, can abolish the therapeutic potential of respiratory motor plasticity (Hayes et al., 2014; Mateika and Komnenov, 2017; Trumbower et al., 2012, 2017) and leave patients vulnerable to respiratory failure. Stimuli which preferentially elicit S-pathway-evoked plasticity are more likely to provide therapeutic benefit after inflammation.

CHAPTER IV

ONE BOUT OF NEONATAL INFLAMMATION IMPAIRS ADULT RESPIRATORY MOTOR PLASTICITY IN MALE AND FEMALE RATS

This chapter includes material previously published in the *eLife* (Hocker et al., 2019) which was co-authored by Sarah A. Beyeler, Alyssa N. Gardner, Stephen M. Johnson, Jyoti J. Watters, Adrianne G. Huxtable. I lead these studies, collected and analyzed all physiological data, analyzed gene expression and immunohistochemistry data, and wrote the paper. Alyssa Gardner collected gene expression data. Sarah Beyeler collected immunohistochemical data, contributed to writing the corresponding methods and results for the data, and gave editorial assistance. Adrianne Huxtable designed and contributed to writing the manuscript. Jyoti Watters contributed to writing the methods and results sections for the gene analysis data. Stephen Johnson, Joyti Watters, and Adrianne Huxtable provided guidance, oversight, and editorial assistance.

Introduction

At birth, neonates transition from a sterile maternal environment into an environment filled with pathogens, microbes, and toxins and must simultaneously begin robust, rhythmic breathing. Respiratory problems represent a significant clinical problem for neonatologists (Martin et al., 2012), especially in preterm infants where breathing is unstable (Poets et al., 1994; Poets and Southall, 1994) and infections are common (Stoll et al., 2002, 2004). Further, inflammation appears to augment respiratory dysfunction in neonates, whereby inflammation depresses hypoxic responses (Olsson et al., 2003;

Rourke et al., 2016) and induces recurrent apneas (Hofstetter et al., 2007). Despite the prevalence of early life inflammation, little is known about the long-lasting consequences of neonatal inflammation on adult neurorespiratory control.

We are beginning to understand the potential for long-term consequences of early life inflammation in other physiological systems. Neonatal inflammation blunts adult immune function (Bilbo et al., 2010; Mouihate et al., 2010; Spencer et al., 2011), increases adult stress reactivity (Grace et al., 2014; Shanks et al., 2000; Wang et al., 2013), impairs adult learning and hippocampal plasticity (Bilbo, 2005; Bilbo et al., 2006), increases the risk of neuropsychiatric disorders (Hornig et al., 1999; Rantakallio et al., 1997), and worsens age-related cognitive decline (Bilbo, 2010). Yet, we know very little about the long-term effects of neonatal inflammation on adult neurorespiratory control.

Respiratory plasticity is an important feature of the neural control of breathing, providing adaptability and maintenance of breathing when the respiratory system is challenged (Fuller and Mitchell, 2017). Phrenic long-term facilitation (pLTF) is a frequently studied adult model of respiratory motor plasticity (Mitchell and Johnson, 2003) and is elicited by at least two distinct cellular signaling pathways: the Q-pathway and the S-pathway (reviewed in Dale-Nagle *et al.*, 2010). The Q-pathway is evoked by moderate acute intermittent hypoxia (mAIH; 3x5 minute hypoxic episodes, PaO_2 35-45 mmHg) and is serotonin dependent, while the S-pathway is evoked by severe AIH (sAIH, PaO_2 25-35 mmHg) and is adenosine dependent (Nichols et al., 2012). Interestingly, Q-pathway-evoked plasticity is undermined by even low levels of acute, adult, systemic inflammation and restored by the non-steroidal anti-inflammatory, ketoprofen (Hocker and Huxtable, 2018; Huxtable et al., 2013; Vinit et al., 2011), while S-pathway-evoked

adult plasticity is inflammation resistant (Agosto-Marlin et al., 2017). Though we are beginning to understand more about the mechanisms of acute, adult inflammation on respiratory motor plasticity (Hocker et al., 2017; Hocker and Huxtable, 2018), we do not know how inflammation in early postnatal life impacts respiratory motor plasticity in the adult. Furthermore, few studies have investigated sex-differences in pLTF (Behan et al., 2002; Dougherty et al., 2017) and we know even less about sex-differences in respiratory control in response to inflammation. Additionally, males are more sensitive acutely to neonatal inflammation leading to higher male mortality in neonates (Bouman et al., 2005; Kentner et al., 2010; Rathod et al., 2017), but our understanding of other sex-differences after neonatal inflammation are unknown. Given the profound effects of neonatal inflammation on other physiological systems, we tested the hypothesis that neonatal inflammation undermines Q-pathway, but not S-pathway, respiratory motor plasticity in adult male and female rats.

Our results indicate that one, neonatal inflammatory challenge completely abolishes adult, AIH-induced Q-pathway and S-pathway respiratory motor plasticity. Despite no lasting increases in adult, inflammatory gene expression, Q-pathway impairment is inflammation-dependent and is restored by acute adult anti-inflammatory treatment. Conversely, S-pathway impairment is inflammation-independent, but can be evoked by intermittent adenosine receptor agonism, suggesting phrenic motor neurons are not impaired. Since astrocytes are a primary source of adenosine during hypoxia (Angelova et al., 2015; Takahashi et al., 2010), they are likely impaired by neonatal inflammation and contributing to impairment of respiratory plasticity. These studies are the first steps toward understanding the lasting effects of neonatal inflammation on adult

respiratory plasticity and suggest neonatal inflammation induces lasting-changes, increasing susceptibility to adult ventilatory control disorders.

Results

Neonatal inflammation acutely delays weight gain and increases male mortality.

Male and female postnatal day 4 (P4) rats were injected with either LPS (Lipopolysaccharide; 1mg/kg, i.p.) or saline. The dose of LPS was based on previous studies demonstrating CNS inflammatory gene expression in neonates (Rourke et al., 2016), as well as our unpublished data (N. Morrison, S. Johnson, J. Watters, A. Huxtable, unpublished observations). Within 24 hours of neonatal LPS injections, there was significantly greater mortality of male pups (8 of 67) than female pups (1 of 55, Fisher's exact test, $p = 0.04$, Fig. 4.1A). No mortality was evident in the saline treated males ($n = 63$) or females ($n = 63$). For the surviving pups, neonatal LPS males weighed significantly less at week 7 (no pairwise weight differences seen in females), but importantly, weights were not different in adults (Fig. 4.1B).

Adult, Q-pathway-evoked pLTF was undermined by neonatal inflammation, and was restored by acute, adult anti-inflammatory treatment.

Q-pathway-evoked pLTF is evident as the increase in integrated phrenic activity 60 minutes after mAIH (PaO_2 35-45 mmHg) in adult, anesthetized rats (Bach and Mitchell, 1996). As expected, in adult males treated with neonatal saline, Q-pathway-evoked pLTF was evident after mAIH (55 ± 33.2% change from baseline, $n = 7$, $p = 0.0006$, Fig. 4.2A and C). However, Q-pathway-evoked pLTF was absent in adult males

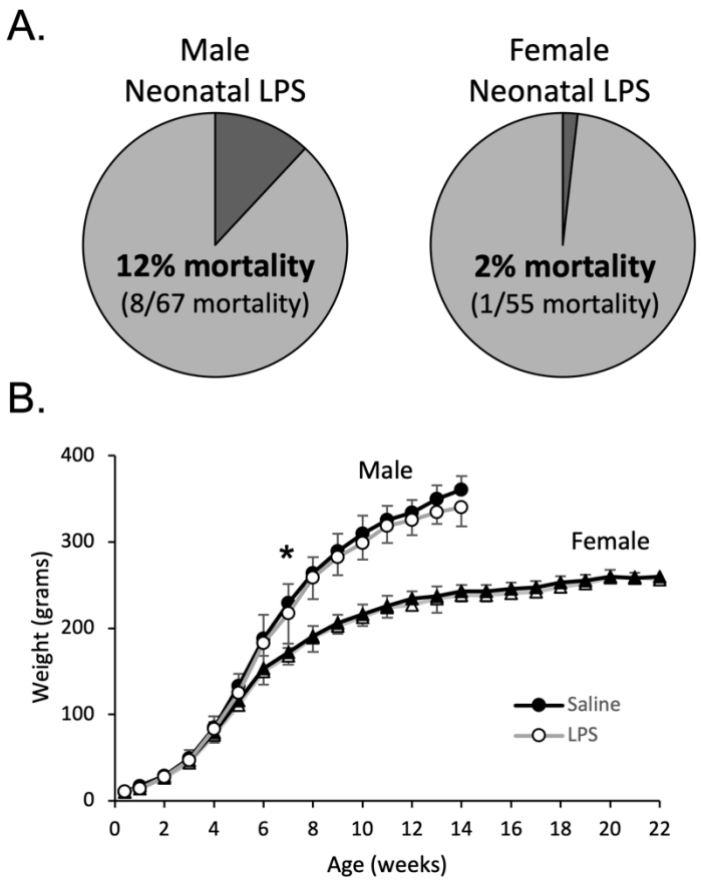

Figure 4.1. Neonatal inflammation increases mortality in neonatal males and transiently delays weight gain in male and female rats. After neonatal inflammation (P4, LPS 1 mg/kg, i.p.) male mortality **(A)** is increased within 24 hours (Fisher's exact test, $p = 0.006$), but not in females ($p = 0.466$), relative to saline controls. Weekly male and female weights **(B)** after neonatal saline or LPS demonstrate a transient impairment in male weight gain, but are unchanged from neonatal groups in adulthood. (* $p < 0.05$, significant pairwise difference within sex)

treated with neonatal LPS (14 ± 49%, n = 12, p = 0.2247 Fig. 4.2A and C). To control for the known effects of estrus cycle hormones on pLTF in females (Behan et al., 2002; Dougherty et al., 2017; Zabka et al., 2001), adult females were ovariectomized 7-8 days before electrophysiology studies. Similar to males, adult females treated with neonatal saline displayed Q-pathway-evoked pLTF (97 ± 63% change from baseline, n = 7, p < 0.0001, Fig. 4.2B and C), while adult females challenged with neonatal LPS did not

express pLTF (-15 ± 43%, n = 6, p = 0.4689, Fig. 4.2B and C). Phrenic amplitude did not change from baseline in the time control group (8 ± 6% change, n = 5, p = 0.6482), regardless of sex or neonatal LPS exposure and was significantly reduced compared to males or females treated with neonatal saline. Between groups, Q-pathway-evoked pLTF was significantly abolished in adults after neonatal LPS compared to adults after neonatal saline for both males (p = 0.0200) males and females (p < 0.0001). Thus, neonatal inflammation induces lasting impairment of adult, Q-pathway-evoked respiratory motor plasticity in both males and females.

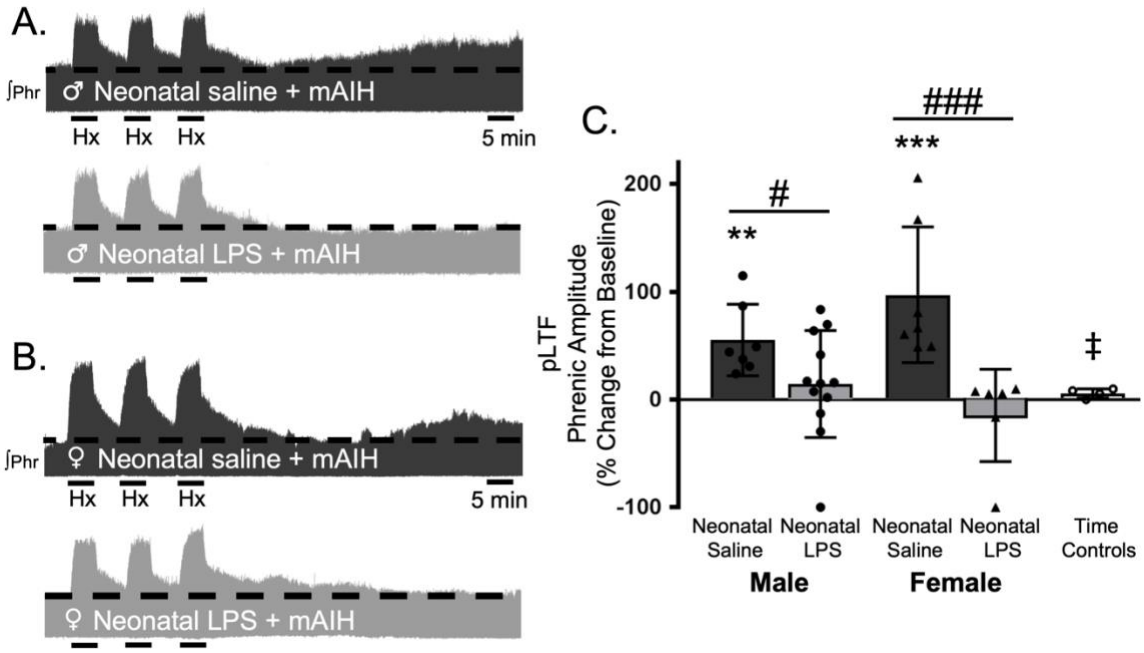

Figure 4.2. Neonatal systemic inflammation undermines adult, Q-pathway-evoked pLTF in male and female rats. Representative integrated phrenic neurograms from male **(A)** and female rats **(B)** after neonatal (P4) saline (top traces, black) or LPS (1 mg/kg, i.p.; bottom traces, grey). Q-pathway-evoked pLTF is evident in adults after neonatal saline as the progressive increase in phrenic nerve amplitude from baseline (dashed line) over 60 minutes following moderate acute intermittent hypoxia (mAIH, 3 x 5 minute episodes, PaO_2 35-45 mmHg). Group data **(C)** demonstrate Q-pathway-evoked pLTF 60 min after mAIH is abolished in adults by neonatal LPS in both males (circles) and females (triangles) and phrenic amplitude in male and female time controls is unchanged from baseline (** p < 0.01, *** p < 0.001 from baseline, # p < 0.05, ### p < 0.001 between groups, ‡ p < 0.05 from adult males and females after neonatal saline).

To test whether this lasting impairment of adult, respiratory motor plasticity was due to ongoing adult inflammation as a result of the neonatal inflammatory LPS challenge, we acutely treated adults with the non-steroidal anti-inflammatory, ketoprofen (12.5 mg/kg, i.p., 3 h), a high dose previously shown to restore plasticity after acute, adult inflammation (Huxtable et al., 2013). Ketoprofen treatment restored Q-pathway-evoked pLTF in adult males treated with neonatal LPS (58 ± 18% change from baseline, $n = 4$, $p = 0.0004$, Fig. 4.3A and C). Ketoprofen also restored Q-pathway-evoked pLTF in adult females treated with neonatal LPS (111 ± 44% from baseline, $n = 5$, $p < 0.0001$, Fig. 4.3B and C). Adults treated with neonatal saline (male: 54 ± 17% from baseline, $n = 4$, 0.0008; female: 89 ± 40%, $n = 5$, $p < 0.0001$) were unaffected by adult ketoprofen treatment. Additionally, phrenic motor amplitude did not change in adult time controls treated with ketoprofen (13 ± 14% change from baseline, $n = 4$, $p = 0.3436$) and was significantly reduced compared to all other groups. Between groups, pLTF was not different between adult males ($p = 0.7605$) or females ($p = 0.2932$) after neonatal saline or neonatal LPS, demonstrating the impairment in Q-pathway-evoked pLTF is inflammation-dependent in both males and females.

Neonatal inflammation did not induce chronic neuroinflammation in adult medulla or cervical spinal cords.

Because the lasting impairment of Q-pathway-evoked pLTF was inflammation-dependent, we examined whether neonatal inflammation had lasting effects on adult neuroinflammation in regions involved in respiratory neural control and motor plasticity.

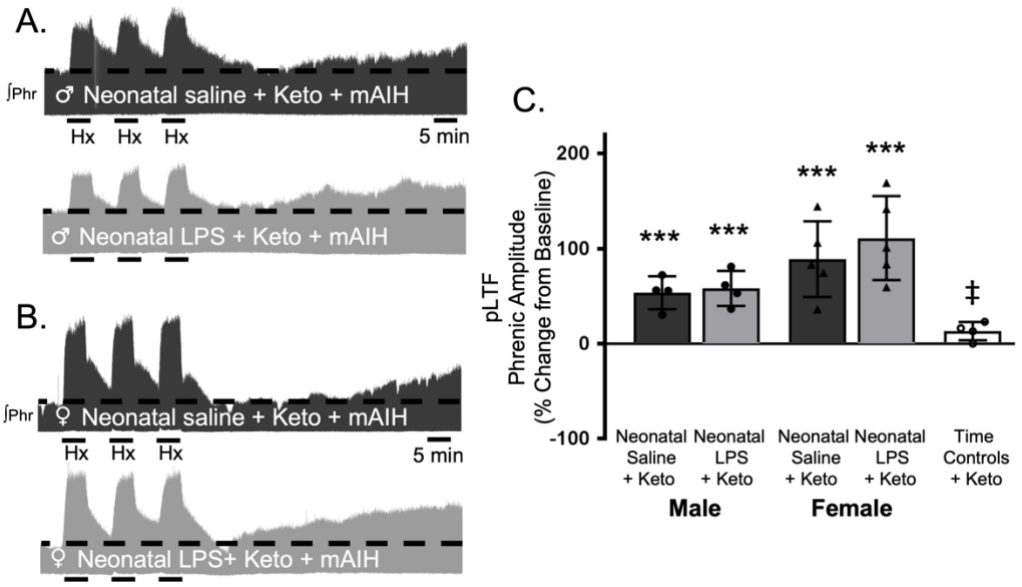

Figure 4.3. Acute, adult anti-inflammatory (ketoprofen, Keto) restores Q-pathway-evoked pLTF after neonatal systemic inflammation in adult male and female rats. Representative integrated phrenic neurograms for adult male **(A)** and female **(B)** rats after neonatal (P4) saline (top traces, black) or LPS (1 mg/kg, i.p.; bottom traces, grey) and acute, adult ketoprofen (12.5 mg/kg, i.p., 3 hr). Q-pathway-evoked pLTF is evident as the progressive increase in phrenic nerve amplitude from baseline (black dashed line) over 60 minutes following moderate acute intermittent hypoxia (mAIH, 3 x 5 minute episodes, PaO_2 35-45 mmHg). Group data **(C)** demonstrate adult ketoprofen restores Q-pathway-evoked pLTF 60 min after mAIH in adults after neonatal LPS in both males (circles) and females (triangles). Phrenic amplitude in male and female time controls is unchanged from baseline. (*** $p < 0.001$ from baseline, ‡ $p < 0.05$ from all other groups).

Since plasticity was abolished in both males and females, data from both sexes were combined for analysis of inflammatory genes. In medullary and cervical spinal homogenates, neonatal LPS did not significantly alter mRNA for adult inflammatory genes (IL-6, IL-1β, TNF-α, or iNOS; Fig. 4.4A and B). However, COX-2 gene expression was reduced in adult spinal cords after neonatal LPS (Fig. 4.4B, $p = 0.001$), suggesting a decrease in COX-dependent inflammatory signaling. Thus, there was no evidence for lasting increases in neuroinflammatory gene expression in adults after a single exposure of neonatal inflammation in respiratory control regions.

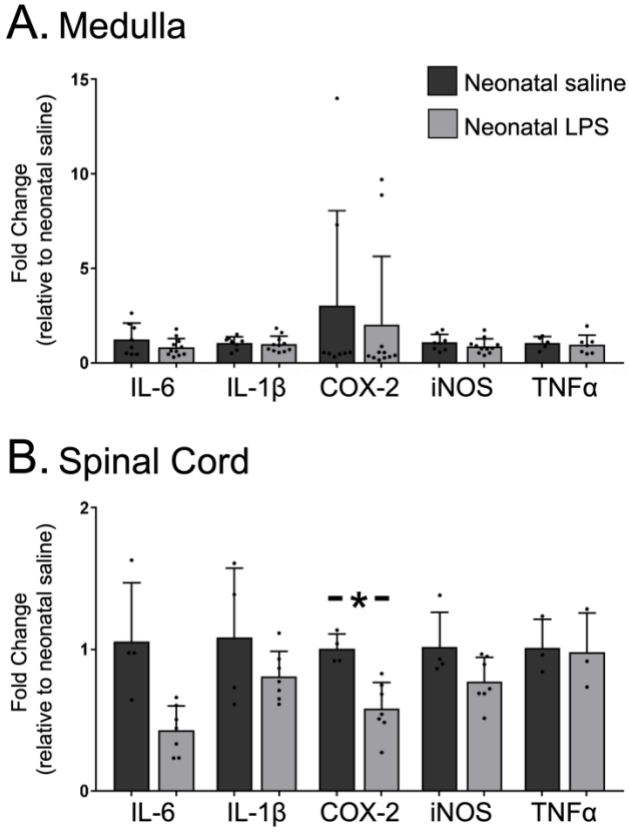

Figure 4.4. Neonatal inflammation does not increase adult medullary or spinal inflammatory gene expression. Homogenate samples isolated from adult medullas showed no significant increase in inflammatory mRNA after neonatal inflammation **(A)**. Similarly, homogenate samples from isolated adult cervical spinal cords **(C)** were not increased by neonatal inflammation, but *COX2* gene expression was significantly decreased in adults after neonatal inflammation (* $p < 0.05$).

Adult S-pathway-evoked pLTF was undermined by neonatal inflammation, not restored by adult anti-inflammatory treatment, but revealed by intermittent adenosine 2A receptor agonism.

S-pathway-evoked pLTF is evident as the increase in integrated phrenic activity 60 minutes after sAIH (PaO_2 25-35 mmHg) in adult rats. As expected, in adult males after neonatal saline, S-pathway-evoked pLTF was evident after sAIH (61 ± 69% change from baseline, n = 5, p = 0.0001, Fig. 4.5A and C). Contrary to our hypothesis, S-

pathway-evoked pLTF was abolished in adult males after neonatal LPS (7 ± 18% change from baseline, n = 4, p = 0.6770, Fig. 4.5A and C). In adult females after neonatal saline, S-pathway-evoked pLTF was evident (102 ± 47% change from baseline, n = 4, p < 0.0001, Fig. 4.5B and C). Similar to adult males treated with neonatal LPS, S-pathway-evoked pLTF was abolished in adult females after neonatal LPS (0 ± 33%, n = 4, p = 0.9796, Fig. 4.5B and C). Phrenic amplitude in the time control group was significantly less than males (p = 0.0147) or females (p < 0.0001) treated with neonatal saline. Between groups, S-pathway-evoked pLTF was significantly reduced after neonatal LPS in both adult males (p = 0.0180) and females (p < 0.0001) compared to adults after neonatal saline. Thus, neonatal inflammation induces lasting impairment of adult, S-pathway-evoked respiratory motor plasticity in both males and females.

To test whether this lasting impairment of adult, S-pathway-evoked plasticity is due to ongoing inflammation in adults after neonatal LPS, we examined sAIH-induced plasticity after an acute, adult treatment with ketoprofen (12.5mg/kg, i.p., 3 h). Ketoprofen did not alter normal expression of S-pathway-evoked pLTF in adult males after neonatal saline (63 ± 22% change from baseline, n = 5, p = 0.0014, Fig. 4.6A and C). However, contrary to the Q-pathway results, adult ketoprofen did not restore S-pathway-evoked pLTF in adult males after neonatal LPS (0 ± 65% change from baseline, n = 5, p = 0.9804, Fig. 4.6A and C). Similarly, adult females treated with neonatal saline also exhibited normal S-pathway-evoked pLTF after adult ketoprofen (130 ± 22% change from baseline, n = 5, 0.0803, Fig. 4.6B and C), and S-pathway-evoked pLTF was not

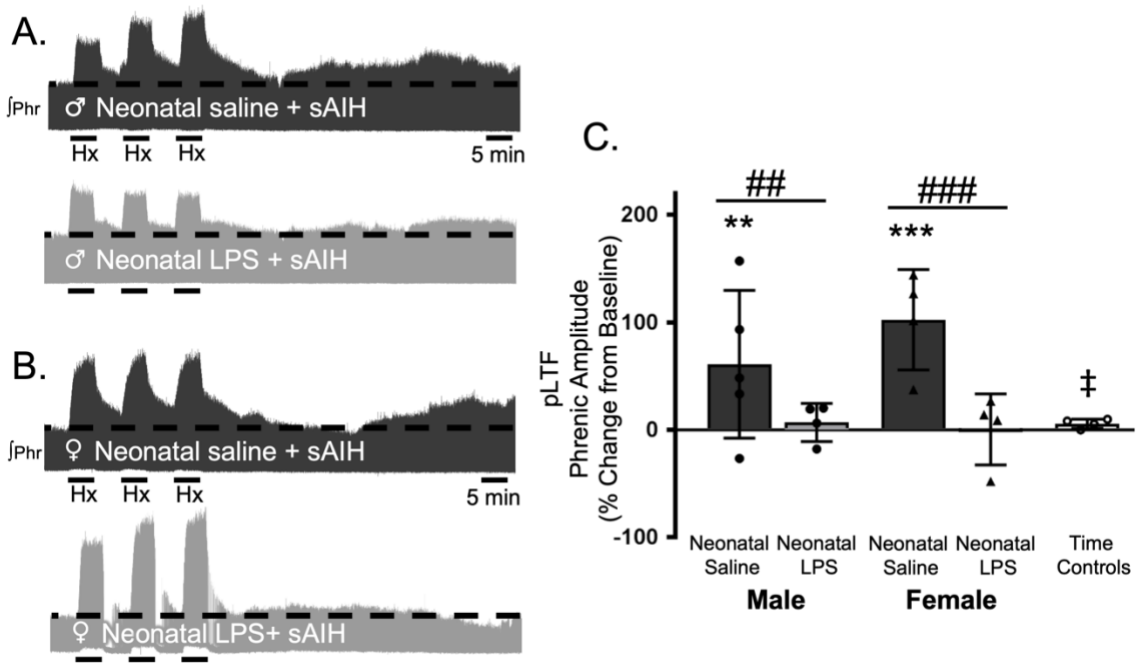

Figure 4.5. Neonatal systemic inflammation undermines adult, S-pathway-evoked pLTF in male and female rats. Representative integrated phrenic neurograms for adult male **(A)** and female **(B)** rats after neonatal (P4) saline (top traces, black) or LPS (1 mg/kg, i.p.; bottom traces, grey). S-pathway-evoked pLTF is evident as the progressive increase in phrenic nerve amplitude from baseline (black dashed line) over 60 minutes following severe acute intermittent hypoxia (sAIH, 3 x 5 minute episodes, PaO_2 25-35 mmHg) in adults after neonatal saline. Group data **(C)** demonstrate S-pathway-evoked pLTF 60 min after sAIH is abolished in adults by neonatal LPS in both males (circles) and females (triangles). Phrenic amplitude in male and female time controls is unchanged from baseline. (** $p < 0.01$, *** $p < 0.001$ from baseline ## $p < 0.01$, ### $p < 0.001$ between groups, ‡ $p < 0.05$ from male and female adults after neonatal saline).

restored by ketoprofen in adult females after neonatal LPS (25 ± 30% change from baseline, n = 6, p = 0.0803, Fig. 4.6B and C). Adult males and females treated with neonatal LPS and adult ketoprofen were not different from time controls (males, p =0.4964; females p = 0.5227). Between groups, S-pathway-evoked pLTF after acute ketoprofen was significantly reduced in adults after neonatal LPS comapred to adults after neonatal saline in both males (p = 0.0019) and females (p < 0.0001). Thus, neonatal

inflammation induces a lasting impairment of adult, S-pathway-evoked respiratory motor plasticity, which is not due to ongoing adult, inflammatory signaling.

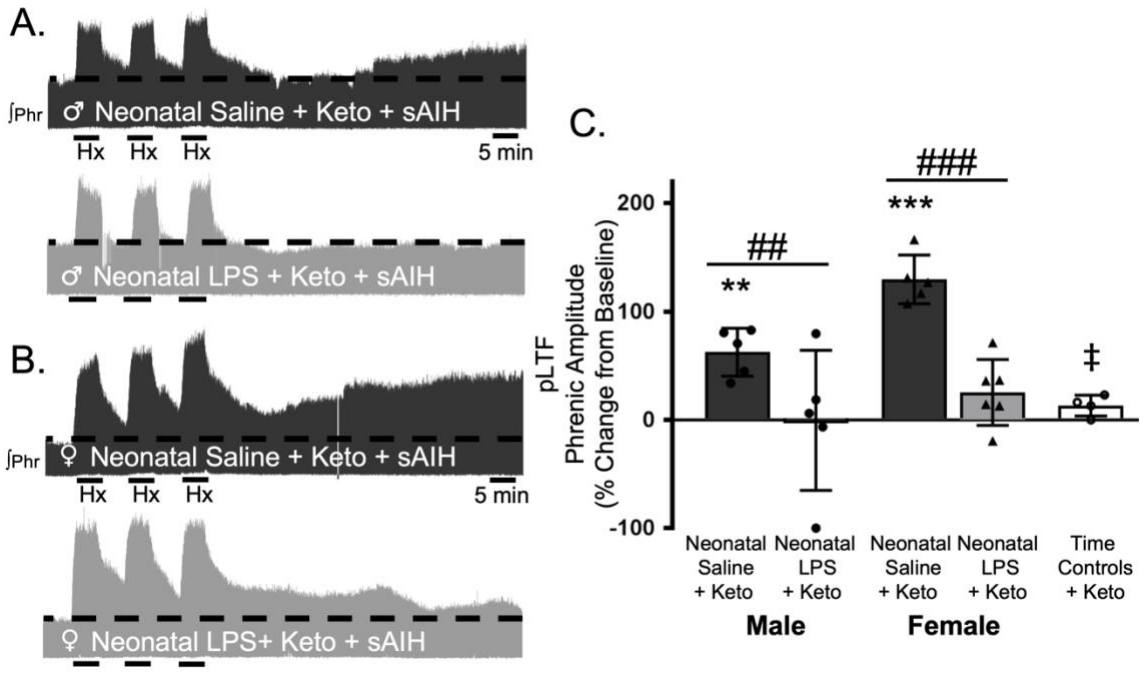

Figure 4.6. Adult, anti-inflammatory (ketoprofen, keto) does not restore S-pathway-evoked pLTF after neonatal systemic inflammation in adult male and female rats. Representative integrated phrenic neurograms for adult male **(A)** and female **(B)** rats after neonatal (P4) saline (top traces, black) or LPS (1 mg/kg, i.p.; bottom traces, grey) and acute, adult ketoprofen (12.5 mg/kg, i.p., 3 hr). S-pathway-evoked pLTF is evident as the progressive increase in phrenic nerve amplitude from baseline (black dashed line) over 60 minutes following severe acute intermittent hypoxia (sAIH, 3 x 5 minute episodes, PaO_2 35-45 mmHg) in adults after neonatal saline. Group data **(C)** demonstrate acute, adult ketoprofen does not restore S-pathway-evoked pLTF 60 min after sAIH after neonatal LPS in adult males (circles) and females (triangles). Phrenic amplitude in male and female time controls is unchanged from baseline. (** $p < 0.01$, *** $p < 0.001$ from baseline, ## $p < 0.01$, ### $p < 0.001$ between groups, ‡ $p < 0.05$ from adult males and females after neonatal saline).

S-pathway-evoked plasticity elicted by sAIH is adenosine dependent (Golder et al., 2008; Nichols et al., 2012) and can be evoked by intermittent CGS-21680, an adenosine 2A receptor agonist. To test if neonatal inflammation is impairing phrenic motor neurons and preventing pLTF, we examined phrenic output after intermittent CGS-

21680 on the cervical spinal cord, around the phrenic motor pool. Intrathecal CGS-21680 (100 µM, 3 x 10 µL) evoked phrenic motor plasticity in adult males after neonatal saline (110 ± 17% change from baseline, n = 4, $p < 0.001$, Fig. 4.7A and C) and females after neonatal saline (127 ± 47%, n = 4, $p < 0.001$, Fig. 4.7B and C). After neonatal LPS, intrathecal CGS-21680 also elicited plasticity in adult males (85 ± 64%, n = 6, $p < 0.001$, Fig. 4.7A and C) and adult females (147 ± 74%, n = 6, $p < 0.001$, Fig. 4.7B and C), demonstrating phrenic motor neurons are not impaired after neonatal inflammation and are capable of S-pathway-evoked plasticity. The vehicle control group was not different from baseline (-3 ± 5% change, n = 4, $p = 0.8891$) and significantly reduced compared to all other groups. Between groups, pLTF was not different between adult males ($p = 0.2841$) or females ($p = 0.4032$) after neonatal saline or neonatal LPS. Thus, adult phrenic motor neurons are not impaired after neonatal inflammation and are capable of plasticity after neonatal inflammation. Therefore, the source of intermittent adenosine release is impaired during sAIH-induced pLTF after neonatal inflammation.

Adult microglia and astrocyte density were not changed by neonatal inflammation.

While there was no evidence for elevated neuroinflammation based on the inflammatory genes evaluated here, the anti-inflammatory drug ketoprofen successfully restored Q-pathway-evoked plasticity. Additionally, our results indicate the impairment in S-pathway-evoked plasticity was likely due to a lasting change in adenosine signaling, possibly as a result of altered astrocytes. Thus, we hypothesized a lasting change in astrocytes and microglia in respiratory control regions, influencing neuronal function and

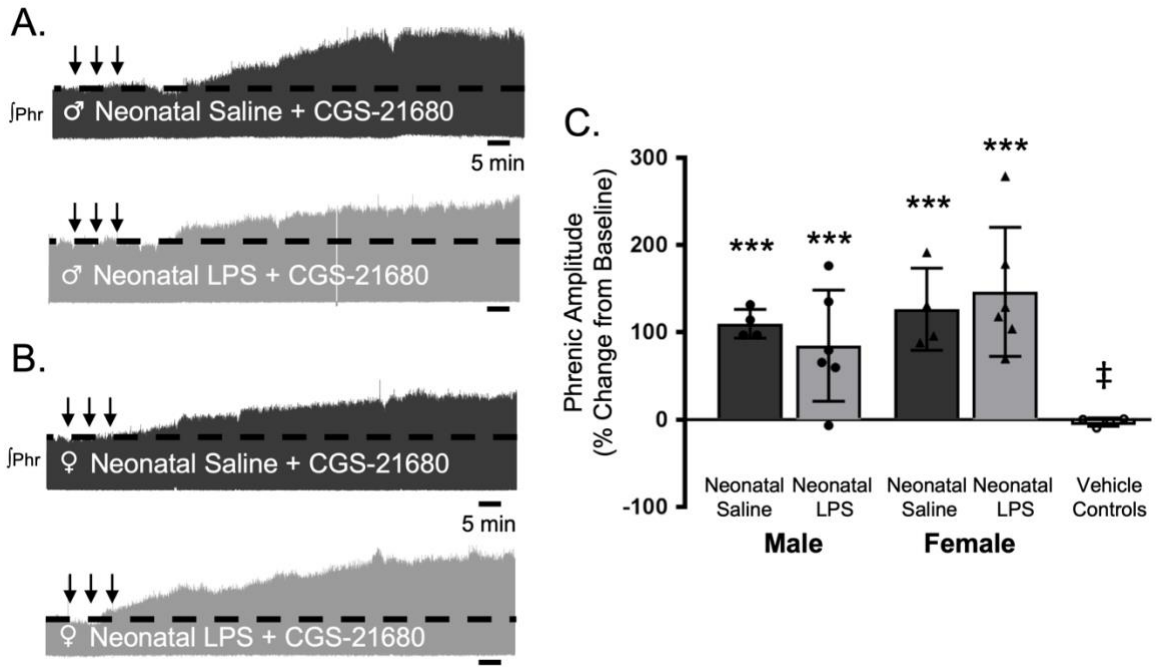

Figure 4.7. Intermittent adult, adenosine receptor agonism reveals plasticity after neonatal systemic inflammation in male and female rats. Representative integrated phrenic neurograms for adult male **(A)** and female **(B)** rats after neonatal (P4) saline (top traces, black) or LPS (1 mg/kg, i.p.; bottom traces, grey). S-pathway-evoked phrenic motor plasticity is evident as the progressive increase in phrenic nerve amplitude from baseline (black dashed line) 90 minutes after intermittent CGS-21680 (100 µM, black arrows, 3 x 5 minutes apart) in adults after neonatal saline. Group data **(C)** demonstrate adult CGS-21680 reveals S-pathway-evoked plasticity after neonatal LPS in adult males (circles) and females (triangles). Phrenic amplitude in male and female vehicle controls is unchanged from baseline. (*** $p < 0.001$ from baseline, ‡ $p < 0.001$ from adult males and females after neonatal saline).

impairing adult plasticity. We evaluated GFAP (astrocytes) and IBA1 (microglia) immunoreactivity in the adult preBötC, the site of respiratory rhythmogenesis (Smith et al., 1991), and in cervical spinal cords in the region of the phrenic motor nucleus, the presumptive site of pLTF (Baker-Herman et al., 2004; Dale et al., 2017; Devinney et al., 2015a). Neonatal inflammation did not alter GFAP ($p = 0.5969$) or IBA1 ($p = 0.6487$) immunoreactivity in adult preBötC in either sex (Fig. 4.8A, B, and E), suggesting astrocyte and microglial density were not changed in adults after neonatal inflammation.

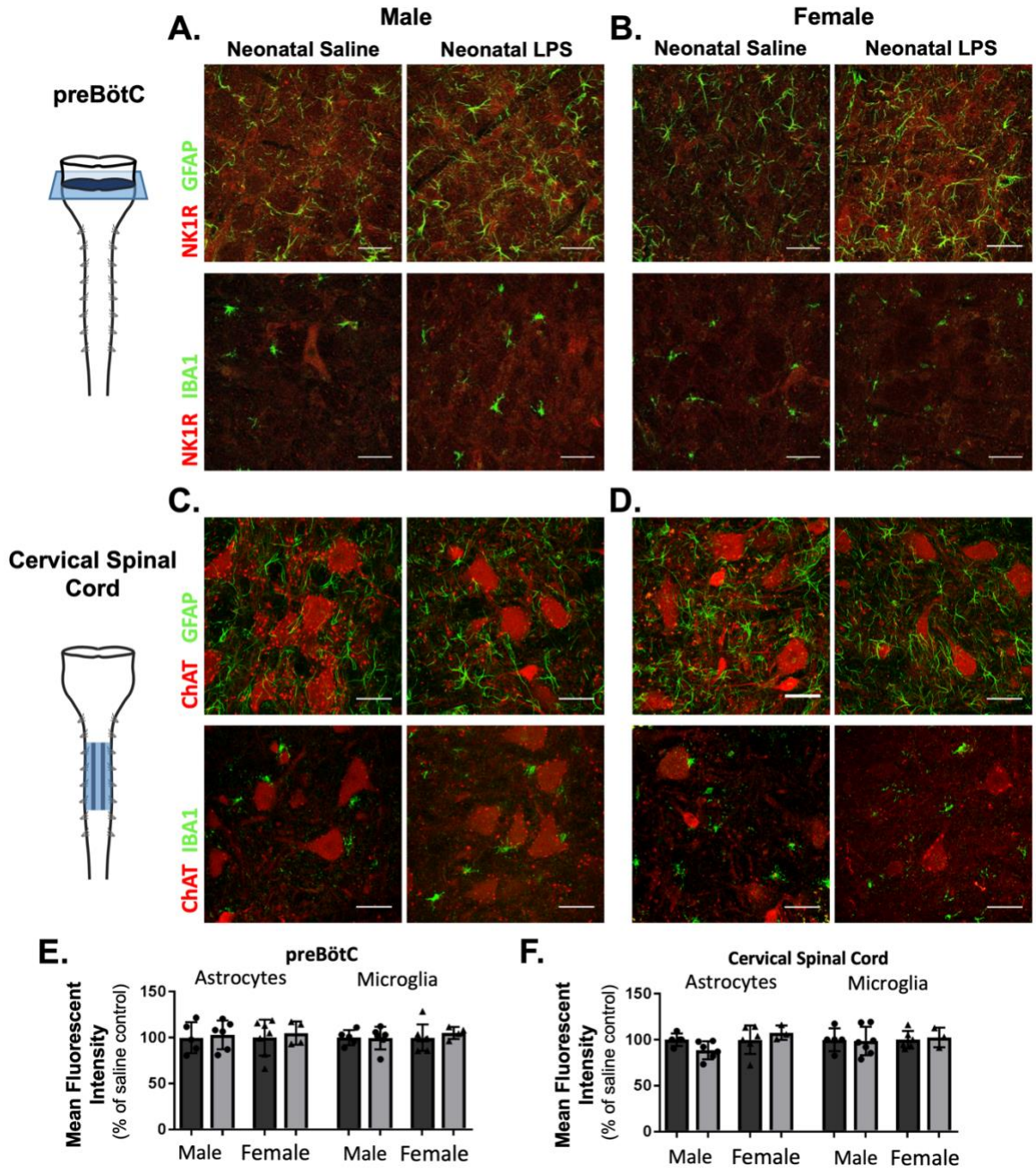

Figure 4.8. Neonatal inflammation does not alter GFAP or IBA1 immunofluorescence in adult preBötzinger Complex or ventral cervical spinal cords. After neonatal LPS (1 mg/kg, i.p., P4), representative confocal images (40x) from adult preBötC (A and B) and cervical spinal cords (C and D) displayed no qualitative differences in immunoreactivity for GFAP (green, astrocytes) or IBA1 (green, microglia) in males (left panels) or females (right panels). PreBötC neurons are labeled with antibodies for NK1R (red, **A and B**) and motor neurons are labeled with antibodies for ChAT (red, C and D). Neonatal inflammation did not significantly change mean fluorescent intensity of either GFAP or IBA1 in the preBötC (**E**) or cervical spinal cord (**F**), suggesting no lasting differences in astrocytes or microglia after neonatal inflammation. Scale bars: 50 µm.

Furthermore, there were no changes in GFAP ($p = 0.7195$) or IBA1 ($p = 0.9254$) immunoreactivity in adult cervical spinal cords (Fig. 4.8C, D and F), suggesting no lasting changes in astrocyte and microglia density in the region of the phrenic motor nucleus. Additionally, no obvious differences in astrocyte or microglial morphology in adult phrenic motor nuclei or the preBötC were seen following neonatal LPS inflammation, suggesting other signaling mechanisms are responsible for impairing adult pLTF.

Acute hypoxic phrenic responses were greater in females, but were unaffected by neonatal inflammation.

Neonatal inflammation did not significantly alter moderate acute hypoxic phrenic amplitude responses within adult males (neonatal saline = 114 ± 41% change from baseline; neonatal LPS = 93 ± 36%) or females (neonatal saline = 185 ± 53%; neonatal LPS = 148 ± 63%, Table 4.1). Hypoxic phrenic amplitude responses were also unaffected by the anti-inflammatory ketoprofen in adult males (neonatal saline + Keto = 118 ± 36%; neonatal LPS + Keto, 118 ± 44%) or females (neonatal saline + Keto, 165 ± 52%; neonatal LPS + Keto, 189 ± 82%, Table 4.1). However, adult females exhibited significantly greater acute phrenic amplitude responses to moderate hypoxia (main effect, $p = 0.0004$).

Phrenic amplitude in response to severe hypoxia was similarly unaltered by neonatal inflammation within adult males (neonatal saline = 139 ± 37% change from baseline; neonatal LPS = 106 ± 10%) or females (neonatal saline = 172 ± 125%; neonatal LPS = 172 ± 26%, Table 4.1). Acute ketoprofen pretreatment did not alter acute hypoxic

phrenic amplitude responses in adult males (neonatal saline = 151 ± 25% change from baseline; neonatal LPS, 174 ± 96%) or females (neonatal saline = 194 ± 45%; neonatal LPS = 235 ± 63%, Table 4.1). Similarly, adult females exhibited a significantly greater acute amplitude response to severe hypoxia than males (main effect, $p = 0.021$).

Table 4.1. Acute, adult hypoxic phrenic responses. Group data for adult, acute hypoxic phrenic responses to moderate (PaO_2 35-45 mmHg) and severe (PaO_2 25-35 mmHg) hypoxia demonstrate no differences after neonatal (P4) saline or LPS (1 mg/kg, i.p), or after adult ketoprofen (12.5 mg/kg, i.p, 3 hr) within each sex. Significant differences between sexes demonstrate larger responses in females after moderate or severe hypoxia († $p < 0.05$, ††† $p < 0.001$). [a] $p < 0.05$ from male neonatal LPS. Moderate hypoxia: neonatal saline male (n = 7), neonatal LPS male (n = 10), neonatal saline female (n = 6), neonatal LPS female (n = 6). Keto + Moderate hypoxia: neonatal saline male (n = 4), neonatal LPS male (n = 4), neonatal saline female (n = 5), neonatal LPS female (n = 5). Severe hypoxia: neonatal saline male (n = 5), neonatal LPS male (n = 4), neonatal saline female (n = 4), neonatal LPS female (n = 4). Keto + Moderate hypoxia: neonatal saline male (n = 5), neonatal LPS male (n = 5), neonatal saline female (n = 5), neonatal LPS female (n = 6)

	Male		**Female** †††	
	Neonatal Saline	Neonatal LPS	Neonatal Saline	Neonatal LPS
Moderate hypoxia	114 ± 41	93 ± 36	185 ± 53[a]	148 ± 63
Keto + Moderate hypoxia	118 ± 36	118 ± 44	165 ± 52	189 ± 82[a]
	Male		**Female** †	
	Neonatal Saline	Neonatal LPS	Neonatal Saline	Neonatal LPS
Severe hypoxia	139 ± 37	106 ± 10	172 ± 125	172 ± 26
Keto + Severe hypoxia	151 ± 25	174 ± 96	194 ± 45	235 ± 63

Physiological parameters and frequency plasticity

All physiological parameters remained within experimental limits (Table 4.1). Neonatal saline or LPS caused no significant changes in adult temperature, $PaCO_2$, PaO_2, or pH at baseline. There were no between group differences in baseline MAP, suggesting no long-lasting cardiovascular changes after neonatal inflammation. No significant changes occurred over time in temperature, pH, or $PaCO_2$ for any group. As expected, MAP and PaO_2 were significantly decreased during hypoxic episodes in experimental groups, but these changes were not evident in time control groups and were not different from baseline values at 60 minutes post-AIH.

Baseline phrenic burst frequency was not significantly different between groups and frequency plasticity, an increase in burst frequency 60 minutes after AIH , was not evident in any group. Phrenic burst frequency did not change after intrathecal CGS-21680.

Table 4.2. (next page) Physiological parameters during electrophysiology experiments. MAP, mean arterial pressure; P_aO_2, arterial oxygen pressure; P_aCO_2, arterial carbon dioxide pressure. Neonatal Saline + mAIH male (n = 7) female (n = 7); Neonatal LPS + mAIH male (n = 12) female (n = 6); Neonatal Saline + Keto + mAIH male (n = 4) female (n = 5); Neonatal LPS + Keto + mAIH male (n = 4) female (n = 5); Neonatal Saline + sAIH male (n = 5) female (n = 4); Neonatal LPS + sAIH male (n = 4) female (n = 4); Neonatal Saline + Keto + sAIH male (n = 5) female (n = 5); Neonatal LPS + Keto + sAIH male (n = 5) female (n = 6); Time Control (n = 5); Time Control + Keto (n = 4). Statistical comparisons: ANOVA-RM, Tukey's post hoc: [a] different from Time control within time point, [b] different from TC + Keto within time point, [c] different from baseline and 60 min, [d] different from baseline, [e] different from female neonatal LPS + Keto + sAIH within time point, [f] different from female LPS within time poi

	Temperature (°C)		P_aO_2 (mmHg)		P_aCO_2 (mmHg)		pH		MAP (mmHg)	
Baseline	Male	Female	Male	Female	Male	Female	Male	Female	Male	Female
Neonatal Saline + mAIH	37.4 ± 0.2	37.4 ± 0.2	254 ± 19	259 ± 53	43.2 ± 5.6	48.9 ± 3.7	7.37 ± 0.06	7.36 ± 0.02	124 ± 9	121 ± 18
Neonatal LPS + mAIH	37.6 ± 0.2	37.5 ± 0.2	266 ± 30	268 ± 24	42.8 ± 4.7[e]	45.0 ± 1.8	7.37 ± 0.04	7.37 ± 0.02	127 ± 10	123 ± 23
Neonatal Saline + Keto + mAIH	37.3 ± 0.1	37.4 ± 0.3	249 ± 21	255 ± 28	41.7 ± 4.9	48.6 ± 3.5	7.38 ± 0.03	7.33 ± 0.02	132 ± 8	121 ± 12
Neonatal LPS + Keto + mAIH	37.4 ± 0.2	37.4 ± 0.3	276 ± 40	283 ± 33	41.5 ± 3.2	47.9 ± 3.6	7.39 ± 0.03	7.34 ± 0.02	129 ± 16	117 ± 14
Neonatal Saline + sAIH	37.6 ± 0.3	37.5 ± 0.2	295 ± 18	266 ± 9	43.3 ± 5.9	47.7 ± 3.1	7.37 ± 0.02	7.36 ± 0.00	133 ± 6	121 ± 19
Neonatal LPS + sAIH	37.4 ± 0.1	37.4 ± 0.4	297 ± 28	264 ± 35	45.3 ± 4.2	47.7 ± 4.0	7.36 ± 0.02	7.36 ± 0.02	135 ± 20	132 ± 14
Neonatal Saline + Keto + sAIH	37.4 ± 0.3	37.5 ± 0.1	256 ± 46	268 ± 29	41.6 ± 2.2[e]	49.9 ± 3.5	7.39 ± 0.03	7.34 ± 0.02	110 ± 12	113 ± 29
Neonatal LPS + Keto + sAIH	37.5 ± 0.2	37.4 ± 0.2	243 ± 45	245 ± 39	42.3 ± 3.4	51.6 ± 6.8	7.37 ± 0.01	7.31 ± 0.04	121 ± 3	129 ± 13
Neonatal Saline + CGS-21680	37.5 ± 0.2	37.3 ± 0.2	268 ± 21	237 ± 14	45.4 ± 5.3	46.2 ± 3	7.36 ± 0.04	7.34 ± 0.03	119 ± 24	121 ± 10
Neonatal LPS + CGS-21680	37.6 ± 0.3	37.4 ± 0.3	247 ± 27	247 ± 21	46.2 ± 2.9	46.6 ± 2.7	7.37 ± 0.02	7.34 ± 0.02	114 ± 12	107 ± 15
Time Controls	37.7 ± 0.1		250 ± 45		49.4 ± 4.0		7.36 ± 0.05		110 ± 10	
Time Controls + Keto	37.5 ± 0.3		250 ± 17		44.0 ± 9.1		7.37 ± 0.06		115 ± 39	
CGS-21680 Vehicle Controls	37.4 ± 0.3		237 ± 40		45.8 ± 0.8		7.37 ± 0.03		110 ± 17	
Hypoxia										
Neonatal Saline + mAIH	37.4 ± 0.2	37.3 ± 0.1	38 ± 2[abc]	40 ± 3[abc]	42.2 ± 5.1[e]	48.8 ± 3.8	7.35 ± 0.07	7.36 ± 0.03[e]	62 ± 23[abc]	65 ± 30[abc]
Neonatal LPS + mAIH	37.5 ± 0.4	37.4 ± 0.1	39 ± 2[abc]	39 ± 4[abc]	43.0 ± 4.8[e]	45.4 ± 2.8	7.36 ± 0.04[e]	7.36 ± 0.02[e]	68 ± 19[abc]	80 ± 21[c]
Neonatal Saline + Keto + mAIH	37.5 ± 0.2	37.4 ± 0.3	38 ± 1[abc]	39 ± 3[abc]	41.9 ± 3.5	48.6 ± 3.7	7.37 ± 0.03[e]	7.32 ± 0.04	62 ± 11[c]	56 ± 6[abc]
Neonatal LPS + Keto + mAIH	37.5 ± 0.2	37.5 ± 0.3	40 ± 2[abc]	39 ± 4[abc]	40.9 ± 2.2[e]	47.8 ± 4.9	7.36 ± 0.04	7.32 ± 0.03	71 ± 14[c]	66 ± 19[c]
Neonatal Saline + sAIH	37.6 ± 0.2	37.4 ± 0.3	29 ± 5[abc]	29 ± 2[abc]	43.5 ± 5.9	47.7 ± 2.3	7.35 ± 0.03	7.32 ± 0.06	58 ± 9[abc]	53 ± 11[abc]
Neonatal LPS + sAIH	37.4 ± 0.3	37.5 ± 0.3	30 ± 4[abc]	31 ± 5[abc]	46.3 ± 4.2	47.3 ± 5.9	7.34 ± 0.03	7.31 ± 0.03	61 ± 20[c]	59 ± 20[abc]
Neonatal Saline + Keto + sAIH	37.4 ± 0.2	37.5 ± 0.2	30 ± 2[abc]	32 ± 3[abc]	42.3 ± 2.2[e]	48.9 ± 3.7	7.36 ± 0.03	7.29 ± 0.03	34 ± 8[abcf]	45 ± 29[abc]
Neonatal LPS + Keto + sAIH	37.3 ± 0.3	37.6 ± 0.2	31 ± 2[abc]	32 ± 1[abc]	42.2 ± 3.2[e]	52.2 ± 5.8	7.34 ± 0.03	7.28 ± 0.06	37 ± 11[abcf]	43 ± 21[abc]
Time Controls	37.6 ± 0.3		226 ± 40		48.7 ± 4.7		7.35 ± 0.04		107 ± 13	
Time Controls + Keto	37.5 ± 0.2		258 ± 13		45.5 ± 9.3		7.37 ± 0.06[e]		109 ± 44	
60 minutes										
Neonatal Saline + mAIH	37.5 ± 0.4	37.3 ± 0.1	234 ± 28	259 ± 22	43.4 ± 5.7	48.6 ± 3.7	7.38 ± 0.05[e]	7.35 ± 0.02	114 ± 9	117 ± 27
Neonatal LPS + mAIH	37.5 ± 0.3	37.4 ± 0.3	253 ± 19	268 ± 23[a]	42.9 ± 4.4[e]	45.2 ± 2.6	7.39 ± 0.04[e]	7.37 ± 0.01	116 ± 14	121 ± 25
Neonatal Saline + Keto + mAIH	37.3 ± 0.2	37.3 ± 0.3	262 ± 14	257 ± 32	42.5 ± 4.9	48.7 ± 4.0	7.38 ± 0.01	7.33 ± 0.04	121 ± 13	115 ± 11
Neonatal LPS + Keto + mAIH	37.6 ± 0.3	37.6 ± 0.3	257 ± 18	276 ± 40[a]	41.5 ± 2.7	47.8 ± 3.6	7.36 ± 0.02	7.34 ± 0.06	123 ± 11	112 ± 18
Neonatal Saline + sAIH	37.5 ± 0.3	37.4 ± 0.2	262 ± 36	258 ± 19	43.7 ± 5.5	47.6 ± 2.9	7.37 ± 0.04	7.32 ± 0.03	135 ± 9	115 ± 24
Neonatal LPS + sAIH	37.7 ± 0.2	37.4 ± 0.2	282 ± 16[a]	266 ± 18	46.2 ± 4.8	47.7 ± 4.5	7.36 ± 0.02	7.35 ± 0.02	127 ± 14	128 ± 17
Neonatal Saline + Keto + sAIH	37.7 ± 0.3	37.4 ± 0.3	248 ± 42	262 ± 9	42.3 ± 2.6	50.2 ± 4.2	7.37 ± 0.03	7.32 ± 0.03[d]	105 ± 10	109 ± 36
Neonatal LPS + Keto + sAIH	37.5 ± 0.2	37.4 ± 0.3	252 ± 24	245 ± 21	42.2 ± 3	51.2 ± 6.9	7.38 ± 0.02	7.31 ± 0.04	117 ± 14	125 ± 19
Neonatal Saline + CGS-21680	37.3 ± 0.3	37.6 ± 0.1	270 ± 46	215 ± 48	45.7 ± 4.9	47 ± 3.3	7.34 ± 0.06	7.35 ± 0.04	112 ± 30	126 ± 21
Neonatal LPS + CGS-21680	37.4 ± 0.4	37.4 ± 0.4	254 ± 26	256 ± 21	46.1 ± 3.2	46.5 ± 3.2	7.37 ± 0.01	7.33 ± 0.04	107 ± 16	101 ± 25
Time Controls	37.5 ± 0.3		220 ± 25		48.4 ± 3.7		7.36 ± 0.04		102 ± 22	
Time Controls + Keto	37.6 ± 0.2		272 ± 21		44.3 ± 8.7		7.37 ± 0.07		111 ± 48	
CGS-21680 Vehicle Controls	37.6 ± 0.2		271 ± 27		45.4 ± 1.6		7.36 ± 0.03		108 ± 7	

Discussion

Although neonatal inflammation is common (Stoll et al., 2002, 2004), little is known concerning how neonatal inflammation alters ventilatory control. Here, we investigated the long-term consequences of neonatal systemic inflammation on adult respiratory motor plasticity, a key feature of the neural control of breathing providing adaptability to respiratory system challenges (Mitchell and Johnson, 2003). We show for the first time that a single inflammatory challenge to neonates completely abolishes AIH-induced Q-pathway and S-pathway-evoked respiratory motor plasticity in adult males and females. Our results indicate a persistent change in adult inflammatory signaling contributes to this impairment since adult anti-inflammatory treatment restores Q-pathway-evoked, but not S-pathway-evoked, pLTF. Further, this is the first evidence of impairment of S-pathway-evoked motor plasticity, suggesting neonatal inflammation likely leads to a further vulnerable adult as this pathway was thought of as a "backup pathway" after acute, adult inflammation (Agosto-Marlin et al., 2017). However, we demonstrate S-pathway plasticity can be revealed by intermittent, spinal adenosine receptor agonism, suggesting astrocyte dysfunction after neonatal inflammation since they are the likely source of adenosine during hypoxia (Angelova et al., 2015; Takahashi et al., 2010). These studies are the first steps toward understanding the lasting effects of neonatal inflammation on adult neurorespiratory control and suggest neonatal inflammation may increase susceptibility to adult ventilatory control disorders.

LPS-induced neonatal inflammation transiently upregulates cytokines in regions involved in respiratory control and plasticity (N. Morrison, S. Johnson, J. Watters, A. Huxtable, unpublished observations), consistent with inflammatory profiles in other CNS

regions (Bilbo and Schwarz, 2012; Jafri et al., 2013; Schwarz and Bilbo, 2011; Wang et al., 2006). Neonatal inflammation also increases male mortality, consistent with clinical male mortality after neonatal inflammation (Person et al., 2014) and is relevant to the increased risk of sudden infant death syndrome for males (Kinney and Thach, 2009). However, similar to other studies (Bilbo et al., 2005; Mouihate et al., 2010; Smith et al., 2014), we found no measurable adult changes in cytokines, or glial number or morphology despite a lasting inflammation-dependent impairment in Q-pathway-evoked pLTF. While, we have previously demonstrated adult Q-pathway pLTF is sensitive to low levels of acute, systemic inflammation (Hocker and Huxtable, 2018; Huxtable et al., 2011, 2013, 2015, 2017; Vinit et al., 2011), this is the first study to demonstrate neonatal inflammation induces lasting changes in inflammatory signaling to undermine adult Q-pathway-evoked pLTF. Additionally, S-pathway-evoked pLTF is not restored by even the high dose of ketoprofen used here, but is revealed by intermittent adenosine 2A receptor agonism on phrenic motor neurons (Seven et al., 2018). While the adenosine 2A receptor agonist may affect other cell-types in the cervical spinal cord and complicate our findings, adenosine 2A receptors are primarily located on phrenic motor neurons in the cervical spinal cord (Seven et al., 2018) and their expression on phrenic motor neurons is required for pLTF (Seven et al., 2018). Thus, these results indicate phrenic motor neurons are not impaired after neonatal inflammation and the loss of S-pathway-evoked plasticity is likely due to impaired adenosine signaling during hypoxia. Furthermore, a likely source of adenosine during hypoxia is astrocytes (Angelova et al., 2015; Takahashi et al., 2010), suggesting neonatal inflammation induces lasting astrocyte-specific changes in the adult spinal cord to impair adult S-pathway-evoked pLTF. Further understanding the

mechanisms impairing distinct forms of respiratory motor plasticity is required to develop plasticity as a therapeutic tool, such as for spinal cord injury and amyotrophic lateral sclerosis (Gonzalez-Rothi et al., 2015; Mitchell, 2008). Additionally, considering the cross-talk between Q- and S-pathways (Dale-Nagle et al., 2010; Fields and Mitchell, 2015; Perim et al., 2018), the response of the respiratory control system likely depends on the functional status of both Q- and S-pathways. Thus, future studies are needed to understand how inflammation modifies cross-talk between Q- and S-pathways and how respiratory motor plasticity can be exploited therapeutically (Gonzalez-Rothi et al., 2015).

The timing of neonatal inflammation is likely a significant factor in how neonatal inflammation impacts adult physiology. Low-levels of cytokines are important for neurodevelopment (Bilbo and Schwarz, 2009), and perturbing the balance of neonatal cytokines during development leads to lasting aberrant effects on neural circuits and developing cells (Reemst et al., 2016). Furthermore, while many components of the respiratory system begin developing *in utero* (Johnson et al., 2017; Mantilla and Sieck, 2008; Pagliardini et al., 2003; Prakash et al., 2000), the respiratory control system undergoes significant postnatal maturation. In these studies, we induced systemic inflammation with LPS at P4, similar to other studies showing long-term consequences of neonatal inflammation in other physiological systems (Bilbo, 2010; Fan et al., 2008; Kohman et al., 2008; Shanks et al., 2000; Walker et al., 2006), supporting the idea that important neural changes occur within the first week of life. Yet, it remains to be determined whether there is a precise critical period where neonatal inflammation impacts respiratory control circuits. However, our data on male mortality after neonatal

LPS are consistent with other critical developmental windows, including a male-specific sensitive period to LPS (Rourke et al., 2016), disproportionate male mortality from neonatal inflammation (Person et al., 2014), the increased risk of sudden infant death syndrome for males (Kinney and Thach, 2009), and increased incidence of obstructive sleep apnea in adults after neonatal inflammation (McNamara and Sullivan, 2000). Thus, these data have important implications for understanding the sex-specific impairment early in life and into adulthood. Additionally, we and others (Spencer et al., 2006) observed a short delay in weight gain after neonatal inflammation, which normalized by weaning, suggesting no lasting effects on growth. Future studies are needed to refine our understanding of the critical periods during development when early-life inflammation induces long-lasting physiological changes to improve our understanding of adult disease and better understand important developmental processes.

While other reports have shown sex differences in neonatal programming of adult neuroinflammatory responses (LaPrairie and Murphy, 2007; Rana et al., 2012), we observed no sex-differences in the effects of neonatal inflammation on adult plasticity. Importantly, this is the first evidence of inflammation abolishing pLTF in females and the first to report sAIH-induced respiratory motor plasticity in females. Females exhibited greater acute hypoxic phrenic amplitude responses relative to males, consistent with previous findings (Bavis et al., 2004; Mortola and Saiki, 1996), despite variability in reports of sex differences in hypoxic ventilatory responses (Behan and Kinkead, 2011). In contrast to our results following neonatal inflammation, neonatal stress alters adult hypoxic responses in a sex-dependent manner, whereby male responses are enhanced and female responses are blunted (Rousseau et al., 2017). Thus, the long-term effects on

respiratory control may be dependent on the type of stressors in early life. Importantly, our experiments were performed in adult, ovariectomized females with exogenously restored estradiol levels to permit respiratory motor plasticity (Behan et al., 2002; Dougherty et al., 2017; Zabka et al., 2003). Therefore, as sex hormones are known to modulate respiratory control and hypoxic responses (Behan and Kinkead, 2011; Nelson et al., 2011), we cannot rule out a confounding role for exogenous estradiol supplementation after ovariectomy. Finally, after neonatal inflammation, we found no differences in adult hypoxic responses, suggesting no lasting change in carotid body responses due to neonatal inflammation. Accordingly, the deficit in adult respiratory motor plasticity after neonatal inflammation is likely a consequence of long-term changes in the spinal cord where pLTF occurs (Baker-Herman et al., 2004; Dale et al., 2017; Devinney et al., 2015a).

While adult anti-inflammatory treatment restored Q-pathway-evoked pLTF, we did not observe increases in inflammatory gene expression in adult medullary or cervical spinal cord homogenates. Thus, while inflammatory signaling contributes to the impairment of adult plasticity, the source of this signaling change remains unclear and will be the topic of future studies. Similarly, others demonstrated no changes in baseline CNS inflammatory markers after neonatal inflammation, but observed priming of glial responses to adult stimuli (Bilbo et al., 2005; Mouihate et al., 2010; Smith et al., 2014), suggesting lasting changes in glia have the potential to underlie impairments in adult respiratory plasticity. Contrary to other reports (Boisse et al., 2005; Kentner et al., 2010), we found spinal COX-2 gene expression was decreased in adulthood, suggesting a decrease in inflammatory signaling, which is unlikely to contribute to the lasting

inflammation-dependent impairment in plasticity. Further, the acute inflammatory impairment of adult respiratory plasticity is COX-independent (Huxtable et al., 2017), emphasizing a role for other inflammatory molecules mediating the lasting impairment in respiratory motor plasticity. Unmeasured inflammatory genes or post-transcriptional changes in inflammatory proteins may be responsible for undermining adult pLTF after neonatal inflammation. Conversely, other perinatal stimuli involving inflammatory signaling, such as maternal care and diet, do have lasting programming effects on adult inflammatory cytokine expression (Bilbo and Schwarz, 2009), but are more complex stimuli than the acute neonatal inflammation in our study. We also observed no change in microglial or astrocyte density and no obvious qualitative changes in morphology in adult medullas or spinal cords after neonatal inflammation. Thus, there are no obvious signs of inflammation in regions contributing to pLTF despite the restoration of Q-pathway-evoked pLTF with ketoprofen. Furthermore, the abolition of S-pathway-evoked pLTF is likely due to lasting changes in adenosine signaling from astrocytes, suggesting an astrocyte-specific change underlies this impairment. Thus, future studies are needed to identify inflammatory mechanisms undermining the Q-pathway and further details of the inflammation-independent mechanism responsible for undermining S-pathway-evoked motor plasticity.

The adult respiratory control network is vulnerable to early life stressors (Bavis et al., 2004; Fournier et al., 2011; Genest et al., 2004), which may undermine the ability to compensate during adult ventilatory control disorders. Our study is the first to demonstrate lasting consequences of neonatal inflammation on adult respiratory control. These deficits in respiratory control are independent of later life events, in contrast to

other studies in which the physiological effects of early life inflammation are not revealed until after an adult stimulus (Bilbo, 2010; Bilbo et al., 2005). We found a single episode of neonatal systemic inflammation induced lasting impairment of both Q- and S-pathway-evoked respiratory motor plasticity in adults. Our results demonstrate the adult impairment of Q-pathway plasticity is dependent on acute inflammatory signaling; however, we observed no lasting increase in adult inflammatory gene expression or the density of astrocytes and microglia. The pharmacological induction of S-pathway-evoked pLTF demonstrates phrenic motor neurons are capable of plasticity and suggest upstream impairment, such as the source of adenosine. While strong evidence supports astrocytes as the primary source of adenosine during hypoxia (Angelova et al., 2015; Takahashi et al., 2010), we cannot rule out other sources of adenosine. Identifying cell-type specific changes underlying lasting physiological impairments will be explored in future studies. Future studies will investigate the lasting effects of neonatal inflammation on isolated microglia and astrocytes to uncover potential mechanisms of adult impairments after neonatal inflammation.

Together, these results indicate two mechanistic pathways to spinal motor plasticity induced by AIH are undermined by neonatal inflammation in rats. Our experimental approach assessed phrenic nerve output in anesthetized rats and may not be generalizable to respiratory control in freely behaving animals or to other forms of motor plasticity. However, AIH induces long-term facilitation of ventilation in humans (Mateika and Komnenov, 2017) and strengthens corticospinal pathways to non-respiratory motor-neurons (Christiansen et al., 2018), suggesting our results likely have relevance to mechanisms of human spinal motor plasticity after AIH. While AIH-induced

respiratory motor plasticity does not necessarily alter normal homeostatic control of ventilation, the general facilitation of spinal motor output has significant therapeutic potential for treating patients with respiratory and non-respiratory motor limitations (Hayes et al., 2014; Nichols et al., 2013; Trumbower et al., 2012, 2017)

In conclusion, this basic science study has major implications for the understanding the neonatal origins of adult ventilatory control disorders. These studies are the first evidence that one neonatal inflammatory exposure induces long-term impairments in adult respiratory control with potential relevance to many respiratory disorders. These findings are particularly relevant since inflammation is common in neonates (Person et al., 2014), especially those born prematurely who are at higher risk for adult disease (Luu et al., 2016). Improving our appreciation of how early life inflammation can influence adult respiratory control will have important consequences for understanding adult disease and susceptibility to respiratory disorders. Additionally, AIH-induced spinal motor plasticity is also a promising therapy to enhance motor recovery after spinal injury (Trumbower et al., 2012). However, not all patients respond to AIH (Hayes et al., 2014; Trumbower et al., 2017) and our findings suggest neonatal inflammatory exposure could contribute to these therapeutic limitations and understanding the mechanisms undermining plasticity will increase the therapeutic potential of AIH-induced spinal motor plasticity.

Methods

All experiments were approved by the Institutional Animal Care and Use Committees at the University of Oregon and the University of Wisconsin-Madison and

conformed to the policies of the National Institute of Health *Guide for the Care and Use of Laboratory Animals*. Male and female Sprague Dawley rats (Envigo Colony 217 and 206) were housed under standard conditions (12:12h light/dark cycle) with food and water *ad libitum*.

Drugs and Materials

LPS (0111:B4, Sigma Chemical) was dissolved and sonicated in sterile saline for neonatal intraperitoneal (i.p.) injections (1 mg/kg). S-(+) Ketoprofen (Keto, Sigma Chemical) was dissolved in ethanol (50%) and sterile saline for acute, adult injections (12.5 mg/ml/kg, i.p., 3 hr). 17-β estradiol was dissolved in sesame oil (Tex Lab Supply, Texas, USA) for acute injections (40 μg/mL/kg, i.p.,3 hr) in adult females after ovariectomy.

The adenosine 2A receptor agonist CGS-21680 was dissolved in fresh artificial cerebrospinal fluid (aCSF: 120mM NaCl, 3mM KCl, 2mM $CaCl_2$, 2mM $MgCl_2$, 23mM $NaHCO_3$, and 10mM glucose) with DMSO (10%) for intrathecal injections.

Neonatal treatments

Timed pregnant rats (E14-17 upon arrival) were purchased in pairs from a commercial vendor (Envigo) and monitored daily. To control for between litter effects, litters were stratified such that each dam fostered similar numbers of male and female pups. On postnatal day 4 (P4), all of the stratified pups with one dam were injected with LPS (1 mg/kg, i.p.), while pups with the control dam were injected with sterile saline (i.p.). The dose of LPS was based on previous studies demonstrating CNS inflammatory gene expression in neonates (Rourke et al., 2016), as well as our unpublished data (N. Morrison, S. Johnson, J. Watters, A. Huxtable, unpublished observations) indicating

CNS inflammation following LPS (1mg/kg). Pups were weighed weekly and weaned at P21. Electrophysiology experiments were conducted once males reached 300g. Females were ovariectomized at approximately 250g, 7-8 days prior to electrophysiology experiments.

Ovariectomy

Ovariectomies were performed as previously described (Dougherty et al., 2017) to control for the known effects of estrus cycle hormones on pLTF (Behan et al., 2002; Dougherty et al., 2017; Zabka et al., 2001). Adult rats were anesthetized with isoflurane and maintained on a nose cone (2.5% in O_2) during surgery. Depth of anesthesia was confirmed by the absence of toe-pinch responses. Bilateral dorsolateral incisions exposed ovarian fat pads. Ovaries were ligated and removed, muscle layers were approximated, and skin incisions were closed with a single dissolvable suture. A single dose of buprenorphine (0.05 g/kg, s.c.) was administered at the end of surgery for pain control and rats recovered in individual cages for 7-8 days before electrophysiology studies. Since pLTF exists in females only when estradiol is high (Dougherty et al., 2017), estradiol levels were restored by injection of 17-β estradiol (40 μg/mL/kg, i.p.) three hours before electrophysiology experiments.

Experimental Groups

All experimental groups consisted of adult male and female rats after a single injection of either neonatal LPS or neonatal saline. To investigate the impact of neonatal systemic inflammation on adult Q-pathway-evoked respiratory motor plasticity, the following experimental groups were used: male neonatal saline + mAIH (n = 7), male

neonatal LPS + mAIH (n = 12), female neonatal saline + mAIH (n = 7), female neonatal LPS + mAIH (n = 6).

To investigate if acute anti-inflammatory treatment restores Q-pathway-evoked respiratory motor plasticity after neonatal inflammation, adults were treated with ketoprofen (12.5 mg/kg, i.p.) three hours before electrophysiology experiments: male neonatal saline + Keto + mAIH (n = 4), male neonatal LPS + Keto + mAIH (n = 4), female neonatal saline + Keto + mAIH (n = 5), female neonatal LPS + Keto + mAIH (n = 5).

To investigate the impact of neonatal systemic inflammation on adult S-pathway-evoked respiratory motor plasticity, we used the following experimental groups: male neonatal saline + sAIH (n = 5), male neonatal LPS + sAIH (n = 4), female neonatal saline + sAIH (n = 4), female neonatal LPS + sAIH (n = 4).

To investigate if acute anti-inflammatory treatment restores S-pathway-evoked respiratory motor plasticity after neonatal inflammation, adults were treated with ketoprofen (12.5 mg/kg, i.p.) three hours before electrophysiology experiments: female neonatal saline + Keto + sAIH (n = 5), male neonatal LPS + Keto + sAIH (n = 5), female neonatal saline + Keto + sAIH (n = 5), female neonatal LPS + Keto + sAIH (n = 6).

To investigate if intermittent, intrathecal CGS-21680 reveals S-pathway-evoked respiratory motor plasticity, we used the following experimental groups: male neonatal saline + CGS-21680 (n = 4), male neonatal LPS + CGS-21680 (n = 6), female neonatal saline + CGS-21680 (n = 4), female neonatal LPS + CGS-21680 (n = 6).

To reduce use of additional animals, and because time control experiments were not statistically different between males or females, time control groups consisted of

animals from each experimental condition. The time control group for studies investigating the Q-pathway (Fig. 4.2) and S-pathway (Fig. 4.5) consisted of adults after neonatal saline (male: n=1; female n=2), neonatal LPS (n = 1 male, 1 female). The time control + Keto group (Figs. 3 and 6) consisted of adults after neonatal saline + Keto (n = 1 male, 1 female) and neonatal LPS + Keto (n = 1 male, 1 female). Vehicle controls for intrathecal CGS-21680 experiments (Fig. 4.7) consisted of adults after neonatal saline (n = 1 male, 1 female) and neonatal LPS (n = 1 male, 1 female).

Electrophysiological studies

Electrophysiological studies have been described in detail previously (Bach and Mitchell, 1996; Baker-Herman and Mitchell, 2002; Huxtable et al., 2013). Rats were anesthetized with isoflurane, tracheotomized, ventilated (Rat Ventilator, VetEquip®), and vagotomized bilaterally. A venous catheter was placed for drug delivery and fluid replacement, and a femoral arterial catheter was used to monitor blood pressure and for arterial blood sampling. Arterial blood samples were analyzed (PaO_2, $PaCO_2$, pH, base excess; Siemens RAPIDLAB® 248) during baseline, during the first hypoxic response, and 15, 30 and 60 minutes post-AIH. Temperature was measured with a rectal temperature probe (Kent Scientific Corporation) and maintained between 37°C and 38°C with a custom heated table. Using a dorsal approach, hypoglossal and phrenic nerves were cut distally, and de-sheathed. Rats were converted to urethane anesthesia (1.8 g/kg i.v.; Sigma-Aldrich), allowed to stabilize for one hour, and paralyzed with pancuronium dibromide (1 mg; Selleck Chemicals).

In rats receiving intrathecal injections, a laminectomy was performed at cervical vertebrae 2 (C2) and a primed, silicone catheter was inserted two millimeters through a

small incision in the dura. The catheter tip extended toward the rostral margin of C4 (Baker-Herman and Mitchell, 2002). CGS-21680 (100 μM) or vehicle (10% DMSO in aCSF) was injected around the phrenic motor pool in three boluses (10 μL) separated by 5 minutes.

Nerves were bathed in mineral oil and placed on bipolar silver wire electrodes. Raw nerve recordings were amplified (10k), filtered (0.1-5 kHz), integrated (50 ms time constant), and recorded (10 kHz sampling rate) for offline analysis (PowerLab and LabChart 8.0, AD Instruments). Apneic and recruitment CO_2 thresholds were determined by changing inspired CO_2 with continuous end-tidal CO_2 monitoring (Kent Scientific Corporation). End tidal CO_2 was set 2 mmHg above the recruitment threshold, whereby arterial blood samples were used to establish baseline $PaCO_2$, which was maintained within 1.5 mmHg of the baseline value throughout. Blood volume and base excess were maintained (±3 MEq/L) by continuous infusion (1-3 mL/h, i.v.) of hetastarch (0.3%) and sodium bicarbonate (0.99%) in lactated ringers. Experiments were excluded if mean arterial pressure deviated more than 20 mmHg from baseline.

All rats (excluding time control rats) received three, 5-minute bouts of either mAIH (~10.5% O_2, PaO_2 35-45 mmHg) or sAIH (~7% O_2, PaO_2 25-35 mmHg). The average amplitude and frequency of 30 consecutive integrated phrenic bursts were taken during baseline, the first acute hypoxic response, and 15, 30, and 60 minutes after AIH and made relative to baseline amplitude. Phrenic nerve activity data for each experimental group were compared using two-way, repeated measures ANOVA with Fisher LSD post hoc tests. Sample sizes were selected based on similar, previous studies and the variance of pLTF in our experience (Hocker and Huxtable, 2018; Huxtable et al.,

2017, 2018). Physiological variables were compared using two-way, repeated measures ANOVA with Tukey's post hoc test. Mean arterial pressure is reported for baseline, the end of the third hypoxic exposure, and 60 minutes after AIH. Acute hypoxic responses were compared using an ANOVA with Fisher LSD post hoc test. Values are means ± SD.

RNA isolation, cDNA synthesis and quantitative PCR experiments

Neonatal rats (P4) were injected with either vehicle (saline) or LPS (1 mg/kg, i.p.) and allowed to mature to ~12 weeks. Adult male and female rats were anesthetized with isoflurane and perfused with PBS (transcardiac). Medulla and cervical spinal cords (C3-C7) were dissected and flash frozen until they were homogenized in Tri-Reagent (Sigma, St. Louis, MO, USA). Glycoblue reagent (Invitrogen, Carlsbad, CA, USA) was used to isolate total RNA, according to the manufacturer's protocol. cDNA was reverse transcribed from 1 µg of total RNA using MMLV reverse transcriptase together with a cocktail of oligo dT and random primers (Promega, Madison, WI, USA), as previously described (Crain et al., 2009), and analyzed using qPCR with PowerSYBR green PCR master mix on an ABI 7500 Fast system. Inflammatory gene expression was analyzed in medulla and spinal cord homogenates using the following primers:
IL-6: 5'-GTG GCT AAG GAC CAA GAC CA and 5'-GGT TTG CCG AGT AGA CCT CA; IL-1β: 5'-CTG CAG ATG CAA TGG AAA GA and 5'-TTG CTT CCA AGG CAG ACT TT; COX-2: 5'-TGT TCC AAC CCA TGT CAA AA and 5'-CGT AGA ATC CAG TCC GGG TA; TNF-α: 5'-TCC ATG GCC CAG ACC CTC ACA C and 5'-TCC GCT TGG TGG TTT GCT ACG; iNOS: 5'-AGG GAG TGT TGT TCC AGG TG and 5'-TCT GCA GGA TGT CTT GAA CG; 18s: 5'-CGG GTG CTC TTA GCT GAG TGT CCC G and 5'-CTC GGG CCT GCT TTG AAC AC.

Wherever possible, primers were designed to span introns (Primer 3 software) and were purchased from Integrated DNA Technologies (Coralville, IA, USA). Primer efficiency was assessed by use of standard curves, as previously reported (Crain and Watters, 2015). Expression of inflammatory genes was made relative to 18s ribosomal RNA calculated using the $2^{-\Delta\Delta CT}$ method (Livak and Schmittgen, 2001). Gene transcripts were considered undetectable, and not included in statistical analyses if their CT values fell outside of the linear range of the standard curve for that primer set, which in most cases was ≥34 cycles.

Immunohistochemistry methods

Upon completion of electrophysiology experiments, rats were perfused (transcardiac) with cold phosphate buffered saline (PBS, pH 7.4), followed by 4% paraformaldehyde (pH 7.4). All brains were removed and immersed in paraformaldehyde until sectioning (Leica VT 1200S vibratome). For immunohistochemistry, transverse medullary and coronal cervical spinal cord sections (40 µm) were washed (PBS) and blocked (PBS, 0.3% Triton, 1% BSA, 2 hours, room temperature) to prevent non-specific antibody binding. For medullary sections, two combinations of primary antibodies were used (PBS, 0.3% Triton, 0.01% BSA, room temperature, 24 hours): (1) rabbit anti-GFAP (1:1000, Millipore AB5804) to label astrocytes and guinea pig anti-NK1R (1:500, Millipore AB15810) to label preBötzinger Complex (preBötC) neurons (Gray et al., 1999), and (2) rabbit anti-IBA1 (1:1000, Wako 019-19741) to label microglia and guinea pig anti-NK1R (1:500, Millipore AB15810) to label preBötC neurons. For the spinal cord, two different combinations of primary antibodies were used (PBS, 0.3% Triton, 0.01% BSA, room temperature, 24 hours): (1) rabbit anti-GFAP (1:1000, Millipore

AB5804) to label astrocytes and goat anti-ChAT (1:300, Millipore AB144p) to label motor neurons, (2) rabbit anti-IBA1 (1:1000, Wako 019-19741) to label microglia and goat anti-ChAT (1:300, Millipore AB144p) to label motor neurons. After primary antibody incubation, sections were rinsed (PBS) and incubated with secondary antibodies (PBS, 0.3% triton, 0.01% BSA, room temperature, 3 hours): donkey-anti-rabbit 647 IgG (1:1000, Life Technologies A31573) to label GFAP and IBA1 primary antibodies, donkey-anti-goat 555 IgG (1:1000, Life Technologies A21432) to label ChAT primary antibody and donkey-anti-guinea pig 488 IgG (1:1000, Alexa Fluor 706-545-148) to label NK1R primary antibody. Sections were washed and mounted onto charged microscope slides, air dried and covered with prolong gold (Life technologies, P36930) to preserve the fluorescence. A glass cover slip was placed over the samples and sealed with clear nail polish. Slides were stored in the dark at 4°C until imaged. All immunohistochemistry experiments contained adult male and female tissues after neonatal saline (medulla: n = 5 males, 7 females; spinal cord: n = 5 males, 6 females) or neonatal LPS (medulla: n = 6 males, 4 females; spinal cord: n = 6 males, 3 females).

Image analysis methods

All immunofluorescent images (1024 x 1024 pixels, 40x magnification) were acquired using a Leica Microsystems CMS GmbH confocal microscope using the LAS X acquisition and viewing software (0.5 µm z-stack step increments). All images were taken using identical laser and gain settings and identically adjusted for contrast/brightness using ImageJ open source software to allow for comparisons across all groups. To quantify the density of microglia and astrocytes, maximum intensity projections for 20 µm of z-stacks from the medulla and cervical spinal cords were

analyzed. Mean fluorescent intensity for each image within a single batch was made relative to the average fluorescent intensities of adults after neonatal saline samples within each sex (Paizs et al., 2009). Data are presented as percent change from adults after neonatal saline within each sex.

Statistical Analysis

GraphPad Prism 7.0 software was used for statistical analyses. Differences in mortality between treatments and between sexes was evaluated with Fisher's exact test. Phrenic nerve activity data for each experimental group were compared using two-way, repeated measures ANOVA with Fisher LSD *post hoc* tests. Physiological variables were compared using two-way, repeated measures ANOVA with Tukey's *post hoc* test. Mean arterial pressure is reported from baseline, the end of the third hypoxic exposure, and 60 minutes after AIH. Acute hypoxic phrenic responses were compared using an ANOVA with Fisher LSD *post hoc* test. Microglial and astrocytic density comparisons were made between groups using a one-way ANOVA with multiple-comparisons *post hoc* tests. For all tests, $p < 0.05$ was considered significant and all data are expressed as mean ± SD.

CHAPTER V

MATERNAL METHADONE DESTABILIZES EARLY NEONATAL BREATHING AND DESENSITIZES NEONATES TO ACUTE METHADONE-INDUCED RESPIRATORY DEPRESSION

This chapter includes unpublished material which was co-authored by Adrianne G. Huxtable. I designed and led these studies, collected and analyzed all data, and wrote the paper. Adrianne Huxtable designed, contributed to writing the manuscript, provided guidance, oversight, and editorial assistance.

Introduction

The misuse of opioids has become a national and public health crisis with greater than 118 Americans dying from opioid overdose daily in 2016, 27% more deaths than the previous year (CDC Wonder). This crisis also carries a significant economic burden, estimated to be $78.5 billion/year (Florence et al., 2016). Significant efforts are underway to curb the misuse of opioids in adults, yet one understudied population in these efforts is pregnant women. Opioid use during pregnancy is on the rise (Epstein et al., 2013; Krans et al., 2015; Stover and Davis, 2015) and a significant need exists to improve treatments for neonates after maternal opioid use (Kraft et al., 2016). Maternal opioid use leads to neonatal abstinence syndrome (NAS), described as dysfunction in the central and autonomic nervous system, and gastrointestinal system in infants (McQueen and Murphy-Oikonen, 2016). NAS results in diverse negative outcomes for the infant,

including; irritability, sleep disturbances, death, and respiratory disturbances (McQueen and Murphy-Oikonen, 2016). The respiratory disturbances are not well characterized, but increased apneas have been described (McQueen and Murphy-Oikonen, 2016; Ward et al., 1986). Yet, despite this increasing population of NAS infants, little is known about the effects of maternal opioids on developing neonatal respiratory control circuitry.

At birth, neonates must have a functional respiratory system capable of robust, rhythmic breathing. Therefore, rhythmic neural activity, initiating at the preBötzinger complex (preBötC, the kernel for respiratory rhythmogenesis) (Smith et al., 1991) is required for development of neural circuitry, respiratory muscles, and the lungs (Greer, 2012; Pagliardini et al., 2003). In rats, development of rhythmogenic respiratory neural networks begins around embryonic day 17 (E17) and continues until birth (Pagliardini *et al.*, 2003). The preBötC is exceptionally sensitive to opioids and is responsible for many of the respiratory depressant effects of opioids (Montandon et al., 2011, 2016; Stucke et al., 2015). Since maternal opioids cross the placenta and delay neurodevelopment (Hauser and Knapp, 2018; Kopecky et al., 1999), they have the potential to suppress rhythmic respiratory activity from the preBötC, and thus, respiratory control networks need to compensate to maintain adequate respiratory function at birth (Gourévitch *et al.*, 2017). Interestingly, the parafacial respiratory group (pFRG) also has rhythmogenic properties during embryonic and early neonatal life (Onimaru and Homma, 2003; Thoby-Brisson and Ramirez, 2001) and may be able to mitigate respiratory instability during early life (Feldman and Del Negro, 2006). However, controlled studies on neonatal breathing after maternal opioids are extremely limited. One study demonstrated medullary respiratory network reorganization after maternal opioid exposure in neonatal

rats (Gourévitch *et al.*, 2017). Another study in guinea pigs shows enhanced hypercapnic ventilatory responses after prenatal opioids (Nettleton et al., 2008), suggesting changes in chemosensitivity after maternal opioids. To our knowledge, the present study is the first investigating changes in neonatal breathing after maternal opioid use in rats. For this study, we tested the effects of maternal methadone to model aspects of maternal opioid use since methadone is a standard of care treatment for maternal opioid dependence (Bhavsar et al., 2018). Additionally, NAS infants are typically treated acutely with opioids, such as methadone, to alleviate NAS symptoms (Davis et al., 2018; Kraft et al., 2016; Pryor et al., 2017). However, opioids dangerously depress breathing in neonates and may cause lasting deficits in neurodevelopment (Attarian et al., 2014). Therefore, we hypothesized that repetitive, daily acute methadone would further destabilize breathing after maternal methadone.

Understanding the acute effects of maternal opioid use is critical to developing more effective treatments for neonates exposed to perinatal opioids. We hypothesize that perinatal methadone exposure during development of the respiratory control system will destabilize neonatal breathing, blunt hypoxic ventilatory responses, and enhance hypercapnic ventilatory responses. Understanding how maternal opioid use alters the respiratory response to acute opioids will contribute to our understanding of how to alleviate the symptoms of NAS without severe respiratory dysfunction.

Methods

All experiments conformed to the policies of the National Institute of Health *Guide for the Care and Use of Laboratory Animals* and were approved by the Institutional Animal Care and Use Committee at the University of Oregon. Timed

pregnant Sprague Dawley Rats (Envigo Colony 217) were ordered to arrive at embryonic day 17 (E17) and were housed under standard conditions with a 12:12h light/dark cycle with food and water *ad libitum*.

Maternal opioid exposure

Since respiratory rhythm generation and fetal breathing movements begin on day E17 in fetal rats (Greer, 2012; Pagliardini et al., 2003), maternal methadone exposure began on E17 to mitigate other developmental effects of methadone and focus on the effects of opioids on developing respiratory circuitry. Each morning from E17 onward, dams were injected with methadone (5 mg/kg, Sigma-Aldrich, subcutaneous) and monitored for at least one hour. After parturition, daily maternal methadone injections continued until postnatal day 5 (P5) (Fig. 5.1). Control dams were injected daily with vehicle (saline, subcutaneous) or were un-treated to control for the potential stress of daily injections. Breathing in neonates (P0-5) born to maternal methadone (MM), maternal saline (MS), and maternal no-treatment (MN) were studied using plethysmography.

In the first study, neonatal baseline ventilation, hypoxic, and hypercapnic ventilatory responses were assessed from P0-5 (Fig. 5.1). Since no differences were found between sexes ($p > 0.05$), male and female rats were combined for maternal methadone (MM: P0 = 8 female, 8 male, P1 = 8 female, 4 male, P2 = 9 female, 4 male, P3 = 7 female, 4 male, P4 = 7 female, 2 male, P5 = 7 female, 2 male), maternal saline (MS: P0 = 8 female, 5 male, P1 = 8 female, 7 male, P2 = 8 female, 7 male, P3 = 5 female, 6 male, P4 = 5 female, 5 male, P5 = 5 female, 6 male), and maternal no treatment (MN:

P0 = 10 female, 12 male, P1 = 7 female, 11 male, P2 = 4 female, 6 male, P3 = 7 female, 9 male, P4 = 6 female, 8 male, P5 = 7 female, 7 male).

In a separate group of neonates in the second study, the combined effects of maternal treatment with daily acute methadone (1mg/kg, i.p.) from P0-5 were assessed (Fig. 5.1). Injections began at P0 and were repeated each day in the same rats until P5. Thus, each neonate received a total of 6 acute, methadone injections by the time they reached P5. For each neonate, baseline breathing was measured for 10 minutes before acute methadone injection. The ventilatory response to acute methadone was monitored for one hour, followed by hypercapnic and hypoxic ventilatory responses. Since no differences were found between sexes, male and female rats exposed to daily acute methadone were combined from each maternal treatment (MM: P0 = 7 female, 7 male, P1 = 6 female, 8 male, P2 = 8 female, 5 male, P3 = 8 female, 7 male, P4 = 8 female, 7 male, P5 = 7 female, 7 male; MS: P0 = 3 female, 6 male, P1 = 3 female, 6 male, P2 = 2 female, 7 male, P3 = 2 female, 7 male, P4 = 3 female, 6 male, P5 = 5 female, 4 male; MN: P0 = 3 female, 4 male, P1 = 2 female, 4 male, P2 = 2 female, 4 male, P3 = 2 female, 4 male, P4 = 2 female, 4 male, P5 = 2 female, 2 male).

Neonatal whole-body plethysmography

Ventilation was measured in awake, freely behaving neonates from P0-5 using custom built whole-body plethysmography. Neonatal rats were individually placed in an acrylic chamber (75 ml volume). Three mass flow controllers (Alicat Scientific) control the concentration of oxygen, nitrogen, and carbon dioxide at a total flow rate of 100 ml/minute. Body surface temperature was maintained throughout experiments at

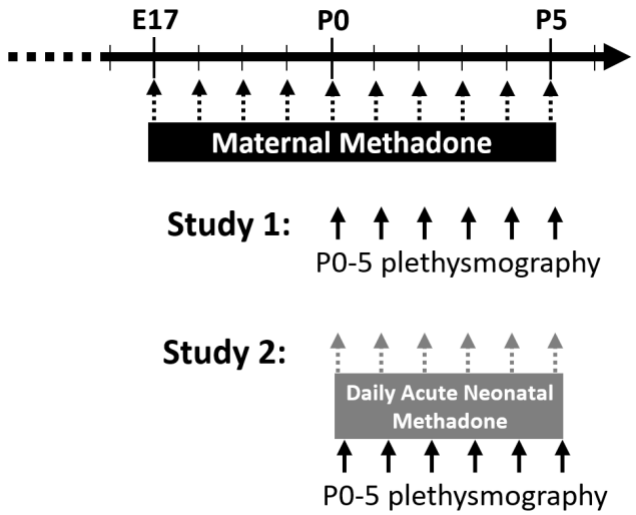

Figure 5.1. Schematic of experimental paradigm for perinatal opioids. Pregnant dams were treated from E17-P5 with daily methadone injections (5mg/kg, s.c.). Control dams were untreated or injected with vehicle (saline). In study 1, baseline breathing, hypercapnic, and hypoxic ventilatory responses in neonates (P0-5) from each maternal treatment group were assessed by whole-body plethysmography. In study 2, neonates from each maternal treatment group were given daily acute methadone (1 mg/kg i.p.) from P0-5. Baseline breathing, ventilatory responses to acute methadone, and hypoxic and hypercapnic ventilatory responses were assessed at P0-5 by whole-body plethysmography.

thermoneutral (Eden and Hanson, 1987; Mortola and Dotta, 1992) by adjusting chamber temperature between 32-34°C with a heating pad (Kent Scientific). A differential pressure transducer (ADInstruments®) attached to the chamber via a dedicated port recorded pressure changes due to ventilation relative to pressure in an identical reference chamber. Data were recorded using LabChart software (PowerLab System, ADInstruments®/ LabChart).

Hypoxic and Hypercapnic ventilatory responses

Hypercapnic ventilatory responses (HCVR) and hypoxic ventilatory responses (HVR) were measured daily (P0-P5). After a baseline recording period (20 min, 21% O_2,

balance N_2), inflow gas switched to 5% CO_2 (10 minutes) to assess hypercapnic ventilatory responses. The HCVR response was assessed during the last two minutes of the hypercapnic stimulus and made relative to baseline V_E taken during the preceding 5 minutes before hypercapnic exposure. After hypercapnia, chambers were returned to normocapnia (21% O_2, balance N_2, 20 min) for neonates to recover (20 minutes). To evaluate hypoxic ventilatory responses, inflow gas was switched to 10% oxygen (10 min). Peak, phase I, HVR was calculated as the maximum rolling average of 50 breaths during the hypoxic stimulus and made relative to baseline V_E in the 5 minutes immediately preceding hypoxia. Phase II, hypoxic ventilatory decline was assessed as the average V_E in the last two minutes of the hypoxic exposure and made relative to baseline V_E in the 5 minutes immediately preceding hypoxia.

Methadone-induced respiratory depression and quantal slowing

Respiratory responses to acute neonatal methadone were measured daily in neonates from P0-P5 after MM, MS, and MN. Neonates were placed in the recording chamber for 10 minutes of baseline recordings. Neonates were removed from the chamber, injected with methadone (1 mg/kg, i.p.) and immediately returned the chamber for continuous recording (1 hour). HCVRs and HVRs were measured one hour after acute methadone injections, as described above.

Quantal slowing is the reduction of breathing frequency by integer multiples of the basal breathing period in response to acute opioids (Mellen et al., 2003). To assess quantal slowing patterns after acute methadone, Poincare plots of normalized breathing

periods were used to identify the presence of breaths clustered at integers of breathing period.

Data Analysis

For all experiments, inspiratory frequency and V_T were analyzed using peak analysis in LabChart (v8, AD Instruments®). Two respiratory variables, tidal volume (V_T) and frequency (breaths/minute) are estimated from the amplitude and the frequency of the pressure recordings. Minute ventilation (V_E) is calculated as the product of frequency and V_T. V_T and V_E were normalized to body weight. Our custom-built plethysmograph is primarily effective for studying respiratory frequency and is not designed for absolute quantification of V_T. Therefore, V_T and V_E are reported as changes relative to baseline.

Apneas were identified as respiratory pauses lasting longer than 2.5 breaths. Post-sigh apneas were defined as an augmented breath with at least twice the mean V_T, followed by an apnea (Marcouiller et al., 2014). To assess respiratory rhythm variability, short-term (SD1) and long-term (SD2) variability were calculated from breath-to-breath intervals during baseline.

Poincaré plots were constructed from a subset of breathing periods taken 25-40 minutes after neonatal exposure to acute methadone. Normalized periods (n) and subsequent periods (n +1) were plotted. A blinded investigator visually coded each plot based on clustering of breaths at integer multiples of the normal breathing period, a feature consistent with quantal slowing.

Statistical comparisons and visualization for all data were performed using R and R studio (version 1.1.463). Differences between means were identified using two-way

ANOVA with Bonferroni correction for multiple comparisons ($\alpha = 0.05$). Values are reported as means ± SD.

RESULTS

Sex had no effect on any respiratory variables ($p > 0.05$); thus, male and female rats were combined for all analyses. Neonatal body weights were similar from P0-P5, regardless of maternal treatment. One exception was a significant reduction in MS P2 weights compared to MM ($p = 0.001$, Table 5.1).

Table 5.1. Maternal methadone does not alter neonatal weight.

		P0	P1	P2	P3	P4	P5
n	**MM**	16	11	22	16	13	11
	MS	13	9	10	14	15	11
	MN	12	9	18	14	15	10
Weight	**MM**	5.3 ± 0.6	6.2 ± 0.5	7.0 ± 0.6	8.7 ± 0.6	10.1 ± 0.6	11.2 ± 1.0
(g)	**MS**	5.3 ± 0.6	5.9 ± 0.5	6.6 ± 0.6	7.7 ± 0.7	9.4 ± 0.5	10.7 ± 1.0
	MN	5.5 ± 0.5	6.0 ± 0.7	8.0 ± 0.5	8.1 ± 0.9	9.1 ± 1.3	10.3 ± 1.3

Mean ± SD; ANOVA-RM, Bonferroni post-hoc, # MN $p<0.05$ from MS.

Maternal methadone destabilizes P0 respiratory rhythm.

At P0, apneas were significantly more frequent after MM ($p < 0.001$ compared to MS and MN, Fig.5. 2A and B), indicating less stable breathing after MM. Apnea duration was greater in P0 neonates after MM and MS compared to MN ($p = 0.002$ and $p = 0.008$ respectively, Fig. 5.2B). Additionally, post-sigh apneas were more frequent in P0 neonates after MM compared to MS ($p = 0.012$) and MN ($p < 0.001$, Fig. 5.2B). At P0, MM treated neonates had more sighs (5.1 ± 2.5 min^{-1}) compared to MN (1.1 ± 0.6 min^{-1}, $p < 0.001$), but the number of sighs was not significantly different from MS (1.9 ± 1.4 min^{-1}, $p = 0.086$). The fraction of sighs followed by an apnea was not significantly different between groups at any age ($p > 0.05$).

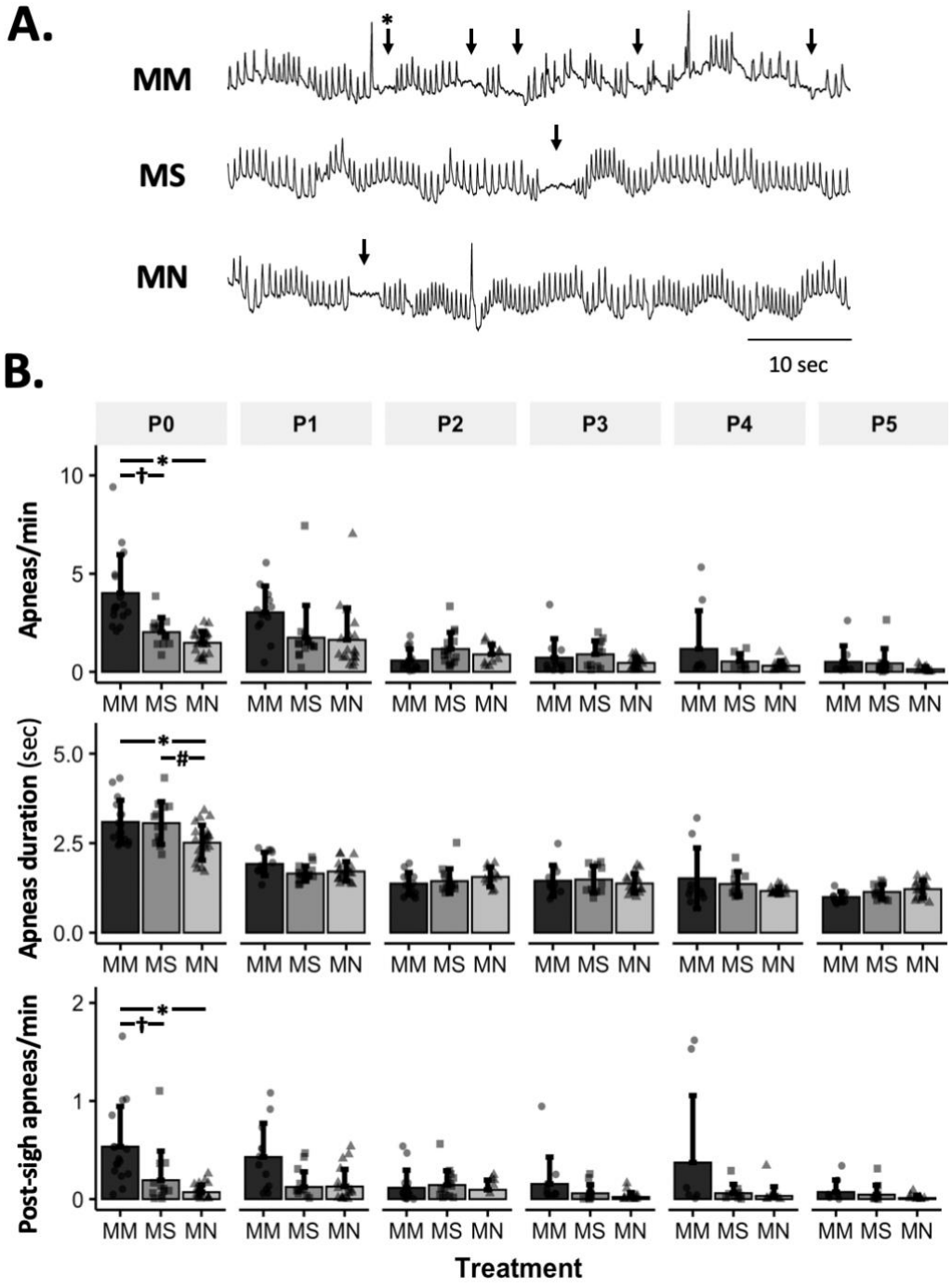

Figure 5.2. Maternal methadone increases apneas at P0. Representative baseline plethysmography traces **(A)** show frequent apneas (↓) and post-sigh apneas (*↓) after maternal methadone (MM, dark bars). Group data (**B**) demonstrate MM increases the frequency (**B, top**) and duration of apneas (**B, middle**) at P0 compared to neonates after maternal saline (MS, grey bars) and maternal no-treatment (MN, light bars). MM also increased the frequency of post-sigh apneas compared to MS and MN neonates at P0 **(B, bottom)**. By P1, the frequency and duration of apneas was not different between treatment groups. ANOVA-RM, Bonferroni post-hoc, * MM $p<0.05$ from MN, † MM $p<0.05$ from MS, # MN $p<0.05$ from MS.

Regardless of maternal treatment, overall baseline breathing was similar between groups, except at P0 (Table 2). At P5, breathing frequency after MM was increased relative to MN neonates ($p = 0.005$), but not MS (Table 2). MM increased V_T at P0 compared to MS ($p < 0.001$) and MN ($p = 0.001$), but V_T was normalized by P1 (Table 2). V_E also increased at P0 after MM compared to MS ($p = 0.017$), but not MN ($p = 0.162$, Table 5.2).

Corresponding to the relative instability at P0 after MM, frequency CV was increased at P0 after MM compared to MN ($p < 0.001$, Table 5.2). Additionally, SD1 and SD2 were elevated in MM and MS at P0 compared to MN ($p < 0.001$, Table 5.2), suggesting both MM and MS cause greater variability in early neonatal breathing pattern.

Maternal Methadone mitigates the hypoxic ventilatory decline at P0, but does not alter peak HVR or HCVR.

To assess if MM altered chemosensitivity, the relative ventilatory response to hypoxia (10% O_2) was analyzed. Phase I, peak ventilatory responses were not different within any age group (Fig. 5.3). However, the phase II hypoxic ventilatory decline was blunted at P0 in MM compared to MS ($p = 0.036$) and MN ($p = 0.027$, Fig. 5.3A and B). After P0, no differences in phase I or phase II HVRs were evident.

The ventilatory response to 5% CO_2 was not different between maternal treatment groups at any age (Fig. 5.4A and B).

Table 5.2. Maternal methadone disrupts baseline breathing at P0.

		P0	P1	P2	P3	P4	P5
n	**MM**	16	11	22	16	13	11
	MS	13	9	10	14	15	11
	MN	12	9	18	14	15	10
Frequency	**MM**	120.3 ± 27.3	155.6 ± 14.9	168.8 ± 30.1	165.4 ± 18.7	173.2 ± 29	202.2 ± 24.8*
(breaths/min)	**MS**	96.5 ± 17.1	138.0 ± 14.6	163.6 ± 19.4	155.6 ± 17	174.2 ± 22.4	183.5 ± 16.2
	MN	104.7 ± 18.7	141.6 ± 14.2	150.9 ± 11.4	157.6 ± 14.9	178.6 ± 12.6	166.1 ± 25.7
V_T	**MM**	0.81 ± 0.16*†	0.82 ± 0.19	0.67 ± 0.16	0.67 ± 0.16	0.79 ± 0.16	0.83 ± 0.20
(ml/100g)	**MS**	0.50 ± 0.10	0.76 ± 0.16	0.72 ± 0.18	0.66 ± 0.04	0.59 ± 0.10	0.64 ± 0.13
	MN	0.57 ± 0.15	0.73 ± 0.10	0.60 ± 0.07	0.66 ± 0.15	0.78 ± 0.22	0.75 ± 0.22
V_E	**MM**	97.4 ± 28.1†	129.0 ± 30.3	117.3 ± 44.1	115.1 ± 35.1	141.7 ± 40.6	177.7 ± 67.8
(ml/min/100g)	**MS**	48.6 ± 14.8	104.4 ± 23.1	118.3 ± 35.4	104.7 ± 15.7	103.4 ± 25.9	123.0 ± 33.1
	MN	61.2 ± 24.2	102.6 ± 16.7	92.1 ± 14.6	104.1 ± 28.4	138.5 ± 40.8	126.3 ± 52.6
Frequency	**MM**	0.92 ± 0.23*	0.64 ± 0.23	0.29 ± 0.11	0.35 ± 0.19	0.43 ± 0.42	0.29 ± 0.07
CV	**MS**	0.73 ± 0.20	0.42 ± 0.07	0.40 ± 0.17	0.35 ± 0.14	0.32 ± 0.1	0.29 ± 0.10
	MN	0.55 ± 0.13	0.42 ± 0.16	0.37 ± 0.11	0.29 ± 0.1	0.27 ± 0.13	0.24 ± 0.07
SD1	**MM**	0.48 ± 0.15*	0.21 ± 0.05	0.13 ± 0.03	0.14 ± 0.05	0.18 ± 0.14	0.10 ± 0.01
	MS	0.50 ± 0.15$^{\#}$	0.18 ± 0.03	0.16 ± 0.08	0.15 ± 0.03	0.13 ± 0.03	0.12 ± 0.02
	MN	0.34 ± 0.12	0.18 ± 0.04	0.15 ± 0.02	0.13 ± 0.02	0.12 ± 0.02	0.13 ± 0.02
SD2	**MM**	0.57 ± 0.19*	0.22 ± 0.08	0.11 ± 0.06	0.14 ± 0.10	0.19 ± 0.23	0.11 ± 0.03
	MS	0.54 ± 0.21$^{\#}$	0.16 ± 0.04	0.14 ± 0.09	0.13 ± 0.06	0.12 ± 0.05	0.11 ± 0.05
	MN	0.34 ± 0.14	0.16 ± 0.06	0.14 ± 0.05	0.11 ± 0.04	0.11 ± 0.05	0.11 ± 0.04
Ti	**MM**	0.26 ± 0.08	0.14 ± 0.03	0.10 ± 0.02	0.1 ± 0.03	0.11 ± 0.06	0.08 ± 0.01
(sec)	**MS**	0.29 ± 0.06	0.13 ± 0.03	0.12 ± 0.04	0.1 ± 0.01	0.09 ± 0.01	0.09 ± 0.01
	MN	0.24 ± 0.08	0.14 ± 0.03	0.11 ± 0.01	0.1 ± 0.02	0.09 ± 0.01	0.09 ± 0.01
Te	**MM**	0.53 ± 0.12	0.33 ± 0.03	0.30 ± 0.06	0.3 ± 0.06	0.31 ± 0.09	0.24 ± 0.04
(sec)	**MS**	0.57 ± 0.10$^{\#}$	0.35 ± 0.04	0.30 ± 0.05	0.32 ± 0.05	0.29 ± 0.05	0.27 ± 0.03
	MN	0.47 ± 0.09	0.34 ± 0.03	0.33 ± 0.04	0.31 ± 0.04	0.27 ± 0.02	0.31 ± 0.05

ANOVA-RM, Bonferroni post-hoc, * MM $p<0.05$ from MN, † MM $p<0.05$ from MS, # MN $p<0.05$ from MS.

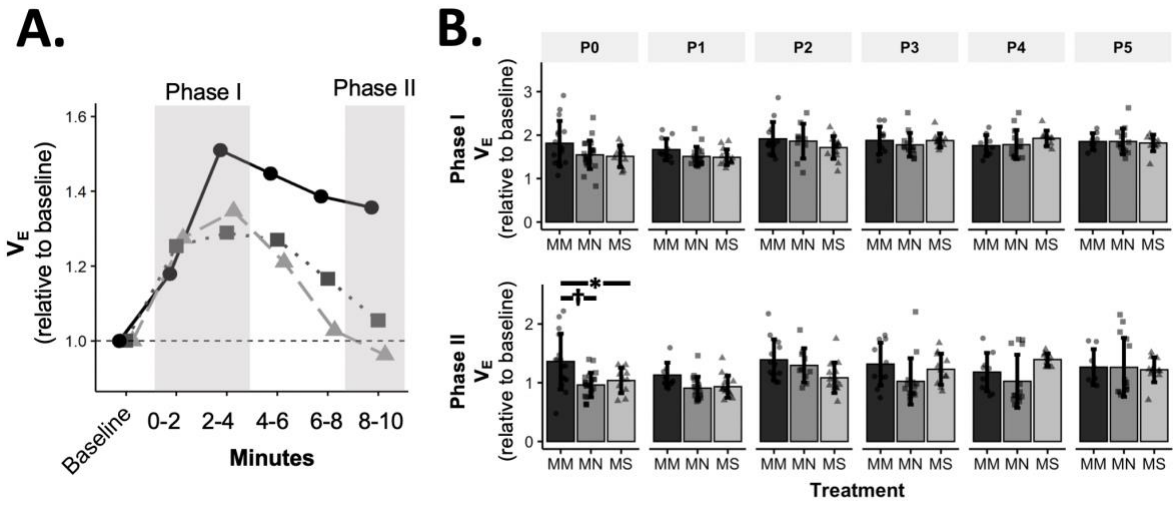

Figure 5.3. Maternal methadone blunts the phase II hypoxic ventilatory depression at P0. Average V_E at P1 for maternal methadone (MM, dark circles, **A**, and bars, **B**), maternal saline (MS, grey boxes, **A**, and bars, **B**), and, maternal no-treatment (MN, light triangles, **A**, and bars, **B**) neonates. Phase I, peak hypoxic ventilatory responses **(B, top)** were unaffected by maternal treatment group or age. However, the phase II hypoxic ventilatory decline **(B, bottom)** was blunted at P0 after MM compared to MN and MS rats, suggesting impaired central hypoxic responses. ANOVA-RM, Bonferroni post-hoc, * MM $p<0.05$ from MN, † MM $p<0.05$ from MS, # MN $p<0.05$ from MS.

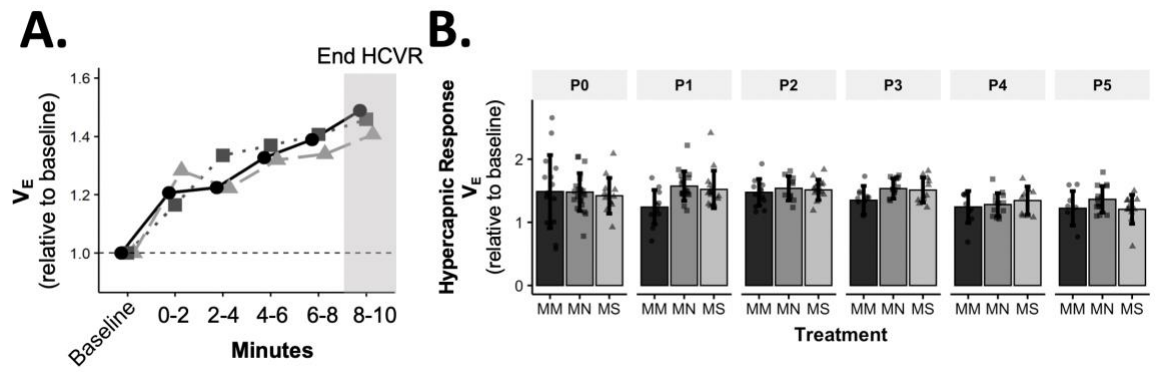

Figure 5.4. Maternal methadone does not alter hypercapnic ventilatory responses (HCVR). Average V_E for maternal methadone (MM, dark circles, **A**, and bars, **B**), maternal saline (MS, grey squares, **A**, and bars, **B**), and, maternal no-treatment (MN, light triangles, **A**, and bars, **B**) neonates demonstrates normal hypercapnic responses after MM **(A)**. No differences in HCVRs after MM, MN, and MS neonates were evident at any age **(B)**. ANOVA-RM, Bonferroni post-hoc, * MM $p<0.05$ from MN, † MM $p<0.05$ from MS, # MN $p<0.05$ from MS.

Daily acute methadone blunts weight gain.

In a separate group of rats from each maternal treatment group, neonates received daily injections of methadone (1 mg/kg, i.p.) starting at P0. After receiving four (P3) or five (P4) treatments with daily acute methadone, weight was blunted at P3 MM ($p = 0.049$) and P4 MM ($p = 0.001$) neonates compared to MS (Table 5.3). However, no differences between MM and MS neonates or MS and MN neonates were evident at any ages.

Table 5.3. Daily acute methadone reduces weight gain in P3 and P4 neonates after maternal methadone.

		P0	P1	P2	P3	P4	P5
n	**MM**	14	14	13	15	15	14
	MS	10	9	9	9	9	9
	MN	8	6	6	6	6	4
Weight	**MM**	5.2 ± 0.7	5.6 ± 0.6	6.7 ± 0.7	7.3 ± 0.9	8.6 ± 1	10 ± 1.2
(g)	**MS**	5.6 ± 0.4	6.3 ± 0.4	7.2 ± 0.6	8.6 ± 0.6	10.3 ± 0.9	11.4 ± 1.5
	MN	5.9 ± 0.9	6.4 ± 1.1	7.6 ± 0.6	8.6 ± 0.9	9.9 ± 0.7	11.8 ± 0.8

Mean ± SD (n); ANOVA-RM, Bonferroni post-hoc, † MM $p<0.05$ from MS.

Daily acute methadone does not alter neonatal breathing after maternal methadone exposure.

Daily acute methadone had no effect on baseline breathing in neonates regardless of maternal treatment (Table 4). Daily acute methadone had no significant effect on the frequency of apneas ($p = 0.395$), average apnea duration ($p = 0.057$), or frequency of post-sigh apneas ($p = 0.430$) between maternal treatment groups, which, contrary to our hypothesis, demonstrates daily acute methadone did not further destabilize neonatal breathing. Baseline frequency ($p = 0.163$), V_T ($p = 0.0737$), V_E ($p = 0.060$), or SD1 ($p = 0.379$) were not different between maternal treatment groups after daily acute methadone, demonstrating baseline ventilation is not impacted by daily acute methadone. There was a

main effect of maternal treatment on SD2 ($p < 0.001$); however, no significant pairwise differences occurred. Ti and Te were also unaltered by daily acute methadone and maternal treatment group ($p = 0.604$ and 0.052 respectively, Table 5.4).

Maternal methadone desensitizes P0-1 neonates from acute methadone-induced frequency depression.

Next, we tested the hypothesis that MM desensitizes neonates to acute methadone-induced respiratory depression. After daily acute methadone (1 mg/kg, i.p.), breathing frequency and V_E were reduced at 20-60 minutes after all maternal treatments at all time points after acute methadone ($p < 0.05$, Fig. 5.5B). For neonates after MS or MN, acute methadone-induced respiratory frequency depression was not different across ages. However, after MM, methadone-induced respiratory depression was blunted in P0 neonates compared to P3 and 4 ($p<0.01$) and blunted in P1 compared to P2-5 neonates ($p < 0.01$). Between groups, methadone-induced respiratory frequency depression was blunted at P0 and P1 in MM compared to MS and MN (Fig. 5.5A and B). MN neonates had a greater frequency depression in response to acute methadone at P2 compared to MS at 40 minutes ($p = 0.028$), and MM at 20 minutes ($p = 0.025$) and 60 minutes ($p = 0.009$). By P3, methadone-induced respiratory frequency depression was similar for all groups (Fig. 5.5B). A compensatory increase in V_T occurred at P0 and P1 in MN and MS neonates relative to MM at 40 and 60 minutes (Fig. 5.5A and B). Despite differences in methadone-induced frequency depression, methadone-induced depressions in V_E were similar for all maternal treatments (Fig. 5.5B) due to the compensatory increase in V_T in MN and MS neonates. However, 40 minutes after methadone at P2, V_E was significantly

reduced in MN neonates compared to MS neonates ($p = 0.043$), but not different from MM treated neonates.

Table 5.4. Daily acute methadone does not change baseline breathing.

		P1	P2	P3	P4	P5
n	**MM**	14	13	15	15	14
	MS	9	9	9	9	9
	MN	6	6	6	6	4
Apneas/min	**MM**	3.2 ± 2.0	0.7 ± 0.5	1.5 ± 2.7†	1.0 ± 0.8	0.5 ± 0.6
	MS	2.9 ± 2.2	5.0 ± 8.2	1.0 ± 0.7	0.4 ± 0.3	1.1 ± 1.6
	MN	4.4 ± 3.6	1.7 ± 2.5	0.8 ± 0.7	0.9 ± 1.3	0.6 ± 0.3
Apnea duration (sec)	**MM**	2.0 ± 0.4	1.3 ± 0.2	1.3 ± 0.4	1.1 ± 0.2	1.0 ± 0.4
	MS	2.3 ± 1.0	1.8 ± 0.6	1.4 ± 0.3	1.2 ± 0.3	1.2 ± 0.6
	MN	1.7 ± 0.5	1.5 ± 0.3	1.4 ± 0.5	1.3 ± 0.3	1.5 ± 0.6
Post-sigh Apneas/min	**MM**	0.5 ± 0.6	0.1 ± 0.1	0.1 ± 0.2	0.1 ± 0.2	0.1 ± 0.2
	MS	0.3 ± 0.3	0.9 ± 2.00	0.2 ± 0.1	0.0 ± 0.0	0.3 ± 0.5
	MN	0.6 ± 0.7	0.3 ± 0.6	0.0 ± 0.1	0.1 ± 0.1	0.0 ± 0.1
Frequency (Breaths/min)	**MM**	149.5 ± 23.4	176.9 ± 19.2	172.2 ± 20.8	192.0 ± 18.8	204.0 ± 40.0
	MS	141.4 ± 22.9	147.8 ± 24.1	166.5 ± 26.4	181.3 ± 24.5	210.8 ± 30.3
	MN	156.7 ± 19.0	159.7 ± 13.0	168.3 ± 37.1	184.6 ± 22.4	203.6 ± 5.7
V_T (ml/100g)	**MM**	0.82 ± 0.13	0.81 ± 0.18	0.70 ± 0.15	0.85 ± 0.19	0.79 ± 0.19
	MS	0.67 ± 0.10	0.76 ± 0.19	0.70 ± 0.09	0.70 ± 0.13	0.81 ± 0.13
	MN	0.94 ± 0.18	0.67 ± 0.10	0.75 ± 0.15	0.67 ± 0.23	0.60 ± 0.09
V_E (ml/min/100g)	**MM**	121.5 ± 29.3	144.9 ± 42.5	124.4 ± 30.7	166.9 ± 42.5	159.6 ± 36.6
	MS	98.1 ± 24.9	112.7 ± 41.0	118.6 ± 26.4	130.3 ± 30.7	175.7 ± 43.9
	MN	149.3 ± 42.5	109.8 ± 22.0	130.3 ± 49.8	131.8 ± 61.5	124.4 ± 22.0
SD1	**MM**	0.25 ± 0.08	0.12 ± 0.02	0.13 ± 0.03	0.12 ± 0.02	0.12 ± 0.05
	MS	0.23 ± 0.10	0.20 ± 0.11	0.14 ± 0.03	0.11 ± 0.02	0.11 ± 0.04
	MN	0.21 ± 0.09	0.15 ± 0.04	0.14 ± 0.04	0.14 ± 0.02	0.11 ± 0.01
SD2	**MM**	0.33 ± 0.11	0.51 ± 0.29	0.7 ± 0.32	0.65 ± 0.35	0.57 ± 0.25
	MS	0.83 ± 0.27	0.78 ± 0.44	0.65 ± 0.37	0.47 ± 0.19	0.86 ± 0.69
	MN	0.86 ± 0.56	1.21 ± 0.48	1.13 ± 0.94	1.1 ± 0.54	0.72 ± 0.34
Ti (sec)	**MM**	0.15 ± 0.04	0.09 ± 0.01	0.1 ± 0.04	0.08 ± 0.01	0.09 ± 0.03
	MS	0.15 ± 0.04	0.13 ± 0.08	0.09 ± 0.01	0.08 ± 0.01	0.09 ± 0.03
	MN	0.14 ± 0.04	0.11 ± 0.01	0.1 ± 0.02	0.08 ± 0.01	0.08 ± 0.01
Te (sec)	**MM**	0.36 ± 0.05	0.28 ± 0.04	0.29 ± 0.04	0.26 ± 0.03	0.25 ± 0.07
	MS	0.38 ± 0.08	0.37 ± 0.08	0.32 ± 0.07	0.28 ± 0.04	0.23 ± 0.04
	MN	0.33 ± 0.06	0.31 ± 0.04	0.31 ± 0.08	0.30 ± 0.05	0.25 ± 0.01

ANOVA-RM, Bonferroni post-hoc, † MM $p<0.05$ from MS.

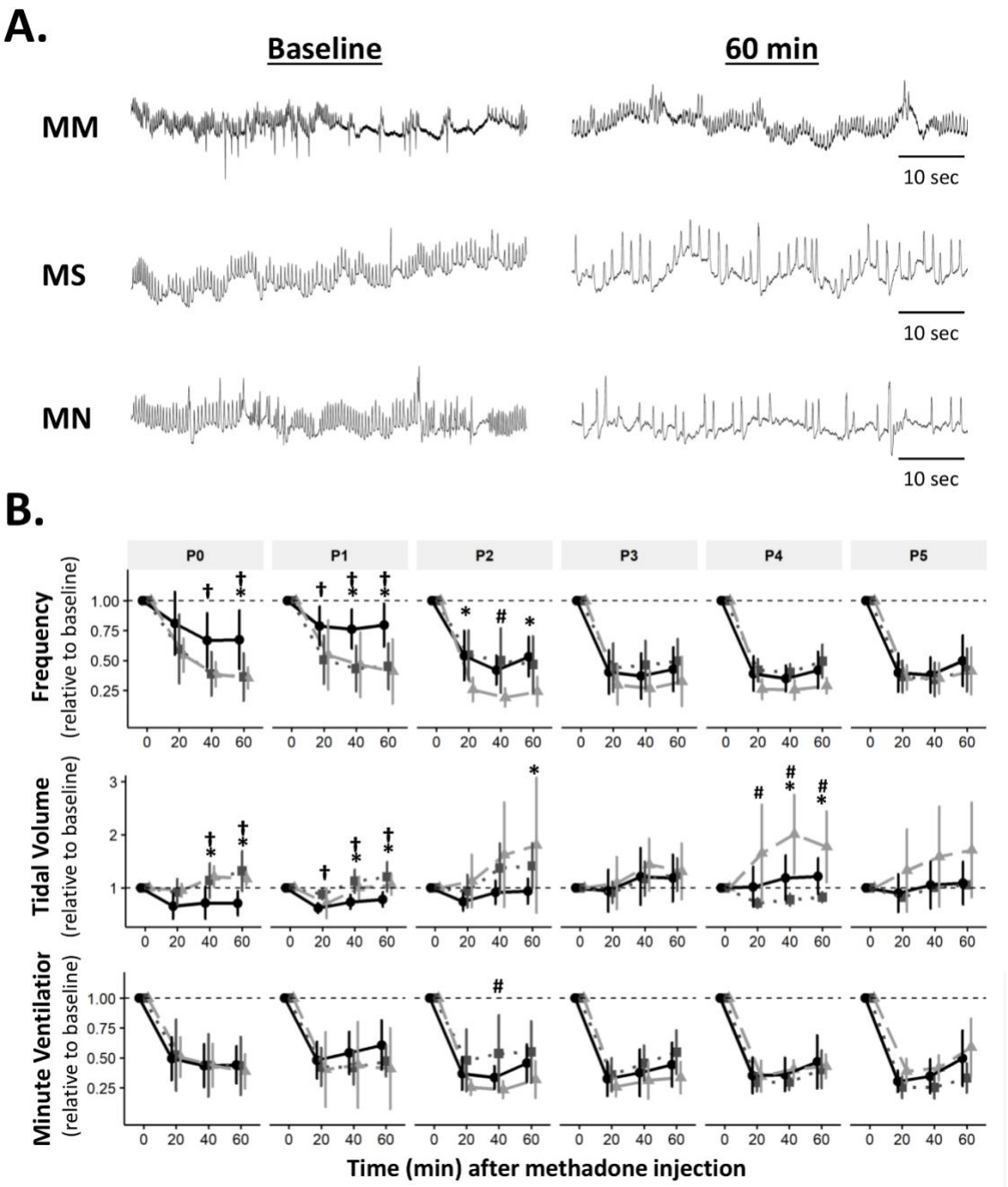

Figure 5.5. Maternal methadone blunts opioid-induced respiratory frequency depression at P0 and P1. Representative plethysmography traces **(A)** before (baseline) and 60 minutes after acute methadone at P0. Group data (**B**) for average breathing frequency, V_T and V_E after maternal methadone (MM, dark circles), maternal no-treatment (MN, grey squares), and maternal saline (MS, light triangles) combined with daily acute methadone (1mg/kg, i.p.). Relative breathing frequency and V_E were significantly reduced from 20-60 minutes after methadone injections in all groups **(B, top)**. At P0 and P1, methadone-induced frequency depression and V_T were blunted after MM compared to MN and MS **(B)**. ANOVA-RM, Bonferroni post-hoc, * MM $p<0.05$ from MN, † MM $p<0.05$ from MS, # MN $p<0.05$ from MS.

Quantal slowing emerges at P2, regardless of maternal treatment.

Quantal slowing is the slowing of respiratory frequency by integer multiples of the normal breathing period (Janczewski and Feldman, 2006; Mellen et al., 2003). Quantal slowing after acute methadone was observed in Poincare plots during the 15 minutes of peak respiratory frequency depression (25-40 minutes post methadone injection, Fig. 5.6A and C). Poincare plots (Fig. 5.6B and D) demonstrated either distributed slowing of respiratory period in younger neonates (P0 methadone response, Fig. 5.6A and B) or quantal slowing in older neonates, evident as distinct groupings of breaths at integer multiples of the normalized period (P5 methadone response, Fig 5.6C and D). Regardless of maternal treatment, quantal slowing emerged at P2 (Fig. 5.6E). The percentage of animals exhibiting quantal slowing from MM, MS, and MN groups highlights the age-dependency of the emergence of quantal slowing (Fig. 5.6E).

Discussion

As the use of opioids during pregnancy increases, improving our understanding of how the neurorespiratory system develops in the presence of opioids is a critical step in understanding how to best treat infants with NAS. Here, we show maternal methadone destabilizes early neonatal respiratory rhythm by increasing apneas and desensitizes neonates to acute methadone-induced frequency depression. The respiratory rhythm instability was most severe in the first day of life after maternal methadone and normalized within the first two days. Contrary to our hypothesis, repeated daily acute methadone after maternal methadone did not significantly alter or further destabilize

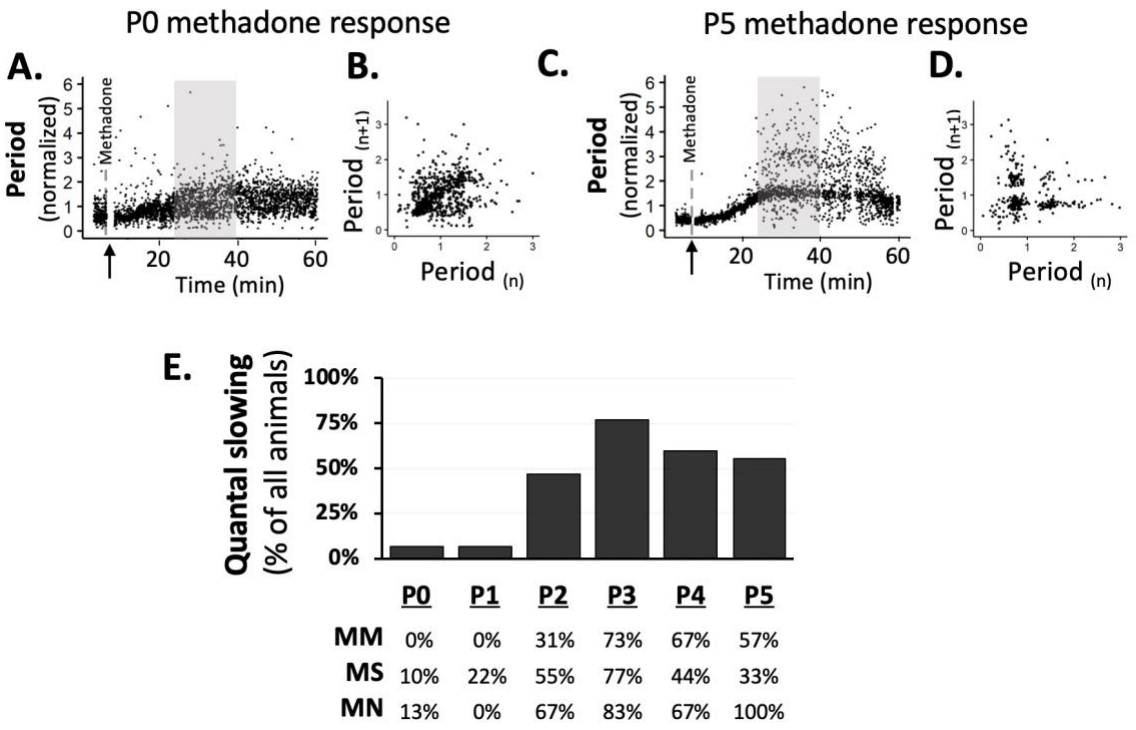

Figure 5.6. During neurorespiratory development, quantal slowing emerges at P2, regardless of maternal treatment. Representative changes in breathing period at P0 **(A and B)** and P5 **(C and D)** after acute methadone (1 mg/kg, i.p.; ↑) demonstrate age-dependent methadone-induced frequency depression. Grey highlighted regions **(A and C)** after methadone injection shown as Poincare plots **(B and D respectively)** to visualize quantal slowing. Quantal slowing is evident as periods clustered at quantal integers of the normal respiratory period at P5, but not P0. Group data highlight that regardless of maternal treatment, quantal slowing emerged at P2 in the majority of animals **(E).**

baseline breathing. However, maternal methadone desensitized neonates to acute methadone-induced respiratory depression at P0-1. Interestingly, the desensitization was normalized rapidly between P1 and P2, the same age at which quantal slowing emerged. These data suggest a significant reorganization of respiratory rhythm generating circuits regardless of maternal treatment at P1-2. Overall, maternal methadone destabilizes the neurorespiratory control system early after birth; however, breathing is rapidly normalized. Thus, while the respiratory control system seems largely resilient to late-

gestational exposure to methadone, there is an initial window of increased vulnerability to apneas, highlighting a particular window where treatment may be necessary.

Maternal methadone increased the prevalence of apneas and post-sigh apneas, and destabilized breathing rhythm in neonates. Though the origin of apneas cannot be identified in this study, the prevalence of apneas suggests dysfunction of the respiratory control network after maternal methadone. This dysfunction could be a result of concentrated neonatal methadone since opioids are known to be higher in fetal tissues compared to maternal levels (Peters et al., 1972) and opioids inhibit rhythm generating regions (Montandon et al., 2011). Neonatal CNS methadone levels can even exceed maternal levels as methadone accumulates in fetuses (Hl and Vin Peters, 1975; Peters et al., 1972), likely due to blunted opioid metabolism in neonates. Furthermore, maternal opioids continue to be transmitted to neonates through breast milk (Hendrickson and McKeown, 2012) and some evidence suggests human neonatal apneas are the result of opioid exposure through maternal milk (Naumburg and Meny, 1988). Therefore, maternal methadone may increase apnea prevalence as a result of high concentrations of methadone impairing neonatal respiratory neural circuitry. However, while concentrated methadone could induce apneas in neonates, methadone suppresses sighs (Bell et al., 2011), which were elevated after MM in P0 neonates. Therefore, elevated neonatal methadone levels alone are unlikely to explain both the increase in apneas and increase in sighs. Since apneas are more common in preterm or very early neonatal infants (Greer, 2012), maternal methadone could alternatively delay neurogenesis (Wu et al., 2014) and accelerate myelination (Hauser and Knapp, 2018; Vestal-Laborde et al., 2014). Therefore, maternal methadone may delay respiratory rhythm generating network

formation as maternal treatments began at E17, the day respiratory rhythm begins (Greer, 2012). A relatively immature respiratory control system could also explain the increased prevalence of apneas after maternal methadone.

Maternal methadone alone did not significantly reduce neonatal weight gain. Other reports (Byrnes and Vassoler, 2018; McLaughlin and Zagon, 1980) suggest longer maternal methadone treatments reduce neonatal weights, suggesting our exposure starting on E17, during a critical period for neurorespiratory development, is not inducing global developmental deficits. However, in combination with daily acute methadone, neonatal weights after MM were reduced at P3-4. Similarly, human infants withdrawing from methadone gain less weight in the first week of life, despite hyperphagia, suggesting altered metabolism after acute methadone (Martinez et al., 1999). Since we did not assess metabolism in our studies, it is unclear if maternal methadone alters neonatal rat metabolism. Further, it is unlikely maternal methadone induces long-lasting deficits in weight gain since adult weights are normalized in other studies with longer maternal methadone treatments (McLaughlin and Zagon, 1980). However, it remains unclear if adult weights are impacted by the combination of maternal methadone and daily acute methadone.

Peak hypoxic responses were unaffected by maternal methadone, demonstrating the respiratory control network can still respond appropriately to hypoxic stimuli. The phase I, peak hypoxic ventilatory response is typically attributed to activation of the peripheral chemosensors in the carotid body (Fung et al., 1996), which express opioid receptors (Ricker et al., 2015) and are inhibited by opioids in adults (Ricker et al., 2015). However, acute opioids also depress hypoxic responses through direct actions on the

brainstem (Bailey et al., 2000; Pattinson, 2008), suggesting a balancing of peripheral and central effects. Thus, the results presented here suggest maternal methadone does not alter carotid body function. Regardless of maternal treatment, the phase I ventilatory response to hypoxia increased substantially in the first 6 days of life, similar to previous reports of HVR development (Liu et al., 2006).

Unlike phase I, the phase II hypoxic ventilatory decline was significantly attenuated after maternal methadone. Phase II is known to be most severe in young neonates (Bissonnette, 2000; Liu et al., 2006; Moss et al., 1987) and is mediated by more complex mechanisms, likely involving changes in metabolism during hypoxia and brainstem signaling (Bissonnette, 2000). Purinergic signaling is significantly involved in hypoxic ventilatory depression, especially in young neonates (Elnazir et al., 1996; Gourine et al., 2005; Rajani et al., 2018), though it remains controversial (Funk and Gourine, 2018). The role of purinergic signaling in perinatal rats changes substantially from fetal to neonatal ages in rats (Huxtable et al., 2009), suggesting maternal methadone may alter the normal development of the purinergic system to blunt the hypoxic ventilatory decline after maternal methadone at P0. Interestingly, and contrary to our findings, human infants from mothers suffering from polysubstance abuse had significantly greater acute hypoxic responses and greater hypoxic ventilatory decline in the first week of life (Ali et al., 2016). However, these effects are confounded by the intake of multiple different types of drugs, which may independently or additively alter development (Nettleton et al., 2008). Thus, maternal methadone blunts the hypoxic ventilatory decline in neonatal rats, though whether this is physiologically advantageous or disadvantageous remains to be determined.

Maternal methadone did not alter hypercapnic ventilatory responses, suggesting the central networks sensing CO_2/pH are not altered by maternal methadone. Unlike the response in rats, maternal methadone or morphine enhances the HCVR in guinea pigs (Nettleton et al., 2008). Contrary to ours and other animal findings, human infants chronically exposed to prenatal methadone have significantly blunted HCVRs, which persist for the first two weeks of life (Olsen and Lees, 1980). These differences in the HCVRs may be explained by species differences, the duration, or timing of maternal methadone exposure. Our paradigm had only 5 days of maternal methadone, while the others last for at least half of gestation, suggesting earlier developmental exposure to methadone may have differential effects on hypercapnic responses.

Maternal methadone had no significant effect on baseline breathing responses to daily, repetitive acute methadone, but desensitized P0-1 neonates to acute methadone-induced respiratory depression. There are at least three explanations for these changes in opioid sensitivity. Firstly, maternal methadone could downregulate expression of opioid receptors in neonates, thereby reducing preBötC sensitivity to opioids from P0-1 and blunting methadone-induced respiratory depression. Maternal buprenorphine downregulates μ-opioid receptors in P1 rat whole brains (Belcheva et al., 1998), demonstrating expression of μ-opioid receptors is influenced by gestational opioids. Additionally, μ-opioid receptors normally increase in the rat brainstem from P3-6 (Kivell et al., 2004) and, as opioid receptor expression increases, methadone-induced respiratory frequency depression likely also increases, potentially explaining the increase in methadone-responses at P3 after maternal methadone. Secondly, competing inhibitory and excitatory actions of opioids in different respiratory regions could explain the blunted

respiratory depression at P0-1 after maternal methadone. While the preBötC rhythm is inhibited by opioids, the pFRG rhythm may be facilitated by opioids in P0-2 rats (Onimaru et al., 2006; Tanabe et al., 2005). Therefore, increased pFRG excitation could counteract depression in the preBötC to blunt methadone-induced frequency depression. Third, *in utero* exposure to methadone could impair preBötC activity during development, such that the respiratory network is more reliant on pFRG rhythm generation in the first two days of neonatal life. Thus, a rhythm generating network dominated by the pFRG would be less sensitive to opioid-induced respiratory depression. Future experiments assessing methadone responses of isolated respiratory circuitry and the developmental expression of opioid receptors would help delineate how maternal methadone alters methadone-induced respiratory depression.

Interestingly, only maternal methadone treated neonates exhibited differential methadone responses over time, due to their blunted acute methadone sensitivity at P0-1. Previous studies are conflicting on the development of opioid-induced frequency depression in rodents. One study demonstrates early μ-opioid receptor-induced respiratory depression is blunted at P1 relative to P10 (Greer et al., 1995), while another suggests respiratory frequency depression is similar between P2 and P8 (Colman and Miller, 2001). Here, methadone sensitivity was unchanged over time in neonates from maternal saline and maternal no treatment groups, suggesting no developmental shifts in opioid sensitivity. However, here we used repetitive daily methadone injections in the same rats from P0-5 and, in many other physiological systems, opioids induce tolerance within the first few exposures in rodents (Ling et al., 1989). Tolerance in the respiratory system has been observed after daily acute fentanyl (Laferrière et al., 2005), though this

has not been observed in other studies (Emery et al., 2016; Levitt and Williams, 2018). Here, we found no evidence for tolerance after repeated daily acute methadone exposure. Furthermore, it is widely thought the respiratory control system does not develop opioid-induced tolerance (Emery et al., 2016; Levitt and Williams, 2018), which increases vulnerability of patients to lethal respiratory depression with opioid over-use.

P0-5 is an important developmental period for respiratory rhythm generating mechanisms during which the dominance of the two respiratory oscillators switches (Huckstepp et al., 2016a). However, the precise timing of the switch is not clear. The phenomenon of quantal slowing represents a physiological means to probe the functional interactions of these two oscillators, whereby quantal slowing occurs when the two oscillators are in phase (Wittmeier et al., 2008) and the preBötC is the dominant inspiratory rhythm generator. Regardless of maternal treatment, quantal slowing emerged in the majority of rats at P2. This change likely reflects a network reorganization at this age irrespective of maternal treatment and suggests a strengthening in connectivity between the pFRG and preBötC. Previous work demonstrates pFRG activity precedes and drives preBötC activity in P0-1 rats (Onimaru and Homma, 2003) and then synchronizes with preBötC activity at P2 (Oku et al., 2007), suggesting quantal slowing may only emerge when the two oscillator's activities are tightly coupled. Additionally, the changes in this coupling of activity may be related to the considerable maturation of neurotransmitter systems occurring at this developmental stage. These changes include large changes in chloride conductance and its inhibition of respiratory rhythm (Ren and Greer, 2008), increased preBötC GABA receptor expression at P2 (Liu and Wong-Riley, 2004), and changes in AMPA receptor subunit expression (Wong-Riley and Liu, 2008).

Such changes may strengthen connections between the preBötC and pFRG, coupling their activity, and contributing to the emergence of quantal slowing at P2. The emergence of quantal slowing and shifts in functional connectivity between oscillators may have important implications for interpreting rhythm generating mechanisms at different neonatal ages. Specifically, the majority of studies on respiratory rhythm generation occur in neonatal rodents in the first week of life; however, the precise age range varies between and within studies. Therefore, investigations of respiratory circuitry before and after P2 may reveal divergent results and should be interpreted with these developmental changes in mind.

In our studies, maternal methadone treatment began on E17 because it is the first day of rhythmic respiratory neural activity, respiratory motor output, and fetal breathing movements in rats (reviewed in Greer, 2012). While other studies focused on the developmental impact of maternal opioids begin earlier to match the period when opioid receptors are first expressed in rodents (Byrnes and Vassoler, 2018), our experimental paradigm was intended to mitigate any other developmental effects of methadone and focus on this important period of neurorespiratory development. Methadone was chosen since it is commonly used as a clinical treatment in pregnant women and neonates (Bhavsar et al., 2018; Davis et al., 2018; Kraft et al., 2016; Pryor et al., 2017). However, methadone is also a non-competitive NMDA antagonist (Laurel Gorman et al., 1997), which may contribute to opioid-induced respiratory depression (Hoffmann et al., 2003). Furthermore, mice lacking NMDA receptors have more apneas in the first few days of life (Poon et al., 2000). However, central respiratory rhythm-generating networks develop normally in the absence of NMDA receptors (Funk et al., 1997) and the increase in

apneas may be due to *in utero* alterations to mechanosensory, chemosensory, or pontine respiratory areas (Funk et al., 1997; Poon et al., 2000). In our study, as we cannot determine the source of apneas, it is unclear if methadone antagonism of NMDA receptors is contributing to early-life respiratory instability.

Endogenous opioid systems modulate neonatal breathing (Jansen and Chernick, 1983) and may be altered by chronic methadone exposure. A surge of endorphins shortly after birth in neonatal brains (Jansen and Chernick, 1983) inhibits the preBötC, causing the pFRG to acutely dominate respiratory rhythm and maintain breathing rhythm (Feldman and Del Negro, 2006; Janczewski and Feldman, 2006). It is unclear if maternal methadone changes in the endogenous opioid system to impair respiratory instability at P0 or blunt early insensitivity to acute methadone. However, it is unlikely alterations in the endogenous opioid system explain the results presented here since maternal methadone in rats did not alter the endogenous opioid system in the neonatal rat ventral respiratory column (Gourévitch et al., 2017).

Understanding how maternal opioids alter neurorespiratory development is important for enhancing treatments for neonates exposed to *in utero* opioids. Our data support the hypothesis that maternal methadone increases apneas and destabilizes neonatal breathing. This instability may be clinically relevant as apneas are more common in babies who die of sudden infant death syndrome (SIDS) (Franco et al., 2003; Kahn et al., 1992) and maternal methadone increases the risk of SIDS (Moon, 2016). Additionally, the hypoxic and hypercapnic ventilatory responses were unaffected by maternal treatment. However, in humans, maternal methadone depresses hypoxic responses (Ward et al., 1992) and hypercapnic responses (Olsen and Lees, 1980),

suggesting differences in species or duration of *in utero* methadone exposure are important. Maternal methadone also blunted the acute response to neonatal methadone, suggesting neonates with NAS may have less respiratory depression after acute opioid treatments. Therefore, NAS infants potentially tolerate higher acute therapeutic doses to mitigate other symptoms of NAS, though the long-term impact of perinatal opioids remains to be determined. This protection from opioid-induced respiratory depression after acute methadone is lost rapidly in rats at P2, likely at the same time as the preBötC becomes the dominant respiratory rhythm generator. It is not clear if humans have a similar developmental trajectory of multiple respiratory rhythm generators as rodents. Importantly, the results presented here demonstrate neurorespiratory disruption by maternal methadone, which may be important for understanding and treating the increasing population of neonates exposed to gestational opioids.

CHAPTER VI

CONCLUSIONS AND FUTURE DIRECTIONS

This discussion will summarize the key findings of each study, describe how the findings advance the current understanding of acute and developmental disruption to respiratory control, and discuss potential future experiments.

Summary of Key Findings

The four aims of this dissertation focus on acute and developmental disruptions to the neurorespiratory control system. The ability of the respiratory control system to adapt and maintain robust breathing is critical to preserving life (Feldman et al., 2010). Acutely, respiratory control is dominated by feedback control mechanisms, like the ventilatory response to hypoxia or hypercapnia. However, plasticity of the respiratory system is fundamental to longer term adaptations. A few physiological examples highlighting this function include acclimatization to altitude, breathing changes during pregnancy, and adapting to disease or injury (Fuller and Mitchell, 2017). In this dissertation, I investigated acute feedback control mechanisms and used phrenic long-term facilitation (pLTF) as a model of respiratory plasticity.

Chapters II and III focused on acute, adult inflammation and the mechanisms by which inflammation disrupts respiratory plasticity. Acute inflammation is common to almost all disorders, diseases, and injuries where breathing is compromised (Hunter, 2012). Respiratory plasticity is thought to confer stability and adaptability of respiratory

control during disease and injury limiting respiratory output (Strey et al., 2013). Therefore, advancing our understanding of how inflammation alters respiratory control is of immediate interest. Furthermore, respiratory plasticity is of particular interest for its therapeutic potential in treating obstructive sleep apnea (Mateika and Komnenov, 2017), facilitating recovery after incomplete spinal cord injury (Hayes et al., 2014; Tester et al., 2014; Trumbower et al., 2012, 2017), and improving function during other motor disorders (Gonzalez-Rothi et al., 2015). All of these pathologies involve some element of inflammation (Arnold and Hagg, 2011; Meisel et al., 2005; Svensson et al., 2012). Thus, translation of these findings toward clinical conditions involving motor limitation and inflammation is major motivation for these studies.

Chapters IV and V focus on perinatal disruption of respiratory control. The respiratory control system must develop and be fully functional at birth and continues to mature during the first two weeks of life, a critical period for neurorespiratory development (Greer, 2012; Liu et al., 2006). Insults to the perinatal respiratory control system can disrupt development and cause long-lasting alterations to respiratory control mechanisms (Bavis et al., 2004). In particular, early life inflammation, which acutely disrupts respiratory control (Poets et al., 1994; Poets and Southall, 1994) and is especially common in pre-term infants (Stoll et al., 2002, 2004), increases the risk of sleep apnea later in life (Tapia et al., 2016). Thus, Chapter IV investigates the lasting impacts of neonatal inflammation on adult respiratory plasticity and contributes to our basic understanding of how early-life insults can alter adult respiratory control. The findings may have implications for adult disease risk and lays the foundation for future studies

investigating underlying mechanisms and the lasting consequences of early-life inflammation.

Chapter V focuses on perinatal opioid exposure, a separate, yet increasingly common perinatal insult. Maternal opioid use is on the rise (Epstein et al., 2013; Krans et al., 2015; Stover and Davis, 2015) and results in infants born with neonatal abstinence syndrome (NAS) (Finnegan *et al.*, 1975; Hudak *et al.*, 2012). NAS is characterized by dysfunction of the central and autonomic nervous system (Kraft et al., 2016). The increase maternal use of opioids and risk of NAS has created a significant clinical need to improve treatments for infants perinatally exposed to opioids (Kraft et al., 2016). Opioids suppress the preBötC activity, which is responsible for respiratory rhythm generation (Smith et al., 1991) and must develop before birth (Greer, 2012). As infants with NAS are more likely to have respiratory instability and apneas (Beckwith and Burke, 2015), Chapter V investigated the impact of maternal opioids on neonatal respiratory control mechanisms. These studies are the first to investigate respiratory control in rats exposed to maternal opioids and provide a basis for future research investigating short and long-term effects of perinatal opioids on respiratory control mechanisms. Specifically, these studies provide novel data regarding the effects of maternal opioids destabilizing neonatal breathing and blunting acute opioid-induced respiratory depression. Understanding mechanisms by which perinatal opioids alter respiratory control will contribute to our ability to treat infants born to opioid-using mothers.

The major findings from Chapter II-V are summarized in figure 6.1.

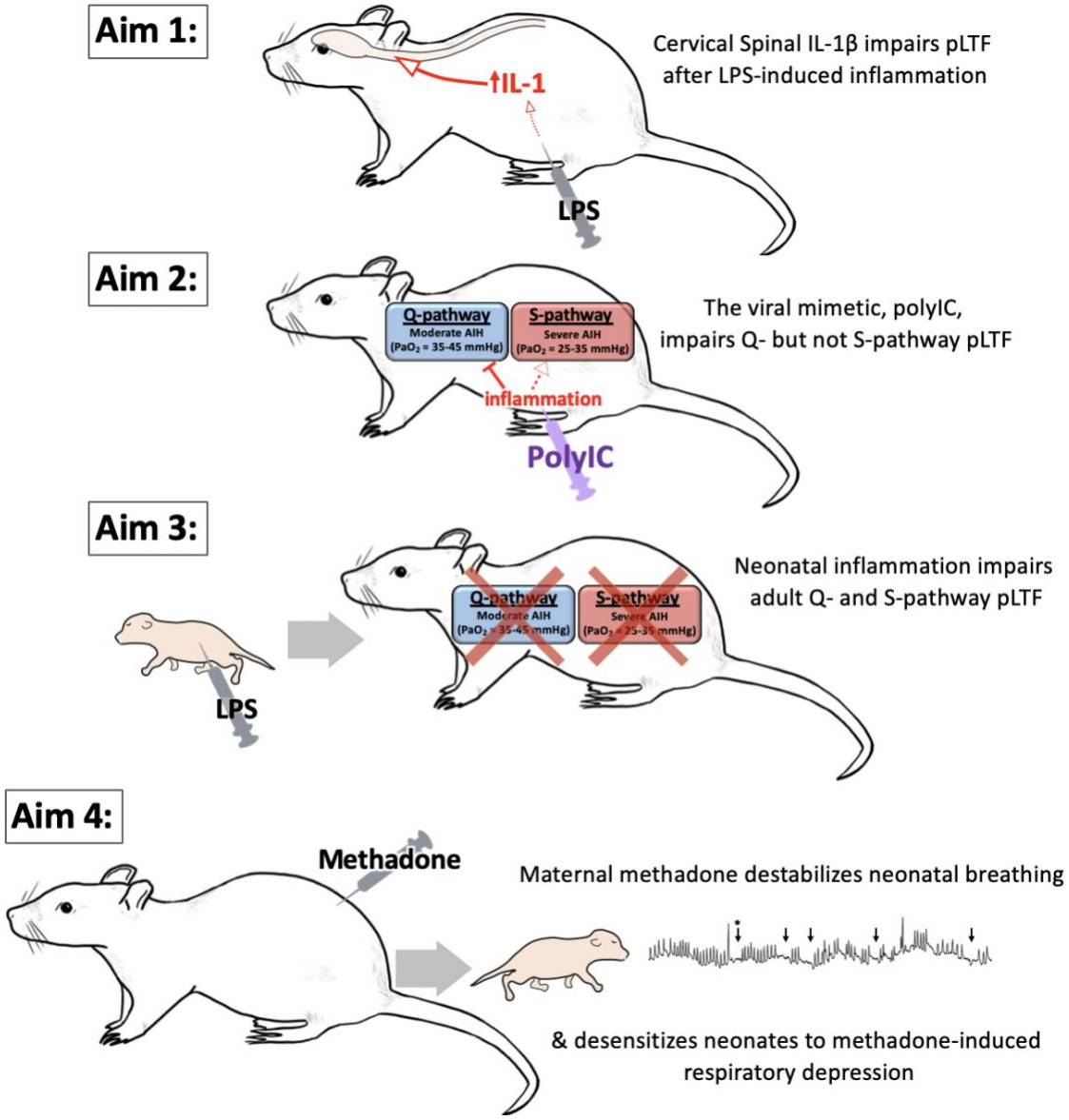

Figure 6.1. Summary of major findings. Aim 1) Both peripheral and cervical spinal IL-1R antagonism restores pLTF after acute, adult inflammation. These data demonstrate peripheral IL-1 signaling back to the CNS and local IL-1 signaling in the cervical spinal cord are both necessary to impair adult pLTF after peripheral inflammation. Aim 2) The viral mimetic polyIC induces inflammation and impairs Q-pathway, but not S-pathway-evoked, pLTF. These data extend and generalize our understanding of the impairment of Q-pathway pLTF by inflammation and confirm the insensitivity of S-pathway pLTF to acute adult inflammation. Aim 3. A single bout of neonatal inflammation impairs adult Q-pathway and S-pathway evoked pLTF, demonstrating long-lasting deficits in adult respiratory control after early-life inflammation. Aim 4. Maternal methadone increases apneas in neonates and desensitizes the neonates to acute methadone-induced respiratory depression.

Aim 1) Interleukin-1 signaling after acute, systemic inflammation undermines adult respiratory motor plasticity (Fig. 6.1).

Previous work has demonstrated inflammation undermines respiratory plasticity and is restored by anti-inflammatory treatment (Huxtable et al., 2013, 2015; Vinit et al., 2011). The study, presented in Chapter II, was the first to demonstrate the importance of a single inflammatory cytokine receptor, IL-1R, in impairing pLTF after acute inflammation, adding to our mechanistic understanding of how systemic inflammation impairs neurorespiratory control mechanisms. Furthermore, these experiments demonstrate the necessity of IL-1R activation in the cervical spinal cord for impairing pLTF after peripheral inflammation. This is the first direct demonstration of local spinal inflammatory cytokines impairing respiratory plasticity, suggesting inflammation is transmitted from the periphery to the cervical spinal cord to impair plasticity. As IL-1R antagonism restored pLTF, we next tested the sufficiency of IL-1β in the cervical spinal cord to impair pLTF. IL-1β is an endogenous inflammatory cytokine activating IL-1R and has no known off-target binding. Exogenous spinal IL-1β was not sufficient to impair pLTF, suggesting other inflammatory signaling mechanisms, likely involving other inflammatory cytokines, are also required. LPS also upregulates other inflammatory cytokines in the cervical spinal cord, including iNOS and COX-2 (Huxtable et al., 2013), which may have additive effects and contribute to the impairment in pLTF after inflammation.

Other IL-1R ligands could be involved in activating IL-1R after LPS-induced inflammation. IL-1α and IL-1β both activate IL-1R, and are thought have to identical biological effects (Dinarello, 2009). However, a recent study suggests IL-1α has distinct

inflammatory effects in the CNS through more potent activation of astrocytes (Liddelow et al., 2017). It is possible spinal IL-1α, presumably still acting through IL-1R, is sufficient for impairing pLTF and should be the topic of future studies.

In a separate model of inflammation induced by intermittent hypoxia, p38 MAPK activation, a kinase downstream of many inflammatory signaling pathways, is required to impair pLTF (Huxtable et al., 2015). Chapter II adds to a working model, whereby peripheral inflammation is transmitted to the cervical spinal cord, activating IL-1Rs which leads to p38 MAPK activation and impairment of pLTF. In the hippocampus, IL-1β activates p38 MAPK and p38 MAPK activation is responsible for attenuating hippocampal plasticity (Curran et al., 2003; Kelly et al., 2003). However, to date, no studies have directly linked IL-1R activation with p38 MAPK activation in impairing respiratory plasticity and thus, should be the topic of future investigations. Additionally, the mechanism by which p38 MAPK impairs plasticity is unknown. One hypothesis suggests p38 MAPK activates protein phosphatase 1 (PP1), which is key to the pattern sensitivity of pLTF (Huxtable et al., 2018). Future studies could use available inhibitors for p38 MAPK and PP1 to further elucidate the mechanisms by which inflammation and IL-1 signaling impairs plasticity in the cervical spinal cord.

Taken together, Chapter II demonstrates the inflammatory impairment in pLTF is due to cervical spinal IL-1 signaling. Furthermore, these studies suggest a more complete working model by which IL-1 signaling activates downstream signaling pathways to impair plasticity. However, the specific cell-types involved in impairing plasticity remain unknown. IL-1R is primarily localized to endothelial cells in the cervical spinal cord (K. Royster, unpublished observations): however, p38 is activated within phrenic motor

neurons after inflammation (Huxtable et al., 2015). Therefore, other intermediate signaling molecules may be responsible for linking IL-1R activation with downstream mechanisms like p38 MAPK activation to impair pLTF. Future investigations should target cell-specific mechanisms of the inflammatory impairment of pLTF.

Aim 2) Viral mimetic-induced inflammation abolishes Q-pathway-evoked, but not S-pathway-evoked, adult respiratory motor plasticity in rats (Fig. 6.1).

Inflammation arises from a variety of sources throughout our lives. Inflammation induced by either LPS or by intermittent hypoxia undermine pLTF (Huxtable et al., 2013, 2015, 2017; Vinit et al., 2011). However, viral-induced inflammation is one of the most common sources of inflammation (Obasi et al., 2014). Chapter III demonstrated the inflammatory impairment of pLTF could be generalized to inflammation induced by a viral mimetic. Therefore, the inflammation-induced impairments in respiratory plasticity are generalizable to different sources of inflammation, suggesting diverse inflammatory stimuli are relevant to altering respiratory control. Additionally, viral infections are particularly common in patients with spinal cord injury (Bracchi-Ricard et al., 2016), which is the focus of using respiratory plasticity as a therapeutic agent (Hayes et al., 2014; Tester et al., 2014; Trumbower et al., 2012, 2017).

While Q-pathway-evoked pLTF is impaired by inflammation, the S-pathway is inflammation-resistant (Agosto-Marlin et al., 2017). Here, we support the findings of the inflammation-resistance of S-pathway using a distinct model of inflammation. This finding has important clinical significance as it suggests an alternative pathway to respiratory plasticity is functional even during inflammation. Thus, this "backup"

pathway could be targeted therapeutically with more severe AIH protocols to elicit beneficial responses in patients not responding to moderate AIH. However, clinicians are often concerned about exposing patients to severe hypoxia. Therefore, future pre-clinical studies should explore different AIH protocols, including more severe AIH, to investigate if more severe paradigms are safe and effective in humans. If more severe AIH is safe and effective, it may prove to be an effective strategy for eliciting plasticity in patients resistant to moderate AIH.

Mechanistically, it is unknown if viral inflammation impairs plasticity via the same mechanisms as LPS or intermittent hypoxia-induced inflammation. Therefore, additional studies could build on our findings by investigating if IL-1R activation is also necessary after polyIC-induced inflammation and if mechanisms downstream of IL-1R, such as p38 MAPK, are also involved. Though these mechanism are likely similar, distinct mechanisms would suggest unique strategies may be needed to mitigate inflammation and elicit plasticity depending on the source of inflammation. However, to date, data suggest inflammatory mechanisms converge and respiratory plasticity can be restored by ketoprofen (Huxtable et al., 2013, 2015). Therefore, treatments targeting downstream inflammatory signaling are likely sufficient to inhibit inflammation and allow for respiratory plasticity regardless of inflammatory stimuli.

Another potential avenue for future research is the role of sleep-deprivation in the inflammatory-impairment of respiratory plasticity. A proposed function of sleep, especially REM sleep, is to prepare for neuroplasticity related to learning and memory (Abel et al., 2013). Furthermore, REM sleep is reduced by each of the inflammation-induced models used to date to impair plasticity; LPS (Schiffelholz and Lancel, 2001),

polyIC (Krueger et al., 1988), and intermittent hypoxia (Polotsky et al., 2006). Thus, sleep deprivation in these models could contribute to deficits in respiratory plasticity. REM sleep loss specifically disrupts cell-mechanisms of hippocampal long-term potentiation (reviewed in Abel et al., 2013), which share features involved in pLTF (Turner et al., 2018), such as cAMP dependence (Grosmark et al., 2012) and downregulated NMDA activity (McDermott et al., 2006). Therefore, REM sleep disruption could also contribute to the cellular mechanisms inhibiting pLTF. However, the precise mechanisms by which sleep deprivation alters cell functions involved in plasticity are unclear. REM sleep deprivation also causes inflammation in rats (Yehuda et al., 2009), suggesting REM sleep disturbances could impair plasticity by inducing inflammation. Future studies should investigate the role of sleep deprivation in impairing pLTF. Does sleep deprivation alone impair pLTF? Is the impairment dependent on inflammatory signaling? Understanding the impact of sleep alterations in regulating respiratory plasticity may be especially relevant in clinical conditions like sleep apnea, where sleep architecture is disrupted and respiratory plasticity may be a therapeutic strategy to reduce symptoms of sleep apnea (Mateika and Komnenov, 2017).

Aim 3) One bout of neonatal inflammation impairs adult respiratory motor plasticity in male and female rats (Fig. 6.1).

Chapter IV shifts from acute inflammation in adults to studying the long-lasting effects of early-life inflammation. While the adult respiratory control system is known to be susceptible to other early-life stressors (Bavis et al., 2004; Fournier et al., 2011; Genest et al., 2004), the lasting effects of early life inflammation are unknown. However,

perinatal inflammation has numerous effects on non-respiratory adult physiological systems (Bilbo, 2005, 2010; Bilbo et al., 2006, 2010; Grace et al., 2014; Hornig et al., 1999; Mouihate et al., 2010; Rantakallio et al., 1997; Shanks et al., 2000; Spencer et al., 2011; Wang et al., 2013). Chapter IV demonstrated, for the first time, a single bout of neonatal inflammation impairs Q- and S-pathways to adult respiratory plasticity. We hypothesize that respiratory plasticity compensates and stabilizes breathing in the face of conditions compromising breathing, such as injury or sleep apnea. Therefore, our findings suggest the respiratory control network is vulnerable to early-life inflammation, which may limit the capacity to compensate to disease or injury later in life and contribute to adult ventilatory control disorders.

We found the impairment of Q-pathway plasticity in adults is dependent on acute inflammatory signaling. However, no lasting increase in adult inflammatory gene expression was evident in relevant CNS regions. It is possible cell-specific inflammatory signaling changes could be responsible for the inflammatory impairment of Q-pathway-evoked pLTF. Future experiments are in progress to identify cell-specific changes in inflammatory signaling related to these findings.

The impairment in S-pathway evoked plasticity was independent of acute inflammatory signaling. However, acute adenosine receptor agonism revealed S-pathway plasticity suggesting upstream impairments, such as the source of adenosine. Astrocytes are likely to be the primary source of adenosine during hypoxia (Angelova et al., 2015; Takahashi et al., 2010). Therefore, future studies implementing genetic strategies to specifically block astrocytic vesicular release (Rajani et al., 2018; Sheikhbahaei et al.,

2018) would be useful in elucidating the role of astrocytes and the source of adenosine in activating S-pathway-evoked plasticity.

Importantly, chapter IV is one of only a few studies investigating respiratory motor plasticity in females (Behan et al., 2002; Dougherty et al., 2017) and is the first to demonstrate a number of findings in female rats. This is the first report to demonstrate the presence of S-pathway-evoked pLTF in females, evoked by either severe AIH or adenosine receptor agonism. The S-pathway may be relevant for therapeutic uses as it is thought to act as an important backup pathway when Q-pathway is impaired. This is also the first demonstration in females of Q-pathway impairment by inflammatory signaling. Thus, though respiratory plasticity is estrus-cycle dependent (Dougherty et al., 2017), mechanisms stimulating or inhibiting respiratory plasticity do not differ by sex. Future experiments should continue to include females, especially translational studies using AIH therapeutically to improve breathing (Tester et al., 2014) and other motor functions (Hayes et al., 2014; Trumbower et al., 2012, 2017).

Aim 4) Maternal methadone destabilizes early neonatal breathing and desensitizes neonates to acute methadone-induced respiratory depression (Fig. 6.1).

Maternal methadone is another common perinatal insult and directly inhibits respiratory rhythm generation. Chapter V demonstrates maternal methadone exposure during respiratory network development (E17-birth) (Greer et al., 2006; Pagliardini et al., 2003), destabilizes neonatal breathing by increasing apneas and post-sigh apneas in P0 neonates. Thus, infants born to opioid using mothers may have exacerbated respiratory instability early in life. This instability may be clinically relevant as apneas are more

common in babies who die of sudden infant death syndrome (SIDS) (Franco et al., 2003; Kahn et al., 1992) and maternal methadone increases the risk of SIDS (Moon, 2016). We also demonstrate a significant blunting of methadone-induced respiratory depression at P0-1 after maternal methadone. As neonates are commonly treated with methadone to mitigate symptoms of withdrawal, this finding suggests neonates may have blunted methadone sensitivity early in life and could tolerate higher doses, though this effect rapidly normalized at P2 in rats. However, higher acute doses in neonates should be balanced with the potential for long-term consequences of opioid exposure in neonates.

Our investigation into the effects of perinatal methadone also provided an opportunity to understand the development of respiratory rhythm generating mechanisms in the first few days of life. During development, two rhythm generating regions contribute to breathing in neonates; the opioid-sensitive preBötC and the opioid-insensitive pFRG (Huckstepp et al., 2016b; Mellen et al., 2003). P0-5 is an important developmental period during which the dominance of these respiratory oscillators switches (Huckstepp et al., 2016b; Onimaru, 2006; Onimaru and Homma, 2003), though the precise timing of this transition is unclear. Chapter V also provides evidence suggesting P2 is the age at which the preBötC and pFRG activity synchronize and therefore, quantal slowing emerges in the presence of opioids (Huckstepp et al., 2016b; Mellen et al., 2003; Wittmeier et al., 2008). Before P2, other reports suggest the pFRG is pre-inspiratory and may drive preBötC inspiratory activity (Onimaru et al., 2006). Thus, these findings provide important context for the interpretation of many studies of respiratory rhythm generation, which typically study rats in the first week of life. Specifically, P0-2 likely represents a unique time in rhythm generating networks where

inspiratory rhythm is driven by pFRG and connections from preBötC to pFRG are relatively weak. After P2, pFRG activity continues to shift toward post-inspiratory/expiratory activity patterns through the first week when it becomes predominately expiratory (Janczewski and Feldman, 2006).

Future studies should focus on understanding the mechanistic effects of maternal methadone in isolated respiratory circuitry, the mechanisms driving breathing instability in P0-1 neonates, and the long-term consequences of perinatal opioid exposure. Experiments in isolated respiratory circuitry will be important for understanding the mechanisms involved in blunting opioid-induced respiratory depression after maternal methadone. Direct application of opioids on the preBötC and in brainstem spinal cord preparations could demonstrate if isolated respiratory circuitry is sufficient to replicate blunted opioid-induced respiratory depression or are other brain regions involved in this change in sensitivity. Next, the mechanisms responsible for respiratory instability and increased apneas after maternal methadone are unknown. One possibility is an increased endogenous opioid system. Upregulated opioid receptors or more available endogenous opioids would inhibit rhythm generation and contribute to breathing instability. Therefore, future studies with acute opioid receptor antagonists in P0-1 neonates after maternal methadone could demonstrate if changes in neonatal rhythm instability were due to elevated endogenous opioids. Finally, are there long-term consequences of perinatal opioid exposure on adult respiratory control? Neonatal opioids may induce opioid hypersensitivity in adults (Kennedy, 2014), making them more susceptible to acute opioid-induced respiratory depression. Also, opioids may induce inflammation

(Wang et al., 2012), which could itself induce many long-lasting physiological changes as demonstrated in Chapter IV.

The potential interplay between opioids and inflammatory signaling raises interesting questions and potentially unites the findings of Chapters II-V. Opioids activate Toll-like receptor 4 (TLR4), the pattern recognition receptor which is activated by LPS, and increase pro-inflammatory signaling (Hutchinson et al., 2009). The most well characterized opioid-induced inflammatory effects are from morphine; however, other clinically relevant opioids (e.g. methadone, oxycodone) also directly activate TLR4 (Grace et al., 2015). Opioid-induced inflammatory signaling occurs in multiple species, whereby chronic intrathecal morphine upregulates spinal inflammatory cytokines in both rodents (Johnston, 2004) and in humans (Zin et al., 2010). These underappreciated opioid signaling pathways mechanistically link opioid actions with inflammation. Thus, perinatal opioids may induce inflammation and have long-lasting consequences, impairing adult respiratory plasticity as demonstrated in chapter IV. Furthermore, acute, adult opioid exposure could induce inflammation and impair respiratory plasticity similar to the inflammatory impairments in pLTF in Chapter II and III. Thus, opioid use in clinical scenarios, such as post-operative care, may limit the adaptability of the respiratory system after surgery. Potential acute opioid-induced impairments in respiratory plasticity may also be relevant for using AIH therapeutically, especially in chronic spinal cord injury patients who are likely to use opioids for pain management (Hand et al., 2018) and are a promising target population for therapeutic AIH (Fuller and Mitchell, 2017; Hayes et al., 2014; Tester et al., 2014; Trumbower et al., 2012, 2017).

Therefore, the interactions between opioids and inflammation in respiratory control are worthy of future investigation.

Conclusions

The respiratory system must be adaptable in order to produce the necessary rhythmic motor output to drive ventilation. Respiratory plasticity is an important feature of this adaptability (Mitchell and Johnson, 2003). Importantly, basic science research into mechanisms of respiratory plasticity has directly led to development of promising therapeutic interventions to promote breathing and other motor function in patients with motor limitations (Fuller and Mitchell, 2017; Hayes et al., 2014; Tester et al., 2014; Trumbower et al., 2012, 2017). However, inflammation may limit the therapeutic benefit of respiratory motor plasticity. Thus, research furthering our understanding of respiratory plasticity, how plasticity can be undermined, and strategies to enhance the benefits of plasticity are critical for future clinical developments.

The research presented in this dissertation contributes to our fundamental understanding of how inflammation impairs adult respiratory plasticity, both acutely and after a single early-life exposure. It also builds on previous research (Agosto-Marlin et al., 2017), suggesting alternative pathways to evoking plasticity (such as severe AIH and S-pathway pLTF) may be beneficial for eliciting therapeutic plasticity in inflammatory conditions. Additionally, it lays the groundwork for future investigations in understanding how early-life inflammation causes lasting respiratory system impairments. Specifically, understanding, region-specific, cell-specific, and molecular

pathway-specific changes after early-life inflammation will help us understand the lasting respiratory impairments after early-life inflammation.

Finally, the impact of maternal opioid use on neonatal breathing is of growing interest as the rates of maternal opioid use continue to rise (Epstein et al., 2013; Kraft et al., 2016; Krans et al., 2015; Stover and Davis, 2015). The research presented here lays the foundation for future studies investigating how perinatal opioids alter the developing endogenous opioid system, how isolated respiratory circuitry is altered by maternal opioids, and what the long-term consequences of perinatal opioids are for adult respiratory control.

REFERENCES CITED

Abel, T., Havekes, R., Saletin, J. M., and Walker, M. P. (2013). Sleep, plasticity and memory from molecules to whole-brain networks. *Curr. Biol.* 23, R774-88. doi:10.1016/j.cub.2013.07.025.

Agosto-Marlin, I. M., Nichols, N. L., and Mitchell, G. S. (2017). Adenosine-dependent phrenic motor facilitation is inflammation resistant. *J. Neurophysiol.* 117, 836–845. doi:10.1152/jn.00619.2016.

Agosto-Marlin, I. M., Nichols, N. L., and Mitchell, G. S. (2018). Systemic inflammation inhibits serotonin receptor 2-induced phrenic motor facilitation upstream from BDNF/TrkB signaling. *J Neurophysiol* 119, 2176–2185. doi:10.1152/jn.

Aleksandrova, N. P., and Danilova, G. A. (2010). Effect of intracerebroventricular injection of interleukin-1-beta on the ventilatory response to hyperoxic hypercapnia. *Eur. J. Med. Res.* 15 Suppl 2, 3–6. doi:10.1186/2047-783X-15-S2-3.

Ali, K., Rossor, T., Bhat, R., Wolff, K., Hannam, S., Rafferty, G. F., et al. (2016). Antenatal substance misuse and smoking and newborn hypoxic challenge response. *Arch. Dis. Child. Fetal Neonatal Ed.* 101, F143–F148. doi:10.1136/archdischild-2015-308491.

Anderson, T. M., Garcia, A. J., Baertsch, N. A., Pollak, J., Bloom, J. C., and Wei, A. D. (2016). A novel excitatory network for the control of breathing. *Nature* 536, 76–80. doi:10.1038/nature18944.

Angelova, P. R., Kasymov, V., Christie, I., Sheikhbahaei, S., Turovsky, E., Marina, N., et al. (2015). Functional Oxygen Sensitivity of Astrocytes. *J. Neurosci.* 35, 10460–10473. doi:10.1523/JNEUROSCI.0045-15.2015.

Arakawa, K., Arakawa, H., Hueston, C. M., and Deak, T. (2014). Effects of the Estrous Cycle and Ovarian Hormones on Central Expression of Interleukin-1 Evoked by Stress in Female Rats. *Neuroendocrinology* 100, 162–177. doi:10.1159/000368606.

Arnold, S. A., and Hagg, T. (2011). Anti-Inflammatory Treatments during the Chronic Phase of Spinal Cord Injury Improve Locomotor Function in Adult Mice. *J. Neurotrauma*. doi:10.1089/neu.2011.1888.

Attarian, S., Tran, L. C., Moore, A., Stanton, G., Meyer, E., and Moore, R. P. (2014). The neurodevelopmental impact of neonatal morphine administration. *Brain Sci.* 4, 321–34. doi:10.3390/brainsci4020321.

Avital, A., Goshen, I., Kamsler, A., Segal, M., Iverfeldt, K., Richter-Levin, G., et al. (2003). Impaired interleukin-1 signaling is associated with deficits in hippocampal memory processes and neural plasticity. *Hippocampus* 13, 826–834. doi:10.1002/hipo.10135.

Bach, K. B., and Mitchell, G. S. (1996). Hypoxia-induced long-term facilitation of respiratory activity is serotonin dependent. *Respir. Physiol.* 104, 251–260. doi:10.1016/0034-5687(96)00017-5.

Bailey, P. L., Lu, J. K., Pace, N. L., Orr, J. A., White, J. L., Hamber, E. A., et al. (2000). Effects of Intrathecal Morphine on the Ventilatory Response to Hypoxia. *N. Engl. J. Med.* 343, 1228–1234. doi:10.1056/NEJM200010263431705.

Baker-Herman, T. L., Fuller, D. D., Bavis, R. W., Zabka, A. G., Golder, F. J., Doperalski, N. J., et al. (2004). BDNF is necessary and sufficient for spinal respiratory plasticity following intermittent hypoxia. *Nat. Neurosci.* 7, 48–55. doi:10.1038/nn1166.

Baker-Herman, T. L., and Mitchell, G. S. (2002). Phrenic long-term facilitation requires spinal serotonin receptor activation and protein synthesis. *J. Neurosci.* 22, 6239–6246. doi:20026595.

Baker-Herman, T. L., and Mitchell, G. S. (2008). Determinants of frequency long-term facilitation following acute intermittent hypoxia in vagotomized rats. *Respir. Physiol. Neurobiol.* 162, 8–17. doi:10.1016/j.resp.2008.03.005.

Balan, K. V, Kc, P., Hoxha, Z., Mayer, C. A., Wilson, C. G., and Martin, R. J. (2011). Vagal afferents modulate cytokine-mediated respiratory control at the neonatal medulla oblongata. *Respir. Physiol. Neurobiol.* 178, 458–464. doi:10.1016/j.resp.2011.03.003.

Bavis, R. W., Olson, E. B., Vidruk, E. H., Fuller, D. D., and Mitchell, G. S. (2004). Developmental plasticity of the hypoxic ventilatory response in rats induced by neonatal hypoxia. *J. Physiol.* 557, 645–660. doi:10.1113/jphysiol.2004.061408.

Beckwith, A. M., and Burke, S. A. (2015). Identification of early developmental deficits in infants with prenatal heroin, methadone, and other opioid exposure. *Clin. Pediatr. (Phila).* 54, 328–335. doi:10.1177/0009922814549545.

Behan, M., and Kinkead, R. (2011). "Neuronal Control of Breathing: Sex and Stress Hormones," in *Comprehensive Physiology* (Hoboken, NJ, USA: John Wiley & Sons, Inc.), 2101–2139. doi:10.1002/cphy.c100027.

Behan, M., Zabka, A. G., and Mitchell, G. S. (2002). Age and gender effects on serotonin - dependent plasticity in respiratory motor control. *Respir. Physiol. Neurobiol.* 131, 65–77. doi:10.1016/S1569-9048(02)00038-1.

Belcheva, M. M., Bohn, L. M., Ho, M. T., Johnson, F. E., Yanai, J., Barron, S., et al. (1998). Brain opioid receptor adaptation and expression after prenatal exposure to buprenorphine. *Dev. Brain Res.* 111, 35–42. doi:10.1016/S0165-3806(98)00117-5.

Bell, H. J., Azubike, E., and Haouzi, P. (2011). The "other" respiratory effect of opioids: suppression of spontaneous augmented ("sigh") breaths. *J. Appl. Physiol.* 111, 1296–1303. doi:10.1152/japplphysiol.00335.2011.

Bellinger, F. P., Madamba, S., and Siggins, G. R. (1993). Interleukin 1?? inhibits synaptic strength and long-term potentiation in the rat CA1 hippocampus. *Brain Res.* 628, 227–234. doi:10.1016/0006-8993(93)90959-Q.

Benyamin, R., Trescot, A. M., Datta, S., Buenaventura, R., Adlaka, R., Sehgal, N., et al. (2008). Opioid complications and side effects. *Pain Physician* 11, S105-20. Available at: http://www.ncbi.nlm.nih.gov/pubmed/18443635 [Accessed May 18, 2018].

Bhavsar, R., Kushnir, A., and Kemble, N. (2018). Incidence and Severity of Neonatal Abstinence Syndrome in Infants with prenatal exposure to Methadone versus Buprenorphine. *Pediatrics* 142, 145–145. doi:10.1542/PEDS.142.1_MEETINGABSTRACT.145.

Bilbo, S. D. (2005). Neonatal Infection-Induced Memory Impairment after Lipopolysaccharide in Adulthood Is Prevented via Caspase-1 Inhibition. *J. Neurosci.* 25, 8000–8009. doi:10.1523/JNEUROSCI.1748-05.2005.

Bilbo, S. D. (2010). Early-life infection is a vulnerability factor for aging-related glial alterations and cognitive decline. *Neurobiol. Learn. Mem.* 94, 57–64. doi:10.1016/J.NLM.2010.04.001.

Bilbo, S. D., Biedenkapp, J. C., Der-Avakian, A., Watkins, L. R., Rudy, J. W., and Maier, S. F. (2005). Neonatal infection-induced memory impairment after lipopolysaccharide in adulthood is prevented via caspase-1 inhibition. *J. Neurosci.* 25, 8000–9. doi:10.1523/JNEUROSCI.1748-05.2005.

Bilbo, S. D., Rudy, J. W., Watkins, L. R., and Maier, S. F. (2006). A behavioural characterization of neonatal infection-facilitated memory impairment in adult rats. *Behav. Brain Res.* 169, 39–47. doi:10.1016/j.bbr.2005.12.002.

Bilbo, S. D., and Schwarz, J. M. (2009). Early-life programming of later-life brain and behavior: a critical role for the immune system. *Front. Behav. Neurosci.* 3, 14. doi:10.3389/neuro.08.014.2009.

Bilbo, S. D., and Schwarz, J. M. (2012). The immune system and developmental programming of brain and behavior. *Front. Neuroendocrinol.* 33, 267–286. doi:10.1016/j.yfrne.2012.08.006.

Bilbo, S. D., Wieseler, J. L., Barrientos, R. M., Tsang, V., Watkins, L. R., and Maier, S. F. (2010). Neonatal bacterial infection alters fever to live and simulated infections in adulthood. *Psychoneuroendocrinology* 35, 369–381. doi:10.1016/j.psyneuen.2009.07.014.

Binshtok, A. M., Wang, H., Zimmermann, K., Amaya, F., Vardeh, D., Shi, L., et al. (2008). Nociceptors are interleukin-1beta sensors. *J. Neurosci.* 28, 14062–73. doi:10.1523/JNEUROSCI.3795-08.2008.

Bissonnette, J. M. (2000). Mechanisms regulating hypoxic respiratory depression during fetal and postnatal life. *Am. J. Physiol. Integr. Comp. Physiol.* 278, R1391–R1400. doi:10.1152/ajpregu.2000.278.6.R1391.

Blain, G. M., Smith, C. A., Henderson, K. S., and Dempsey, J. A. (2010). Peripheral chemoreceptors determine the respiratory sensitivity of central chemoreceptors to CO_2. *J. Physiol.* 588, 2455–2471. doi:10.1113/jphysiol.2010.187211.

Boisse, L., Spencer, S. J., Mouihate, A., Vergnolle, N., and Pittman, Q. J. (2005). Neonatal immune challenge alters nociception in the adult rat. *Pain* 119, 133–141. doi:10.1016/j.pain.2005.09.022.

Bouman, A., Heineman, M. J., and Faas, M. M. (2005). Sex hormones and the immune response in humans. *Hum. Reprod. Update* 11, 411–423. doi:10.1093/humupd/dmi008.

Bracchi-Ricard, V., Zha, J., Smith, A., Lopez-Rodriguez, D. M., Bethea, J. R., and Andreansky, S. (2016). Chronic spinal cord injury attenuates influenza virus-specific antiviral immunity. *J. Neuroinflammation*. doi:10.1186/s12974-016-0574-y.

Broytman, O., Baertsch, N. A., and Baker-Herman, T. L. (2013). Spinal TNF is necessary for inactivity-induced phrenic motor facilitation. *J. Physiol.* 591, 5585–98. doi:10.1113/jphysiol.2013.256644.

Byrnes, E. M., and Vassoler, F. M. (2018). Modeling prenatal opioid exposure in animals: Current findings and future directions. *Front. Neuroendocrinol.* 51, 1–13. doi:10.1016/j.yfrne.2017.09.001.

Carrithers, M. D. (2014). Innate immune viral recognition: Relevance to CNS infections. *Handb. Clin. Neurol.* 123, 215–223. doi:10.1016/B978-0-444-53488-0.00009-2.

Cashman, J. N. (1996). The Mechanisms of Action of NSAIDs in Analgesia. *Drugs* 52, 13–23. doi:10.2165/00003495-199600525-00004.

Ching, S., Zhang, H., Belevych, N., He, L., Lai, W., Pu, X. -a., et al. (2007). Endothelial-Specific Knockdown of Interleukin-1 (IL-1) Type 1 Receptor Differentially Alters CNS Responses to IL-1 Depending on Its Route of Administration. *J. Neurosci.* 27, 10476–10486. doi:10.1523/JNEUROSCI.3357-07.2007.

Christiansen, L., Urbin, M., Mitchell, G. S., and Perez, M. A. (2018). Acute intermittent hypoxia enhances corticospinal synaptic plasticity in humans. *Elife* 7. doi:10.7554/eLife.34304.

Colman, A. S., and Miller, J. H. (2001). Modulation of breathing by m 1 and m 2 opioid receptor stimulation in neonatal and adult rats. Available at: www.elsevier.com/locate/resphysiol [Accessed July 11, 2019].

Crain, J. M., and Watters, J. J. (2015). Microglial P2 Purinergic Receptor and Immunomodulatory Gene Transcripts Vary By Region, Sex, and Age in the Healthy Mouse CNS HHS Public Access. 3. doi:10.4172/2329-8936.1000124.

Cunha, T. M., Verri, W. a, Schivo, I. R., Napimoga, M. H., Parada, C. a, Poole, S., et al. (2008). Crucial role of neutrophils in the development of mechanical inflammatory hypernociception. *J. Leukoc. Biol.* 83, 824–32. doi:10.1189/jlb.0907654.

Dale-Nagle, E. A., Hoffman, M. S., MacFarlane, P. M., and Mitchell, G. S. (2010). Multiple pathways to long-lasting phrenic motor facilitation. *Adv. Exp. Med. Biol.* 669, 225–30. doi:10.1007/978-1-4419-5692-7_45.

Dale, E. A., Fields, D. P., Devinney, M. J., and Mitchell, G. S. (2017). Phrenic motor neuron TrkB expression is necessary for acute intermittent hypoxia-induced phrenic long-term facilitation. *Exp. Neurol.* 287, 130–136. doi:10.1016/j.expneurol.2016.05.012.

Dantzer, R. (2009). Cytokine, sickness behavior, and depression. *Immunol. Allergy Clin. North Am.* 29, 247–64. doi:10.1016/j.iac.2009.02.002.

Davis, J. M., Shenberger, J., Terrin, N., Breeze, J. L., Hudak, M., Wachman, E. M., et al. (2018). Comparison of Safety and Efficacy of Methadone vs Morphine for Treatment of Neonatal Abstinence Syndrome. *JAMA Pediatr.* 172, 741. doi:10.1001/jamapediatrics.2018.1307.

Del Negro, C. A., Koshiya, N., Butera, R. J., and Smith, J. C. (2002). Persistent Sodium Current, Membrane Properties and Bursting Behavior of Pre-Bötzinger Complex Inspiratory Neurons In Vitro. *J. Neurophysiol.* 88.

Devinney, M. J., Fields, D. P., Huxtable, A. G., Peterson, T. J., Dale, E. A., and Mitchell, G. S. (2015a). Phrenic Long-Term Facilitation Requires PKC theta Activity within Phrenic Motor Neurons. *J. Neurosci.* 35, 8107–8117. doi:Doi 10.1523/Jneurosci.5086-14.2015.

Devinney, M. J., Huxtable, A. G., Nichols, N. L., and Mitchell, G. S. (2015b). Hypoxia-induced phrenic long-term facilitation: emergent properties. 3–5. doi:10.1111/nyas.12085.Hypoxia-induced.

Di Filippo, M., Chiasserini, D., Gardoni, F., Viviani, B., Tozzi, A., Giampà, C., et al. (2013). Effects of central and peripheral inflammation on hippocampal synaptic plasticity. *Neurobiol. Dis.* doi:10.1016/j.nbd.2012.12.009.

Di Filippo, M., Sarchielli, P., Picconi, B., and Calabresi, P. (2008). Neuroinflammation and synaptic plasticity: theoretical basis for a novel, immune-centred, therapeutic approach to neurological disorders. *Trends Pharmacol. Sci.* 29, 402–412. doi:10.1016/j.tips.2008.06.005.

Dinarello, C. A. (2009). Immunological and Inflammatory Functions of the Interleukin-1 Family. doi:10.1146/annurev.immunol.021908.132612.

Dougherty, B. J., Kopp, E. S., and Watters, J. J. (2017). Nongenomic Actions of 17-β Estradiol Restore Respiratory Neuroplasticity in Young Ovariectomized Female Rats. *J. Neurosci.* 37, 6648–6660. doi:10.1523/JNEUROSCI.0433-17.2017.

Eden, B. Y. G. J., and Hanson, M. A. (1987). Maturation of the respiratory response to acute hypoxia. *J Physiol*, 1–9.

Elnazir, B., Marshall, J. M., and Kumar, P. (1996). Postnatal development of the pattern of respiratory and cardiovascular response to systemic hypoxia in the piglet: the roles of adenosine. *J. Physiol.* 492, 573–585. doi:10.1113/jphysiol.1996.sp021330.

Emery, M. J., Groves, C. C., Kruse, T. N., Shi, C., and Terman, G. W. (2016). Ventilation and the Response to Hypercapnia after Morphine in Opioid-naive and Opioid-tolerant Rats. *Anesthesiology* 124, 945–957. doi:10.1097/ALN.0000000000000997.

Epstein, R. A., Bobo, W. V., Martin, P. R., Morrow, J. A., Wang, W., Chandrasekhar, R., et al. (2013). Increasing pregnancy-related use of prescribed opioid analgesics. *Ann. Epidemiol.* 23, 498–503. doi:10.1016/j.annepidem.2013.05.017.

Fan, L.-W., Tien, L.-T., Mitchell, H. J., Rhodes, P. G., and Cai, Z. (2008). α-Phenyl-n-tert-butyl-nitrone ameliorates hippocampal injury and improves learning and memory in juvenile rats following neonatal exposure to lipopolysaccharide. *Eur. J. Neurosci.* 27, 1475–1484. doi:10.1111/j.1460-9568.2008.06121.x.

Feldman, J. L. (1986). Neurophysiology of Breathing in Mammals. *Compr. Physiol.*, 463–524. doi:10.1002/cphy.cp010409.

Feldman, J. L., and Del Negro, C. A. (2006). Looking for inspiration: new perspectives on respiratory rhythm. *Nat. Rev. Neurosci.* 7.

Feldman, J. L., and Kam, K. (2015). Facing the challenge of mammalian neural microcircuits: taking a few breaths may help. *J. Physiol*.

Feldman, J. L., Mitchell, G. S., and Nattie, E. E. (2010). Breathing: Rhythmicity, Plasticity, Chemosensitivity. 239–266. doi:10.1146/annurev.neuro.26.041002.131103.Breathing.

Feldman, J. L., Negro, C. Del, and Gray, P. (2013). Understanding the Rhythm of Breathing: So Near, Yet So Far. *Annu. Rev. Physiol* 75, 423–52.

Fields, D. P., and Mitchell, G. S. (2015). Spinal metaplasticity in respiratory motor control. *Front. Neural Circuits* 9, 2. doi:10.3389/fncir.2015.00002.

Finnegan, L. P., Connaughton, J. F., Kron, R. E., and Emich, J. P. (1975). Neonatal abstinence syndrome: assessment and management. *Addict. Dis.* 2, 141–58. Available at: http://www.ncbi.nlm.nih.gov/pubmed/1163358.

Florence, C. S., Zhou, C., Luo, F., and Xu, L. (2016). The Economic Burden of Prescription Opioid Overdose, Abuse, and Dependence in the United States, 2013. *Med. Care* 54, 901–906. doi:10.1097/mlr.0000000000000625.

Forsberg, D., Horn, Z., Tserga, E., Smedler, E., Silberberg, G., Shvarev, Y., et al. (2016). CO2-evoked release of PGE2 modulates sighs and inspiration as demonstrated in brainstem organotypic culture. *Elife* 5, 1–41. doi:10.7554/eLife.14170.

Fortier, M.-E., Kent, S., Ashdown, H., Poole, S., Boksa, P., and Luheshi, G. N. (2004). The viral mimic, polyinosinic:polycytidylic acid, induces fever in rats via an interleukin-1-dependent mechanism. *Am J Physiol Regul Integr Comp Physiol* 287, 759–766. doi:10.1152/ajpregu.00293.2004.-Polyinosinic:polycytidylic.

Fournier, S., Joseph, V., and Kinkead, R. (2011). Influence of juvenile housing conditions on the ventilatory, thermoregulatory, and endocrine responses to hypoxia of adult male rats. *J. Appl. Physiol.* 111, 516–523. doi:10.1152/japplphysiol.00370.2011.

Franco, P., Verheulpen, D., Valente, F., Kelmanson, I., de Broca, A., Scaillet, S., et al. (2003). Autonomic responses to sighs in healthy infants and in victims of sudden infant death. *Sleep Med.* 4, 569–577. doi:10.1016/S1389-9457(03)00107-2.

Fuller, D. D., and Mitchell, G. S. (2017). Respiratory neuroplasticity – Overview, significance and future directions. *Exp. Neurol.* 287, 144–152. doi:10.1016/j.expneurol.2016.05.022.

Fung, M.-L., Wang, W., Darnall, R. A., and St. John, W. M. (1996). Characterization of ventilatory responses to hypoxia in neonatal rats. *Respir. Physiol.* 103, 57–66. doi:10.1016/0034-5687(95)00077-1.

Funk, G. D. (2013). Neuromodulation: Purinergic signaling in respiratory control. *Compr. Physiol.* 3, 331–363. doi:10.1002/cphy.c120004.

Funk, G. D., and Gourine, A. V (2018). CrossTalk proposal: a central hypoxia sensor contributes to the excitatory hypoxic ventilatory response. *J. Physiol.* 596, 2935–2938. doi:10.1113/JP275707.

Funk, G. D., Johnson, S. M., Smith, J. C., Dong, X.-W., Lai, J., and Feldman, J. L. (1997). Functional Respiratory Rhythm Generating Networks in Neonatal Mice Lacking NMDAR1 Gene. *J. Neurophysiol.* 78, 1414–1420. doi:10.1152/jn.1997.78.3.1414.

Galic, M. A., Riazi, K., and Pittman, Q. J. (2012). Cytokines and brain excitability. *Front. Neuroendocrinol.* 33, 116–125. doi:10.1016/j.yfrne.2011.12.002.

Genest, S.-E., Gulemetova, R., Laforest, S., Drolet, G., and Kinkead, R. (2004). Neonatal maternal separation and sex-specific plasticity of the hypoxic ventilatory response in awake rat. *J. Physiol.* 554, 543–557. doi:10.1113/jphysiol.2003.052894.

Giles, J. A., Greenhalgh, A. D., Davies, C. L., Denes, A., Shaw, T., Coutts, G., et al. (2015). Requirement for interleukin-1 to drive brain inflammation reveals tissue-specific mechanisms of innate immunity. *Eur. J. Immunol.* 45, 525–530. doi:10.1002/eji.201444748.

Golder, F. J. (2009). Spinal NMDA receptor activation is necessary for de novo, but not the maintenance of, A2a receptor-mediated phrenic motor facilitation. *J. Appl. Physiol.* 107, 217–223. doi:10.1152/japplphysiol.00183.2009.

Golder, F. J., Ranganathan, L., Satriotomo, I., Hoffman, M., Lovett-Barr, M. R., Watters, J. J., et al. (2008). Spinal Adenosine A2a Receptor Activation Elicits Long-Lasting Phrenic Motor Facilitation. *J. Neurosci.* 28, 2033–2042. doi:10.1523/JNEUROSCI.3570-07.2008.

Gonzalez-Rothi, E. J., Lee, K.-Z., Dale, E. A., Reier, P. J., Mitchell, G. S., and Fuller, D. D. (2015). Intermittent hypoxia and neurorehabilitation. *J. Appl. Physiol.* 119, 1455–65. doi:10.1152/japplphysiol.00235.2015.

Gourevitch, B., Cai, J., and Mellen, N. (2017). Cellular and network-level adaptations to in utero methadone exposure along the ventral respiratory column in the neonate rat. *Exp. Neurol.* 287, 288–297. doi:10.1016/j.expneurol.2016.03.020.

Gourévitch, B., Cai, J., and Mellen, N. (2017). Cellular and network-level adaptations to in utero methadone exposure along the ventral respiratory column in the neonate rat. *Exp. Neurol.* 287, 288–297. doi:10.1016/j.expneurol.2016.03.020.

Gourine, A. V., and Funk, G. D. (2017). On the existence of a central respiratory oxygen sensor. *J. Appl. Physiol.*, jap.00194.2017. doi:10.1152/japplphysiol.00194.2017.

Gourine, A. V, Kasymov, V., Marina, N., Tang, F., Figueiredo, M. F., Lane, S., et al. (2010). Astrocytes control breathing through pH-dependent release of ATP. *Science* 329, 571–575. doi:10.1126/science.1190721.

Gourine, A. V, Llaudet, E., Dale, N., and Spyer, K. M. (2005). Behavioral/Systems/Cognitive Release of ATP in the Ventral Medulla during Hypoxia in Rats: Role in Hypoxic Ventilatory Response. doi:10.1523/JNEUROSCI.3763-04.2005.

Grace, P. M., Maier, S. F., and Watkins, L. R. (2015). Opioid-induced central immune signaling: implications for opioid analgesia. *Headache* 55, 475–89. doi:10.1111/head.12552.

Grace, P. M., Ramos, K. M., Rodgers, K. M., Wang, X., Hutchinson, M. R., Lewis, M. T., et al. (2014). Activation of adult rat CNS endothelial cells by opioid-induced toll-like receptor 4 (TLR4) signaling induces proinflammatory, biochemical, morphological, and behavioral sequelae. *Neuroscience* 280, 299–317. doi:10.1016/j.neuroscience.2014.09.020.

Gray, P. A., Rekling, J. C., Bocchiaro, C. M., and Feldman, J. L. (1999). Modulation of respiratory frequency by peptidergic input to rhythmogenic neurons in the preBötzinger complex. *Science* 286, 1566–8. Available at: http://www.ncbi.nlm.nih.gov/pubmed/10567264 [Accessed September 11, 2018].

Greer, J. J. (2012). Control of breathing activity in the fetus and newborn. *Compr. Physiol.* 2, 1873–1888. doi:10.1002/cphy.c110006.

Greer, J. J., Carter, J. E., and al-Zubaidy, Z. (1995). Opioid depression of respiration in neonatal rats. *J. Physiol.* 485, 845–855. doi:10.1113/jphysiol.1995.sp020774.

Greer, J. J., Funk, G. D., and Ballanyi, K. (2006). Preparing for the first breath: prenatal maturation of respiratory neural control. *J. Physiol.* 570, 437–444. doi:10.1113/jphysiol.2005.097238.

Gresham, K., Boyer, B., Mayer, C., Foglyano, R., Martin, R., and Wilson, C. G. (2011). Airway inflammation and central respiratory control: results from in vivo and in vitro neonatal rat. *Respir. Physiol. Neurobiol.* 178, 414–21. doi:10.1016/j.resp.2011.05.008.

Grosmark, A. D., Mizuseki, K., Pastalkova, E., Diba, K., and Buzsáki, G. (2012). REM Sleep Reorganizes Hippocampal Excitability. *Neuron* 75, 1001–1007. doi:10.1016/j.neuron.2012.08.015.

Guyenet, P. G., and Bayliss, D. A. (2015). Review Neural Control of Breathing and CO 2 Homeostasis. doi:10.1016/j.neuron.2015.08.001.

Hand, B. N., Krause, J. S., and Simpson, K. N. (2018). Dose and Duration of Opioid Use in Propensity Score–Matched, Privately Insured Opioid Users With and Without Spinal Cord Injury. *Arch. Phys. Med. Rehabil.* 99, 855–861. doi:10.1016/J.APMR.2017.12.004.

Hauser, K. F., and Knapp, P. E. (2018). Opiate Drugs with Abuse Liability Hijack the Endogenous Opioid System to Disrupt Neuronal and Glial Maturation in the Central Nervous System. *Front. Pediatr.* 5, 294. doi:10.3389/fped.2017.00294.

Hayes, H. B., Jayaraman, A., Herrmann, M., Mitchell, G. S., Rymer, W. Z., and Trumbower, R. D. (2014). Daily intermittent hypoxia enhances walking after chronic spinal cord injury A randomized trial. *Neurology* 82, 104–113. doi:10.1212/01.WNL.0000437416.34298.43.

Hayes, J. A., Wang, X., and Del Negro, C. A. (2012). Cumulative lesioning of respiratory interneurons disrupts and precludes motor rhythms in vitro. *Proc. Natl. Acad. Sci. U. S. A.* 109, 8286–91. doi:10.1073/pnas.1200912109.

Hendrickson, R. G., and McKeown, N. J. (2012). Is maternal opioid use hazardous to breast-fed infants? *Clin. Toxicol.* 50, 1–14. doi:10.3109/15563650.2011.635147.

Hl, V., and Vin Peters, M. A. (1975). Development of a "blood brain barrier" to methadone in the newborn rat. *J. Pharmacol. Exp. Ther.* 192, 513–520. Available at: https://illiad.uoregon.edu/illiad/oru/illiad.dll?Action=10&Form=75&Value=739373 [Accessed July 19, 2019].

Hocker, A. D., Beyeler, S. A., Gardner, A. N., Johnson, S. M., Watters, J. J., and Huxtable, A. G. (2019). One bout of neonatal inflammation impairs adult respiratory motor plasticity in male and female rats. *Elife* 8. doi:10.7554/eLife.45399.

Hocker, A. D., and Huxtable, A. G. (2018). IL-1 receptor activation undermines respiratory motor plasticity after systemic inflammation. 1. 223134. Available at: https://www.physiology.org/doi/pdf/10.1152/japplphysiol.01051.2017 [Accessed June 4, 2018].

Hocker, A. D., Stokes, J. A., Powell, F. L., and Huxtable, A. G. (2017). The impact of inflammation on respiratory plasticity. *Exp. Neurol.* 287, 243–253. doi:10.1016/j.expneurol.2016.07.022.

Hoffmann, V. L. ., Vermeyen, K. M., Adriaensen, H. F., and Meert, T. F. (2003). Effects of NMDA receptor antagonists on opioid-induced respiratory depression and acute antinociception in rats. *Pharmacol. Biochem. Behav.* 74, 933–941. doi:10.1016/S0091-3057(03)00020-0.

Hofstetter, A. O., Saha, S., Siljehav, V., Jakobsson, P.-J., and Herlenius, E. (2007). The induced prostaglandin E2 pathway is a key regulator of the respiratory response to infection and hypoxia in neonates. *Proc. Natl. Acad. Sci. U. S. A.* 104, 9894–9899. doi:10.1073/pnas.0611468104.

Hornig, M., Weissenböck, H., Horscroft, N., and Lipkin, W. I. (1999). An infection-based model of neurodevelopmental damage. *Proc. Natl. Acad. Sci. U. S. A.* 96, 12102–7. doi:10.1073/pnas.96.21.12102.

Hosoi, T., Okuma, Y., and Nomura, Y. (2000). Electrical stimulation of afferent vagus nerve induces IL-1beta expression in the brain and activates HPA axis. *Am. J. Physiol. Integr. Comp. Physiol.* 279, R141–R147.

Hu, X., Yu, J., Crosby, S. D., and Storch, G. A. (2013). Gene expression profiles in febrile children with defined viral and bacterial infection. *Proc. Natl. Acad. Sci. U. S. A.* 110, 12792–7. doi:10.1073/pnas.1302968110.

Huckstepp, R. T., Henderson, L. E., Cardoza, K. P., and Feldman, J. L. (2016a). Interactions between respiratory oscillators in adult rats. *Elife* 5, e14203. doi:10.7554/eLife.14203.

Huckstepp, R. T. R., Cardoza, K. P., Henderson, L. E., and Feldman, J. L. (2018). Distinct parafacial regions in control of breathing in adult rats. *PLoS One* 13, e0201485. doi:10.1371/journal.pone.0201485.

Huckstepp, R. T. R., Henderson, L. E., Cardoza, K. P., and Feldman, J. L. (2016b). Interactions between respiratory oscillators in adult rats. *Elife* 5, 1–22. doi:10.7554/eLife.14203.

Hudak, M. L., Tan, R. C., COMMITTEE ON DRUGS, T. C. O., COMMITTEE ON FETUS AND NEWBORN, T. C. O. F. A., American Academy of Pediatrics, H., Das, A., et al. (2012). Neonatal drug withdrawal. *Pediatrics* 129, e540-60. doi:10.1542/peds.2011-3212.

Hunter, P. (2012). The inflammation theory of disease. The growing realization that chronic inflammation is crucial in many diseases opens new avenues for treatment. *EMBO Rep.* 13, 968–70. doi:10.1038/embor.2012.142.

Hutchinson, M. R., Shavit, Y., Grace, P. M., Rice, K. C., Maier, S. F., and Watkins, L. R. (2011). Exploring the neuroimmunopharmacology of opioids: an integrative review of mechanisms of central immune signaling and their implications for opioid analgesia. *Pharmacol. Rev.* 63, 772–810. doi:10.1124/pr.110.004135.

Hutchinson, M. R., Zhang, Y., Shridhar, M., Evans, J. H., Buchanan, M. M., Zhao, T. X., et al. (2009). Evidence that opioids may have toll-like receptor 4 and MD-2 effects. *Brain Behav. Immun.* 24, 83–95. doi:10.1016/j.bbi.2009.08.004.

Huxtable, A. G., Kopp, E., Doughtery, B. J., Watters, J. J., and Mitchell, G. S. (2017). Cyclooxygenase enzyme activity does not impair respiratory motor plasticity after one night of intermittent hypoxia. *Respir. Physiol. Neurobiol.* doi:10.1016/j.resp.2017.12.004.

Huxtable, A. G., Peterson, T. J., Ouellette, J. N., Watters, J. J., and Mitchell, G. S. (2018). Spinal protein phosphatase 1 constrains respiratory plasticity after sustained hypoxia. *J. Appl. Physiol.* 125, 1440–1446. doi:10.1152/japplphysiol.00641.2018.

Huxtable, A. G., Smith, S. M. C., Peterson, T. J., Watters, J. J., and Mitchell, G. S. (2015). Intermittent Hypoxia-Induced Spinal Inflammation Impairs Respiratory Motor Plasticity by a Spinal p38 MAP Kinase-Dependent Mechanism. *J. Neurosci.* 35, 6871–80. doi:10.1523/JNEUROSCI.4539-14.2015.

Huxtable, A. G., Smith, S. M. C., Vinit, S., Watters, J. J., and Mitchell, G. S. (2013). Systemic LPS induces spinal inflammatory gene expression and impairs phrenic long-term facilitation following acute intermittent hypoxia. *J. Appl. Physiol.* 114, 879–87. doi:10.1152/japplphysiol.01347.2012.

Huxtable, A. G., Vinit, S., Windelborn, J. A., Crader, S. M., Guenther, C. H., Watters, J. J., et al. (2011). Systemic inflammation impairs respiratory chemoreflexes and plasticity. *Respir. Physiol. Neurobiol.* 178, 482–489. doi:10.1016/j.resp.2011.06.017.

Huxtable, A. G., Zwicker, J. D., Poon, B. Y., Pagliardini, S., Vrouwe, S. Q., Greer, J. J., et al. (2009). Tripartite purinergic modulation of central respiratory networks during perinatal development: the influence of ATP, ectonucleotidases, and ATP metabolites. *J. Neurosci.* 29, 14713–25. doi:10.1523/JNEUROSCI.2660-09.2009.

Iwase, K., Miyanaka, K., Shimizu, A., Nagasaki, A., Gotoh, T., Mori, M., et al. (2000). Induction of endothelial nitric-oxide synthase in rat brain astrocytes by systemic lipopolysaccharide treatment. *J. Biol. Chem.* 275, 11929–33. doi:10.1074/JBC.275.16.11929.

Jafri, A., Belkadi, A., Zaidi, S. I. A., Getsy, P., Wilson, C. G., and Martin, R. J. (2013). Lung inflammation induces IL-1β expression in hypoglossal neurons in rat brainstem. *Respir. Physiol. Neurobiol.* 188, 21–28. doi:10.1016/j.resp.2013.04.022.

Janczewski, W. A., and Feldman, J. L. (2006). Distinct rhythm generators for inspiration and expiration in the juvenile rat. *J. Physiol.* 570, 407–420. doi:10.1113/jphysiol.2005.098848.

Jansen, A. H., and Chernick, V. (1983). Development of Respiratory Control. Available at: www.physiology.org/journal/physrev [Accessed July 12, 2019].

Johnson, S. M., Randhawa, K. S., Epstein, J. J., Gustafson, E., Hocker, A. D., Huxtable, A. G., et al. (2017). Gestational intermittent hypoxia increases susceptibility to neuroinflammation and alters respiratory motor control in neonatal rats. *Respir. Physiol. Neurobiol.*, 0–1. doi:10.1016/j.resp.2017.11.007.

Johnston, I. N. (2004). A Role for Proinflammatory Cytokines and Fractalkine in Analgesia, Tolerance, and Subsequent Pain Facilitation Induced by Chronic Intrathecal Morphine. *J. Neurosci.* 24, 7353–7365. doi:10.1523/JNEUROSCI.1850-04.2004.

Kahn, A., Groswasser, J., Rebuffat, E., Sottiaux, M., Blum, D., Foerster, tM, et al. (1992). Sleep and Cardiorespiratory Characteristics of Infant Victims of Sudden Death: A Prospective Case-Control Study. Available at: https://academic.oup.com/sleep/article-abstract/15/4/287/2749268 [Accessed July 8, 2019].

Kam, K., Worrell, J. W., Janczewski, W. A., Cui, Y., and Feldman, J. L. (2013a). Distinct inspiratory rhythm and pattern generating mechanisms in the preBötzinger complex. *J. Neurosci.* 33, 9235–45. doi:10.1523/JNEUROSCI.4143-12.2013.

Kam, K., Worrell, J. W., Ventalon, C., Emiliani, V., and Feldman, J. L. (2013b). Emergence of Population Bursts from Simultaneous Activation of Small Subsets of preBötzinger Complex Inspiratory Neurons Kaiwen. *J. Neurosci.* 33, 3332–3338. doi:10.1523/JNEUROSCI.4574-12.2013.Emergence.

Katsuki, H., Nakai, S., Hirai, Y., Akaji, K., Kiso, Y., and Satoh, M. (1990). Interleukin-1β inhibits long-term potentiation in the CA3 region of mouse hippocampal slices. *Eur. J. Pharmacol.* 181, 323–326. doi:10.1016/0014-2999(90)90099-R.

Kennedy, A. (2014). An investigation of the effects of fentanyl on respiratory control. Available at: http://theses.gla.ac.uk/5998/1/2014Kennedyphd.pdf [Accessed June 2, 2019].

Kentner, A. C., McLeod, S. A., Field, E. F., and Pittman, Q. J. (2010). Sex-dependent effects of neonatal inflammation on adult inflammatory markers and behavior. *Endocrinology* 151, 2689–2699. doi:10.1210/en.2009-1101.

Kinney, H. C., and Thach, B. T. (2009). The Sudden Infant Death Syndrome. *N. Engl. J. Med.* 361, 795–805. doi:10.1056/NEJMra0803836.

Kivell, B. M., Day, D. J., McDonald, F. J., and Miller, J. H. (2004). Developmental expression of μ and δ opioid receptors in the rat brainstem: evidence for a postnatal switch in μ isoform expression. *Dev. Brain Res.* 148, 185–196. doi:10.1016/J.DEVBRAINRES.2003.12.002.

Koch, H., Caughie, C., Elsen, F. P., Doi, A., Garcia, A. J., Zanella, S., et al. (2015). Prostaglandin E2 differentially modulates the central control of eupnoea, sighs and gasping in mice. *J. Physiol.* 593, 305–19. doi:10.1113/jphysiol.2014.279794.

Kocherlakota, P. (2014). Neonatal Abstinence Syndrome. *Pediatrics* 134, e547–e561. doi:10.1542/peds.2013-3524.

Kohman, R. A., Tarr, A. J., Sparkman, N. L., Bogale, T. M. H., and Boehm, G. W. (2008). Neonatal endotoxin exposure impairs avoidance learning and attenuates endotoxin-induced sickness behavior and central IL-1β gene transcription in adulthood. *Behav. Brain Res.* 194, 25–31. doi:10.1016/J.BBR.2008.06.018.

Konat, G. W., Borysiewicz, E., Fil, D., and James, I. (2009). Peripheral challenge with double-stranded RNA elicits global up-regulation of cytokine gene expression in the brain. *J. Neurosci. Res.* doi:10.1002/jnr.21958.

Kopecky, E. A., Simone, C., Knie, B., and Koren, G. (1999). Transfer of morphine across the human placenta and its interaction with naloxone. *Life Sci.* 65, 2359–2371. doi:10.1016/S0024-3205(99)00503-2.

Kottick, a., and Del Negro, C. a. (2015). Synaptic Depression Influences Inspiratory-Expiratory Phase Transition in Dbx1 Interneurons of the preBotzinger Complex in Neonatal Mice. *J. Neurosci.* 35, 11606–11611. doi:10.1523/JNEUROSCI.0351-15.2015.

Kraft, W. K., Stover, M. W., and Davis, J. M. (2016). Neonatal abstinence syndrome: Pharmacologic strategies for the mother and infant. *Semin. Perinatol.* 40, 203–212. doi:10.1053/j.semperi.2015.12.007.

Krans, E. E., Cochran, G., and Bogen, D. L. (2015). Caring for Opioid-dependent Pregnant Women: Prenatal and Postpartum Care Considerations. *Clin. Obstet. Gynecol.* 58, 370–379. doi:10.1097/GRF.0000000000000098.

Krasowska-Zoladek, A., Banaszewska, M., Kraszpulski, M., and Konat, G. W. (2007). Kinetics of inflammatory response of astrocytes induced by TLR3 and TLR4 ligation. *J. Neurosci. Res.* 85, 205–212. doi:10.1002/jnr.21088.

Krueger, J. M., Majde, J. A., Blatteis, C. M., Endsley, J., Ahokas, R. A., and Cady, A. B. (1988). Polyriboinosinic:polyribocytidylic acid enhances rabbit slow-wave sleep. *Am. J. Physiol. Integr. Comp. Physiol.* 255, R748–R755. doi:10.1152/ajpregu.1988.255.5.R748.

Kuzmich, N., Sivak, K., Chubarev, V., Porozov, Y., Savateeva-Lyubimova, T., and Peri, F. (2017). TLR4 Signaling Pathway Modulators as Potential Therapeutics in Inflammation and Sepsis. *Vaccines* 5, 34. doi:10.3390/vaccines5040034.

Laferrière, A., Colin-Durand, J., and Ravé Moss, I. (2005). Ontogeny of respiratory sensitivity and tolerance to the mu-opioid agonist fentanyl in rat. *Dev. Brain Res.* 156, 210–217. doi:10.1016/J.DEVBRAINRES.2005.03.002.

LaPrairie, J. L., and Murphy, A. Z. (2007). Female rats are more vulnerable to the long-term consequences of neonatal inflammatory injury. *Pain* 132, S124–S133. doi:10.1016/J.PAIN.2007.08.010.

Laurel Gorman, A., Elliott, K. J., and Inturrisi, C. E. (1997). The d- and l- isomers of methadone bind to the non-competitive site on the N-methyl-d-aspartate (NMDA) receptor in rat forebrain and spinal cord. *Neurosci. Lett.* 223, 5–8. doi:10.1016/S0304-3940(97)13391-2.

Laye, S., Bluthe, R. M., Kent, S., Combe, C., Medina, C., Parnet, P., et al. (1995). Subdiaphragmatic vagotomy blocks induction of IL-1 beta mRNA in mice brain in response to peripheral LPS. *Am J Physiol* 268, R1327-31. Available at: http://www.ncbi.nlm.nih.gov/pubmed/7771597 [Accessed September 29, 2017].

Leirão, I. P., Silva, C. A., Gargaglioni, L. H., Da Silva, G. S. F., Leirão, I. P., and Silva, C. A. (2017). Hypercapnia-induced active expiration increases in sleep and enhances ventilation in unanaesthetized rats. *J Physiol* 00000, 1–0. doi:10.1113/JP274726.

Levitt, E. S., and Williams, J. T. (2018). Desensitization and Tolerance of Mu Opioid Receptors on Pontine Kölliker-Fuse Neurons. *Mol. Pharmacol.* 93, 8–13. doi:10.1124/mol.117.109603.

Liddelow, S. A., Guttenplan, K. A., Clarke, L. E., Bennett, F. C., Bohlen, C. J., Schirmer, L., et al. (2017). Neurotoxic reactive astrocytes are induced by activated microglia. *Nature* 541, 481–487. doi:10.1038/nature21029.

Ling, G. S. F., Paul, D., Simantov, R., and Pasternak, G. W. (1989). Differential development of acute tolerance to analgesia, respiratory depression, gastrointestinal transit and hormone release in a morphine infusion model. *Life Sci.* 45, 1627–1636. doi:10.1016/0024-3205(89)90272-5.

Liu, Q., Lowry, T. F., and Wong-Riley, M. T. T. (2006). Postnatal changes in ventilation during normoxia and acute hypoxia in the rat: implication for a sensitive period. *J. Physiol.* 577, 957–70. doi:10.1113/jphysiol.2006.121970.

Liu, Q., and Wong-Riley, M. T. T. (2004). Developmental changes in the expression of GABA $_A$ receptor subunits α1, α2, and α3 in the rat pre-Bötzinger complex. *J. Appl. Physiol.* 96, 1825–1831. doi:10.1152/japplphysiol.01264.2003.

Livak, K. J., and Schmittgen, T. D. (2001). Analysis of Relative Gene Expression Data Using Real-Time Quantitative PCR and the 2−ΔΔCT Method. *Methods* 25, 402–408. doi:10.1006/meth.2001.1262.

Luu, T. M., Katz, S. L., Leeson, P., Thébaud, B., and Nuyt, A.-M. (2016). Preterm birth: risk factor for early-onset chronic diseases. *CMAJ* 188, 736–46. doi:10.1503/cmaj.150450.

Maier, S. F., Wiertelak, E. P., Martin, D., and Watkins, L. R. (1993). Interleukin-1 mediates the behavioral hyperalgesia produced by lithium chloride and endotoxin. *Brain Res.* 623, 321–324. doi:10.1016/0006-8993(93)91446-Y.

Mantilla, C. B., and Sieck, G. C. (2008). Key aspects of phrenic motoneuron and diaphragm muscle development during the perinatal period. *J. Appl. Physiol.* 104, 1818–27. doi:10.1152/japplphysiol.01192.2007.

Marcouiller, F., Boukari, R., Laouafa, S., Lavoie, R., and Joseph, V. (2014). The Nuclear Progesterone Receptor Reduces Post-Sigh Apneas during Sleep and Increases the Ventilatory Response to Hypercapnia in Adult Female Mice. *PLoS One* 9, e100421. doi:10.1371/journal.pone.0100421.

Martin, R. J., Di Fiore, J. M., MacFarlane, P. M., and Wilson, C. G. (2012). "Physiologic Basis for Intermittent Hypoxic Episodes in Preterm Infants," in *Advances in experimental medicine and biology*, 351–358. doi:10.1007/978-94-007-4584-1_47.

Martinez, A., Kastner, B., and Taeusch, H. W. (1999). Hyperphagia in neonates withdrawing from methadone. *Arch. Dis. Child. Fetal Neonatal Ed.* 80, F178-82. doi:10.1136/fn.80.3.f178.

Mateika, J. H., and Komnenov, D. (2017). Intermittent hypoxia initiated plasticity in humans: A multipronged therapeutic approach to treat sleep apnea and overlapping co-morbidities. *Exp. Neurol.* 287, 113–129. doi:10.1016/J.EXPNEUROL.2016.05.011.

Matsumoto, M., and Seya, T. (2008). TLR3: Interferon induction by double-stranded RNA including poly(I:C). *Adv. Drug Deliv. Rev.* 60, 805–812. doi:10.1016/J.ADDR.2007.11.005.

Matsuwaki, T., Shionoya, K., Ihnatko, R., Eskilsson, A., Kakuta, S., Dufour, S., et al. (2017). Involvement of interleukin-1 type 1 receptors in lipopolysaccharide- induced sickness responses. *Brain Behav. Immun.* 66, 165–176. doi:10.1016/j.bbi.2017.06.013.

McCartney, S., Vermi, W., Gilfillan, S., Cella, M., Murphy, T. L., Schreiber, R. D., et al. (2009). Distinct and complementary functions of MDA5 and TLR3 in poly(I:C)-mediated activation of mouse NK cells. *J. Exp. Med.* 206, 2967–2976. doi:10.1084/JEM.20091181.

McDermott, C. M., Hardy, M. N., Bazan, N. G., and Magee, J. C. (2006). Sleep deprivation-induced alterations in excitatory synaptic transmission in the CA1 region of the rat hippocampus. *J. Physiol.* 570, 553. doi:10.1113/JPHYSIOL.2005.093781.

McGuire, M., Liu, C., Cao, Y., and Ling, L. (2008). Formation and maintenance of ventilatory long-term facilitation require NMDA but not non-NMDA receptors in awake rats. *J. Appl. Physiol.* 105, 942–50. doi:10.1152/japplphysiol.01274.2006.

McGuire, M., Zhang, Y., White, D. P., and Ling, L. (2004). Serotonin receptor subtypes required for ventilatory long-term facilitation and its enhancement after chronic intermittent hypoxia in awake rats. *Am. J. Physiol. Regul. Integr. Comp. Physiol.* 286, R334-41. doi:10.1152/ajpregu.00463.2003.

McGuire, M., Zhang, Y., White, D. P., and Ling, L. (2005). Phrenic long-term facilitation requires NMDA receptors in the phrenic motonucleus in rats. *J. Physiol.* 567, 599–611. doi:10.1113/jphysiol.2005.087650.

McLaughlin, P. J., and Zagon, I. S. (1980). Body and organ development of young rats maternally exposed to methadone. *Neonatology* 38, 185–196. doi:10.1159/000241363.

McNamara, F., and Sullivan, C. E. (2000). The genesis of adult sleep apnoea in childhood. *Thorax* 55, 964–969. doi:10.1136/thorax.55.11.964.

McQueen, K., and Murphy-Oikonen, J. (2016). Neonatal Abstinence Syndrome. *N. Engl. J. Med.* 375, 2468–2479. doi:10.1056/NEJMra1600879.

Meisel, C., Schwab ||, J. M., Prass, K., Meisel, A., and Dirnagl, U. (2005). CENTRAL NERVOUS SYSTEM INJURY□INDUCED IMMUNE DEFICIENCY SYNDROME. doi:10.1038/nrn1765.

Mellen, N. M., Janczewski, W. A., Bocchiaro, C. M., and Feldman, J. L. (2003). Opioid-induced quantal slowing reveals dual networks for respiratory rhythm generation. *Neuron* 37, 821–6. doi:10.1016/S0896-6273(03)00092-8.

Mitchell, G. S. (2008). "Respiratory plasticity following intermittent hypoxia: A guide for novel therapeutic approaches to ventilatory control disorders?," in *Genetic Basis for Respiratory Control Disorders*, 291–311. doi:10.1007/978-0-387-70765-5_17.

Mitchell, G. S., and Johnson, S. M. (2003). Invited Review: Neuroplasticity in respiratory motor control. *J. Appl. Physiol.* 94, 358–374. doi:10.1152/japplphysiol.00523.2002.

Molina-Holgado, E., Ortiz, S., Molina-Holgado, F., and Guaza, C. (2000). Induction of COX-2 and PGE $_2$ biosynthesis by IL-1β is mediated by PKC and mitogen-activated protein kinases in murine astrocytes. *Br. J. Pharmacol.* 131, 152–159. doi:10.1038/sj.bjp.0703557.

Montandon, G., Qin, W., Liu, H., Ren, J., Greer, J. J., and Horner, R. L. (2011). PreBotzinger complex neurokinin-1 receptor-expressing neurons mediate opioid-induced respiratory depression. *J. Neurosci.* 31, 1292–301. doi:10.1523/JNEUROSCI.4611-10.2011.

Montandon, G., Ren, J., Victoria, N. C., Liu, H., Wickman, K., Greer, J. J., et al. (2016). G-protein–gated Inwardly Rectifying Potassium Channels Modulate Respiratory Depression by Opioids. *Anesthesiology* 124, 641–650. doi:10.1097/ALN.0000000000000984.

Moon, R. Y. (2016). SIDS and Other Sleep-Related Infant Deaths: Evidence Base for 2016 Updated Recommendations for a Safe Infant Sleeping Environment. *Pediatrics* 138, e20162940. doi:10.1542/peds.2016-2940.

Mortola, J. P., and Dotta, a (1992). Effects of hypoxia and ambient temperature on gaseous metabolism of newborn rats. *Am. J. Physiol.* 263, R267–R272. Available at: www.physiology.org/journal/ajpregu [Accessed October 3, 2018].

Mortola, J. P., and Saiki, C. (1996). Ventilatory response to hypoxia in rats: gender differences. *Respir. Physiol.* 106, 21–34. doi:10.1016/0034-5687(96)00064-3.

Moss, I. R., Ruhold, M., Dahlin, I., Fredholm, B. B., Nyberg, F., and Langercrantz, H. (1987). Respiratory and neuroendocrine responses of piglets to hypoxia during postnatal development. *Acta Physiol. Scand.* 131, 533–541. doi:10.1111/j.1748-1716.1987.tb08273.x.

Mouihate, A., Galic, M. A., Ellis, S. L., Spencer, S. J., Tsutsui, S., and Pittman, Q. J. (2010). Early Life Activation of Toll-Like Receptor 4 Reprograms Neural Anti-Inflammatory Pathways. *J. Neurosci.* 30, 7975–7983. doi:10.1523/JNEUROSCI.6078-09.2010.

Mulkey, D. K., Stornetta, R. L., Weston, M. C., Simmons, J. R., Parker, A., Bayliss, D. A., et al. (2004). Respiratory control by ventral surface chemoreceptor neurons in rats. *Nat. Neurosci.* 7, 1360–1369. doi:10.1038/nn1357.

Nattie, E., and Li, A. (2009). Central chemoreception is a complex system function that involves multiple brain stem sites. *J. Appl. Physiol.* 106, 1464–6. doi:10.1152/japplphysiol.00112.2008.

Naumburg, E. G., and Meny, R. G. (1988). Breast Milk Opioids and Neonatal Apnea. *Am. J. Dis. Child.* 142, 11–12. doi:10.1001/archpedi.1988.02150010017005.

Nelson, N. R., Bird, I. M., and Behan, M. (2011). Testosterone restores respiratory long term facilitation in old male rats by an aromatase-dependent mechanism. *J. Physiol.* 589, 409–421. doi:10.1113/jphysiol.2010.198200.

Nettleton, R. T., Wallisch, M., and Olsen, G. D. (2008). Respiratory effects of chronic in utero methadone or morphine exposure in the neonatal guinea pig. *Neurotoxicol. Teratol.* 30, 448–454. doi:10.1016/j.ntt.2008.03.063.

Nichols, N. L., Dale, E. A., and Mitchell, G. S. (2012). Severe acute intermittent hypoxia elicits phrenic long-term facilitation by a novel adenosine-dependent mechanism. *J. Appl. Physiol.* 112, 1678–88. doi:10.1152/japplphysiol.00060.2012.

Nichols, N. L., Gowing, G., Satriotomo, I., Nashold, L. J., Dale, E. A., Suzuki, M., et al. (2013). Intermittent Hypoxia and Stem Cell Implants Preserve Breathing Capacity in a Rodent Model of Amyotrophic Lateral Sclerosis. *Am. J. Respir. Crit. Care Med.* 187, 535–542. doi:10.1164/rccm.201206-1072OC.

Nicodemus, C. F., and Berek, J. S. (2010). TLR3 agonists as immunotherapeutic agents. *Immunotherapy* 2, 137–140. doi:10.2217/imt.10.8.

Obasi, C. N., Barrett, B., Brown, R., Vrtis, R., Barlow, S., Muller, D., et al. (2014). Detection of viral and bacterial pathogens in acute respiratory infections. *J. Infect.* 68, 125–30. doi:10.1016/j.jinf.2013.10.013.

Oku, Y., Masumiya, H., and Okada, Y. (2007). Postnatal developmental changes in activation profiles of the respiratory neuronal network in the rat ventral medulla. *J Physiol* 585, 175–186. doi:10.1113/jphysiol.2007.138180.

Olsen, G. D., and Lees, M. H. (1980). Ventilatory response to carbon dioxide of infants following chronic prenatal methadone exposure. *J. Pediatr.* 96, 983–989. doi:10.1016/S0022-3476(80)80622-6.

Olsson, A., Kayhan, G., Lagercrantz, H., and Herlenius, E. IL-1␣ Depresses Respiration and Anoxic Survival via a Prostaglandin-Dependent Pathway in Neonatal Rats. doi:10.1203/01.PDR.0000076665.62641.A2.

Olsson, A., Kayhan, G., Lagercrantz, H., and Herlenius, E. (2003). IL-1b depresses respiration and anoxic survival via a prostaglandin-dependent pathway in neonatal rats. *Pediatr. Res.* 54, 326–331. doi:10.1203/01.PDR.0000076665.62641.A2.

Onimaru, H. (2006). Point:Counterpoint: The parafacial respiratory group (pFRG)/pre-Botzinger complex (preBotC) is the primary site of respiratory rhythm generation in the mammal. *J. Appl. Physiol.* 100, 2094–2098. doi:10.1152/japplphysiol.00119.2006.

Onimaru, H., and Homma, I. (2003). A novel functional neuron group for respiratory rhythm generation in the ventral medulla. *J. Neurosci.* 23, 1478–1486. doi:10.1016/j.neuroscience.2004.11.041.

Onimaru, H., Kumagawa, Y., and Homma, I. (2006). Respiration-Related Rhythmic Activity in the Rostral Medulla of Newborn Rats. *J. Neurophysiol.* 96, 55–61. doi:10.1152/jn.01175.2005.

Pace, R. W., Mackay, D. D., Feldman, J. L., and Negro, C. A. Del (2007). Role of persistent sodium current in mouse pre otzinger Complex neurons and respiratory rhythm generation. *J Physiol* 5802, 485–496. doi:10.1113/jphysiol.2006.124602.

Pagliardini, S., Ren, J., and Greer, J. J. (2003). Ontogeny of the pre-Bötzinger complex in perinatal rats. *J. Neurosci.* 23, 9575–84. Available at: http://www.ncbi.nlm.nih.gov/pubmed/14573537.

Paizs, M., Engelhardt, J. I., and SiklÓs, L. (2009). Quantitative assessment of relative changes of immunohistochemical staining by light microscopy in specified anatomical regions. *J. Microsc.* 234, 103–112. doi:10.1111/j.1365-2818.2009.03146.x.

Pan, W., Banks, W. A., and Kastin, A. J. (1997). Permeability of the blood–brain and blood–spinal cord barriers to interferons. *J. Neuroimmunol.* 76, 105–111. doi:10.1016/S0165-5728(97)00034-9.

Paton, J. F. R., Abdala, A. P. L., Koizumi, H., Smith, J. C., and St-John, W. M. (2006). Respiratory rhythm generation during gasping depends on persistent sodium current. *Nat. Neurosci.* 9, 311–313. doi:10.1038/nn1650.

Pattinson, K. T. S. (2008). Opioids and the control of respiration. *Br. J. Anaesth.* 100, 747–758. doi:10.1093/bja/aen094.

Peña, F., Parkis, M. A., Tryba, A. K., and Ramirez, J. M. (2004). Differential contribution of pacemaker properties to the generation of respiratory rhythms during normoxia and hypoxia. *Neuron* 43, 105–117. doi:10.1016/j.neuron.2004.06.023.

Perim, R. R., Fields, D. P., and Mitchell, G. S. (2018). Cross-talk inhibition between 5-HT $_{2B}$ and 5-HT $_{7}$ receptors in phrenic motor facilitation via NADPH oxidase and PKA. *Am. J. Physiol. Integr. Comp. Physiol.* 314, R709–R715. doi:10.1152/ajpregu.00393.2017.

Person, M. K., Esposito, D. H., Holman, R. C., Mehal, J. M., and Stoll, B. J. (2014). Risk factors for infectious disease death among infants in the United States. *Pediatr. Infect. Dis. J.* 33, e280-5. doi:10.1097/INF.0000000000000414.

Peters, M. A., Tur, M., and Buchenauer, D. (1972). The distribution of methadone in the nonpregnant, pregnant and fetal rat after acute methadone treatment. *J. Pharmacol. Exp. Ther.* 181, 273–278. Available at: https://illiad.uoregon.edu/illiad/oru/illiad.dll?Action=10&Form=75&Value=739374 [Accessed July 19, 2019].

Poets, C. F., Samuels, M. P., and Southall, D. P. (1994). Epidemiology and pathophysiology of apnoea of prematurity. *Neonatology* 65, 211–219. doi:10.1159/000244055.

Poets, C. F., and Southall, D. P. (1994). Recent developments in research into sudden infant death. *Thorax* 49, 196–197. doi:10.1136/thx.49.3.196.

Polotsky, V. Y., Rubin, A. E., Balbir, A., Dean, T., Smith, P. L., Schwartz, A. R., et al. (2006). Intermittent hypoxia causes REM sleep deficits and decreases EEG delta power in NREM sleep in the C57BL/6J mouse. *Sleep Med.* 7, 7–16. doi:10.1016/J.SLEEP.2005.06.006.

Poon, C.-S., Zhou, Z., and Champagnat, J. (2000). NMDA Receptor Activity In Utero Averts Respiratory Depression and Anomalous Long-Term Depression in Newborn Mice. *J. Neurosci.* 20, RC73–RC73. doi:10.1523/jneurosci.20-09-j0003.2000.

Powell, F. ., Milsom, W. ., and Mitchell, G. . (1998). Time domains of the hypoxic ventilatory response. *Respir. Physiol.* 112, 123–134. doi:10.1016/S0034-5687(98)00026-7.

Prakash, Y. S., Mantilla, C. B., Zhan, W.-Z., Smithson, K. G., and Sieck, G. C. (2000). Phrenic motoneuron morphology during rapid diaphragm muscle growth. *J. Appl. Physiol.* 89, 563–572. doi:10.1152/jappl.2000.89.2.563.

Pryor, J. R., Maalouf, F. I., Krans, E. E., Schumacher, R. E., Cooper, W. O., and Patrick, S. W. (2017). The opioid epidemic and neonatal abstinence syndrome in the USA: a review of the continuum of care. *Arch. Dis. Child. Fetal Neonatal Ed.* 102, F183–F187. doi:10.1136/archdischild-2015-310045.

Quan, N., He, L., and Lai, W. (2003). Endothelial activation is an intermediate step for peripheral lipopolysaccharide induced activation of paraventricular nucleus. *Brain Res. Bull.* 59, 447–452. doi:10.1016/S0361-9230(02)00951-6.

Rajani, V., Zhang, Y., Jalubula, V., Rancic, V., SheikhBahaei, S., Zwicker, J. D., et al. (2018). Release of ATP by pre-Bötzinger complex astrocytes contributes to the hypoxic ventilatory response via a Ca^{2+} -dependent $P2Y_1$ receptor mechanism. *J. Physiol.* 596, 3245–3269. doi:10.1113/JP274727.

Rana, S. A., Aavani, T., and Pittman, Q. J. (2012). Sex effects on neurodevelopmental outcomes of innate immune activation during prenatal and neonatal life. *Horm. Behav.* 62, 228–236. doi:10.1016/j.yhbeh.2012.03.015.

Rantakallio, P., Jones, P., Moring, J., and Von Wendt, L. (1997). Association between central nervous system infections during childhood and adult onset schizophrenia and other psychoses: A 28-year follow-up. *Int. J. Epidemiol.* 26, 837–843. doi:10.1093/ije/26.4.837.

Rathod, K. S., Kapil, V., Velmurugan, S., Khambata, R. S., Siddique, U., Khan, S., et al. (2017). Accelerated resolution of inflammation underlies sex differences in inflammatory responses in humans. *J. Clin. Invest.* 127, 169–182. doi:10.1172/JCI89429.

Reemst, K., Noctor, S. C., Lucassen, P. J., and Hol, E. M. (2016). The Indispensable Roles of Microglia and Astrocytes during Brain Development. *Front. Hum. Neurosci.* 10, 566. doi:10.3389/fnhum.2016.00566.

Reimer, T., Brcic, M., Schweizer, M., and Jungi, T. W. (2008). poly(I:C) and LPS induce distinct IRF3 and NF-κB signaling during type-I IFN and TNF responses in human macrophages. *J. Leukoc. Biol.* 83, 1249–1257. doi:10.1189/jlb.0607412.

Reimers, J., Wogensen, L. D., Welinder, B., Hejnaes, K. R., Poulsen, S. S., Nillson, P., et al. (1991). The Pharmacokinetics, Distribution and Degradation of Human Recombinant Interleukin 1beta in Normal Rats. *Scand. J. Immunol.* 34, 597–617. doi:10.1111/j.1365-3083.1991.tb01583.x.

Ren, J., and Greer, J. J. (2008). "Modulation of Perinatal Respiratory Rhythm by GABAA- and Glycine Receptor-mediated Chloride Conductances," in (Springer, New York, NY), 149–153. doi:10.1007/978-0-387-73693-8_26.

Ribeiro, A. P., Mayer, C. A., Wilson, C. G., Martin, R. J., and MacFarlane, P. M. (2017). Intratracheal LPS administration attenuates the acute hypoxic ventilatory response: Role of brainstem IL-1β receptors. *Respir. Physiol. Neurobiol.* 242, 45–51. doi:10.1016/j.resp.2017.03.005.

Ricker, E. M., Pye, R. L., Barr, B. L., and Wyatt, C. N. (2015). "Selective mu and kappa Opioid Agonists Inhibit Voltage-Gated Ca2+ Entry in Isolated Neonatal Rat Carotid Body Type I Cells," in *Advances in experimental medicine and biology*, 49–54. doi:10.1007/978-3-319-18440-1_6.

Rothwell, N. J., and Luheshi, G. N. (2000). Interleukin 1 in the brain: Biology, pathology and therapeutic target. *Trends Neurosci.* 23, 618–625. doi:10.1016/S0166-2236(00)01661-1.

Rourke, K. S., Mayer, C. A., and MacFarlane, P. M. (2016). A critical postnatal period of heightened vulnerability to lipopolysaccharide. *Respir. Physiol. Neurobiol.* 232, 26–34. doi:10.1016/j.resp.2016.06.003.

Rousseau, J.-P., Tenorio-Lopes, L., Baldy, C., Janes, T. A., and Fournier, S. (2017). On the origins of sex-based differences in respiratory disorders: Lessons and hypotheses from stress neuroendocrinology in developing rats. *Respir. Physiol. Neurobiol.* 245, 105–121. doi:10.1016/J.RESP.2017.03.013.

Rubin, J. E., Hayes, J. A., Mendenhall, J. L., and Del Negro, C. A. (2009). Calcium-activated nonspecific cation current and synaptic depression promote network-dependent burst oscillations. *Proc. Natl. Acad. Sci. U. S. A.* 106, 2939–44. doi:10.1073/pnas.0808776106.

Schiffelholz, T., and Lancel, M. (2001). Sleep changes induced by lipopolysaccharide in the rat are influenced by age Downloaded from. *Am J Physiol Regul. Integr. Comp Physiol* 280, 398–403. doi:10.220.32.247.

Schneider, H., Pitossi, F., Balschun, D., Wagner, A., del Rey, A., and Besedovsky, H. O. (1998). A neuromodulatory role of interleukin-1beta in the hippocampus. *Proc. Natl. Acad. Sci. U. S. A.* 95, 7778–83. doi:10.1073/pnas.95.13.7778.

Schwarz, J. M., and Bilbo, S. D. (2011). The Immune System and the Developing Brain. *Colloq. Ser. Dev. Brain* 2, 1–128. doi:10.4199/C00045ED1V01Y201110DBR004.

Seven, Y. B., Perim, R. R., Hobson, O. R., Simon, A. K., Tadjalli, A., and Mitchell, G. S. (2018). Phrenic motor neuron adenosine 2A receptors elicit phrenic motor facilitation. *J. Physiol.* 596, 1501–1512. doi:10.1113/JP275462.

Shanks, N., Windle, R. J., Perks, P. a, Harbuz, M. S., Jessop, D. S., Ingram, C. D., et al. (2000). Early-life exposure to endotoxin alters hypothalamic-pituitary-adrenal function and predisposition to inflammation. *Proc. Natl. Acad. Sci.* 97, 5645–5650. doi:10.1073/pnas.090571897.

Sheikhbahaei, S., Turovsky, E. A., Hosford, P. S., Hadjihambi, A., Theparambil, S. M., Liu, B., et al. (2018). Astrocytes modulate brainstem respiratory rhythm-generating circuits and determine exercise capacity. *Nat. Commun.* 9, 370. doi:10.1038/s41467-017-02723-6.

Siljehav, V., Olsson Hofstetter, A., Jakobsson, P.-J., and Herlenius, E. (2012). mPGES-1 and prostaglandin E2: vital role in inflammation, hypoxic response, and survival. *Pediatr. Res.* 72, 460–7. doi:10.1038/pr.2012.119.

Smith, C. A., Blain, G. M., Henderson, K. S., and Dempsey, J. A. (2015). Peripheral chemoreceptors determine the respiratory sensitivity of central chemoreceptors to CO_2 : role of carotid body CO_2. *J. Physiol.* 593, 4225–4243. doi:10.1113/JP270114.

Smith, J. C., Abdala, A. P. L., Borgmann, A., Rybak, I. A., and Paton, J. F. R. (2013). Brainstem respiratory networks: Building blocks and microcircuits. *Trends Neurosci.* 36, 152–162. doi:10.1016/j.tins.2012.11.004.

Smith, J. C., Abdala, A. P. L., Rybak, I. a, and Paton, J. F. R. (2009). Structural and functional architecture of respiratory networks in the mammalian brainstem. *Philos. Trans. R. Soc. B Biol. Sci.* 364, 2577–2587. doi:10.1098/rstb.2009.0081.

Smith, J., Ellenberger, H., Ballanyi, K., Richter, D., and Feldman, J. (1991). Pre-Botzinger complex: a brainstem region that may generate respiratory rhythm in mammals. *Science (80-.).* 254, 726–729. doi:10.1126/science.1683005.

Smith, P. L. P., Hagberg, H., Naylor, A. S., and Mallard, C. (2014). Neonatal Peripheral Immune Challenge Activates Microglia and Inhibits Neurogenesis in the Developing Murine Hippocampus. *Dev. Neurosci.* 36, 119–131. doi:10.1159/000359950.

Spencer, S. J., Galic, M. a, and Pittman, Q. J. (2011). Neonatal programming of innate immune function. *Am. J. Physiol. Endocrinol. Metab.* 300, E11–E18. doi:10.1152/ajpendo.00516.2010.

Spencer, S. J., Martin, S., Mouihate, A., and Pittman, Q. J. (2006). Early-life immune challenge: defining a critical window for effects on adult responses to immune challenge. *Neuropsychopharmacology* 31, 1910–1918. doi:10.1038/sj.npp.1301004.

Starkhammar, M., Kumlien Georén, S., Swedin, L., Dahlén, S.-E., Adner, M., and Cardell, L. O. (2012). Intranasal Administration of poly(I:C) and LPS in BALB/c Mice Induces Airway Hyperresponsiveness and Inflammation via Different Pathways. *PLoS One* 7, e32110. doi:10.1371/journal.pone.0032110.

Stoll, B. J., Hansen, N., Fanaroff, A. A., Wright, L. L., Carlo, W. A., Ehrenkranz, R. A., et al. (2002). Changes in pathogens causing early-onset sepsis in very low birth weight infants. *N. Engl. J. Med.* 347, 240–247. doi:10.1056/NEJMoa012657.

Stoll, B. J., Hansen, N. I., Adams-Chapman, I., Fanaroff, A. A., Hintz, S. R., Vohr, B. R., et al. (2004). Neurodevelopmental and growth impairment among extremely low-birth-weight infants with neonatal infection. *J. Am. Med. Assoc.* 292, 2357–2365. doi:10.1001/jama.292.19.2357.

Stover, M. W., and Davis, J. M. (2015). Opioids in pregnancy and neonatal abstinence syndrome. *Semin. Perinatol.* 39, 561–565. doi:10.1053/j.semperi.2015.08.013.

Strey, K. A., Baertsch, N. A., and Baker-Herman, T. L. (2013). Inactivity-induced respiratory plasticity: protecting the drive to breathe in disorders that reduce respiratory neural activity. *Respir. Physiol. Neurobiol.* 189, 384–94. doi:10.1016/j.resp.2013.06.023.

Stucke, A. G., Miller, J. R., Prkic, I., Zuperku, E. J., Hopp, F. A., and Stuth, E. A. E. (2015). Opioid-induced Respiratory Depression Is Only Partially Mediated by the preBötzinger Complex in Young and Adult Rabbits In Vivo. *Anesthesiology* 122, 1288–1298. doi:10.1097/ALN.0000000000000628.

Svensson, M., Venge, P., Janson, C., and Lindberg, E. (2012). Relationship between sleep-disordered breathing and markers of systemic inflammation in women from the general population. *J. Sleep Res.* 21, 147–154. doi:10.1111/j.1365-2869.2011.00946.x.

Takahashi, T., Otsuguro, K., Ohta, T., and Ito, S. (2010). Adenosine and inosine release during hypoxia in the isolated spinal cord of neonatal rats. *Br. J. Pharmacol.* 161, 1806–16. doi:10.1111/j.1476-5381.2010.01002.x.

Takakura, A. C. T., Moreira, T. S., Colombari, E., West, G. H., Stornetta, R. L., and Guyenet, P. G. (2006). Peripheral chemoreceptor inputs to retrotrapezoid nucleus (RTN) CO_2 -sensitive neurons in rats. *J. Physiol.* 572, 503–523. doi:10.1113/jphysiol.2005.103788.

Takeda, M., Tanimoto, T., Kadoi, J., Nasu, M., Takahashi, M., Kitagawa, J., et al. (2007). Enhanced excitability of nociceptive trigeminal ganglion neurons by satellite glial cytokine following peripheral inflammation. *Pain* 129, 155–166. doi:10.1016/j.pain.2006.10.007.

Takeda, S., Ph, D., Eriksson, L. I., Yamamoto, Y., and Joensen, H. (2001). Opioid Action on Respiratory Neuron Activity of the. *Anesthesiology* 95, 740–749. Available at: http://anesthesiology.pubs.asahq.org/article.aspx?articleid=1944668 [Accessed June 3, 2019].

Tan, W., Pagliardini, S., Yang, P., Janczewski, W. A., and Feldman, J. L. (2010a). Projections of preBötzinger complex neurons in adult rats. *J. Comp. Neurol.* 518, 1862–78. doi:10.1002/cne.22308.

Tan, W., Pagliardini, S., Yang, P., Janczewski, W. A., and Feldman, J. L. (2010b). Projections of preBötzinger complex neurons in adult rats. *J. Comp. Neurol.* 518, 1862–78. doi:10.1002/cne.22308.

Tanabe, A., Fujii, T., and Onimaru, H. (2005). Facilitation of respiratory rhythm by a μ-opioid agonist in newborn rat pons–medulla–spinal cord preparations. *Neurosci. Lett.* 375, 19–22. doi:10.1016/J.NEULET.2004.10.058.

Tapia, I. E., Shults, J., Doyle, L. W., Nixon, G. M., Cielo, C. M., Traylor, J., et al. (2016). Perinatal Risk Factors Associated with the Obstructive Sleep Apnea Syndrome in School-Aged Children Born Preterm. *Sleep* 39, 737–42. doi:10.5665/sleep.5618.

Terrando, N., Rei Fidalgo, A., Vizcaychipi, M., Cibelli, M., Ma, D., Monaco, C., et al. (2010). The impact of IL-1 modulation on the development of lipopolysaccharide-induced cognitive dysfunction. *Crit. care* 14, R88. doi:10.1186/cc9019.

Tester, N. J., Fuller, D. D., Fromm, J. S., Spiess, M. R., Behrman, A. L., and Mateika, J. H. (2014). Long-Term Facilitation of Ventilation in Humans with Chronic Spinal Cord Injury. *Am J Respir Crit Care Med* 189, 57–65. doi:10.1164/rccm.201305-0848OC.

Thoby-brisson, M., and Greer, J. J. (2010). Neural Control of Perinatal Respiration Anatomical and functional development of the pre-Bo ¨ tzinger complex in prenatal rodents. *J. Appl. Physiol.*, 1213–1219. doi:10.1152/japplphysiol.01061.2007.

Thoby-Brisson, M., Karlén, M., Wu, N., Charnay, P., Champagnat, J., and Fortin, G. (2009). Genetic identification of an embryonic parafacial oscillator coupling to the preBötzinger complex. *Nat. Neurosci.* 12, 1028–1035. doi:10.1038/nn.2354.

Thoby-Brisson, M., and Ramirez, J. M. (2001). Identification of two types of inspiratory pacemaker neurons in the isolated respiratory neural network of mice. *J. Neurophysiol.* 86, 104–12. doi:20/15/5858 [pii].

Trumbower, R. D., Hayes, H. B., Mitchell, G. S., Wolf, S. L., and Stahl, V. A. (2017). Effects of acute intermittent hypoxia on hand use after spinal cord trauma. *Neurology* 89, 1904–1907. doi:10.1212/WNL.0000000000004596.

Trumbower, R. D., Jayaraman, A., Mitchell, G. S., and Rymer, W. Z. (2012). Exposure to Acute Intermittent Hypoxia Augments Somatic Motor Function in Humans With Incomplete Spinal Cord Injury. *Neurorehabil. Neural Repair* 26, 163–172. doi:10.1177/1545968311412055.

Turner, S., Streeter, K. A., Greer, J., Mitchell, G. S., and Fuller, D. D. (2018). Pharmacological modulation of hypoxia-induced respiratory neuroplasticity. *Respir. Physiol. Neurobiol.* 256, 4–14. doi:10.1016/J.RESP.2017.11.008.

Turrin, N. P., Gayle, D., Ilyin, S. E., Flynn, M. C., Langhans, W., Schwartz, G. J., et al. (2001). Pro-inflammatory and anti-inflammatory cytokine mRNA induction in the periphery and brain following intraperitoneal administration of bacterial lipopolysaccharide. *Brain Res. Bull.* 54, 443–453. doi:10.1016/S0361-9230(01)00445-2.

Vestal-Laborde, A. A., Eschenroeder, A. C., Bigbee, J. W., Robinson, S. E., and Sato-Bigbee, C. (2014). The Opioid System and Brain Development: Effects of Methadone on the Oligodendrocyte Lineage and the Early Stages of Myelination. *Dev. Neurosci.* 36, 409–421. doi:10.1159/000365074.

Vinit, S., Windelborn, J. A., and Mitchell, G. S. (2011). Lipopolysaccharide attenuates phrenic long-term facilitation following acute intermittent hypoxia. *Respir. Physiol. Neurobiol.* 176, 130–5. doi:10.1016/j.resp.2011.02.008.

Walker, F. R., Hodyl, N. A., Krivanek, K. M., and Hodgson, D. M. (2006). Early life host-bacteria relations and development: Long-term individual differences in neuroimmune function following neonatal endotoxin challenge. *Physiol. Behav.* 87, 126–134. doi:10.1016/j.physbeh.2005.09.008.

Wang, K.-C., Fan, L.-W., Kaizaki, A., Pang, Y., Cai, Z., and Tien, L.-T. (2013). Neonatal lipopolysaccharide exposure induces long-lasting learning impairment, less anxiety-like response and hippocampal injury in adult rats. *Neuroscience* 234, 146–157. doi:10.1016/j.neuroscience.2012.12.049.

Wang, X., Loram, L. C., Ramos, K., de Jesus, A. J., Thomas, J., Cheng, K., et al. (2012). Morphine activates neuroinflammation in a manner parallel to endotoxin. *Proc. Natl. Acad. Sci.* 109, 6325–6330. doi:10.1073/pnas.1200130109.

Wang, X., Rousset, C. I., Hagberg, H., and Mallard, C. (2006). Lipopolysaccharide-induced inflammation and perinatal brain injury. *Semin. Fetal Neonatal Med.* 11, 343–353. doi:10.1016/J.SINY.2006.04.002.

Ward, S. L., Bautista, D. B., Woo, M. S., Chang, M., Schuetz, S., Wachsman, L., et al. (1992). Responses to hypoxia and hypercapnia in infants of substance-abusing mothers. *J. Pediatr.* 121, 704–9. doi:10.1016/s0022-3476(05)81896-7.

Ward, S. L. D., Schuetz, S., Krishna, V., Bean, X., Wingert, W., Wachsman, L., et al. (1986). Abnormal Sleeping Ventilatory Pattern in Infants of Substance-Abusing Mothers. *Am. J. Dis. Child.* 140, 1015–1020. doi:10.1001/archpedi.1986.02140240061028.

Wittmeier, S., Song, G., Duffin, J., and Poon, C.-S. (2008). Pacemakers handshake synchronization mechanism of mammalian respiratory rhythmogenesis. *Proc. Natl. Acad. Sci. U. S. A.* 105, 18000–5. doi:10.1073/pnas.0809377105.

Wong-Riley, M. T. T., and Liu, Q. (2008). Neurochemical and physiological correlates of a critical period of respiratory development in the rat. *Respir. Physiol. Neurobiol.* doi:10.1016/j.resp.2008.04.014.

Wu, C. C., Hung, C. J., Shen, C. H., Chen, W. Y., Chang, C. Y., Pan, H. C., et al. (2014). Prenatal buprenorphine exposure decreases neurogenesis in rats. *Toxicol. Lett.* 225, 92–101. doi:10.1016/j.toxlet.2013.12.001.

Yamato, M., Tamura, Y., Eguchi, A., Kume, S., Miyashige, Y., Nakano, M., et al. (2014). Brain interleukin-1β and the intrinsic receptor antagonist control peripheral toll-like receptor 3-mediated suppression of spontaneous activity in rats. *PLoS One*. doi:10.1371/journal.pone.0090950.

Yang, C. F., and Feldman, J. L. (2018). Efferent projections of excitatory and inhibitory preBötzinger Complex neurons. *J. Comp. Neurol.* 526, 1389–1402. doi:10.1002/cne.24415.

Yehuda, S., Sredni, B., Carasso, R. L., and Kenigsbuch-Sredni, D. (2009). REM Sleep Deprivation in Rats Results in Inflammation and Interleukin-17 Elevation. *J. Interf. Cytokine Res.* 29, 393–398. doi:10.1089/jir.2008.0080.

Yin, M.-J., Yamamoto, Y., and Gaynor, R. B. (1998). The anti-inflammatory agents aspirin and salicylate inhibit the activity of IκB kinase-β. *Nature* 396, 77–80. doi:10.1038/23948.

Zabka, A. G., Behan, M., Mitchell, G. S., Aitken, M., Franklin, J., Pierson, D., et al. (2001). Selected contribution: Time-dependent hypoxic respiratory responses in female rats are influenced by age and by the estrus cycle. *J. Appl. Physiol.* 91, 2831–8. doi:10.1016/0034-5687(96)00017-5.

Zabka, A. G., Mitchell, G. S., Olson, E. B., and Behan, M. (2003). Selected Contribution: Chronic intermittent hypoxia enhances respiratory long-term facilitation in geriatric female rats. *J. Appl. Physiol.* 95. Available at: http://jap.physiology.org/content/95/6/2614.full.pdf+html [Accessed July 31, 2017].

Zhang, R. X., Li, A., Liu, B., Wang, L., Ren, K., Zhang, H., et al. (2008). IL-1ra alleviates inflammatory hyperalgesia through preventing phosphorylation of NMDA receptor NR-1 subunit in rats. *Pain* 135, 232–239. doi:10.1016/j.pain.2007.05.023.

Zhu, C.-B., Lindler, K. M., Owens, A. W., Daws, L. C., Blakely, R. D., and Hewlett, W. A. (2010). Interleukin-1 receptor activation by systemic lipopolysaccharide induces behavioral despair linked to MAPK regulation of CNS serotonin transporters. *Neuropsychopharmacology* 35, 2510–20. doi:10.1038/npp.2010.116.

Zhu, X., Levasseur, P. R., Michaelis, K. A., Burfeind, K. G., and Marks, D. L. (2016). A distinct brain pathway links viral RNA exposure to sickness behavior. *Sci. Rep.* 6, 29885. doi:10.1038/srep29885.

Zin, C. S., Nissen, L. M., O'Callaghan, J. P., Moore, B. J., and Smith, M. T. (2010). Preliminary Study of the Plasma and Cerebrospinal Fluid Concentrations of IL-6 and IL-10 in Patients with Chronic Pain Receiving Intrathecal Opioid Infusions by Chronically Implanted Pump for Pain Management. *Pain Med.* 11, 550–561. doi:10.1111/j.1526-4637.2010.00821.x.